ДОКЛАДЫ
АКАДЕМИИ НАУК СССР

4625-1

M. I. T. Lincoln Laboratory
MAR 2 1959
Received - Library

PROCEEDINGS OF THE ACADEMY OF SCIENCES

OF THE USSR

Physical Chemistry Section

(DOKLADY AKADEMII NAUK SSSR)

IN ENGLISH TRANSLATION

VOL. 118 NOS. 1-6

CONSULTANTS BUREAU, INC.
227 WEST 17TH STREET, NEW YORK 11, N. Y.
an agency for the interpretation of international knowledge

PROCEEDINGS OF THE ACADEMY OF SCIENCES OF THE USSR

(DOKLADY AKADEMII NAUK SSSR)

Section: PHYSICAL CHEMISTRY

Volume 118, Issues 1-6

January-February 1958

Editorial Board:

Acad. L.A. Artsimovich, Acad. A.G. Betekhtin, Acad. S.V. Vekshinskii,
Acad. B.A. Kazanskii, Acad. A.N. Kolmogorov (Asst. to Editor in Chief),
Acad. A.L. Kursanov, Acad. S.A. Lebedev, Acad. A.I. Oparin (Editor in Chief),
Acad. E.N. Pavlovskii, Acad. L.I. Sedov, Acad. N.M. Strakhov,
Acad. A.N. Frumkin (Asst. to Editor in Chief)

(A Publication of the Academy of Sciences of the USSR)

IN ENGLISH TRANSLATION

Copyright, 1958

CONSULTANTS BUREAU, INC.
227 West 17th Street
New York 11, N. Y.

Printed in the United States

Annual Subscription $160.00
Single Issue 35.00

Note: The sale of photostatic copies of any portion of this copyright translation is expressly prohibited by the copyright owners. A complete copy of any article in this issue may be purchased from the publisher for $5.00.

SIGNIFICANCE OF ABBREVIATIONS MOST FREQUENTLY ENCOUNTERED IN SOVIET PERIODICALS

FIAN	Phys. Inst. Acad. Sci. USSR.
GDI	Water Power Inst.
GITI	State Sci.-Tech. Press
GITTL	State Tech. and Theor. Lit. Press
GONTI	State United Sci.-Tech. Press
Gosenergoizdat	State Power Press
Goskhimizdat	State Chem. Press
GOST	All-Union State Standard
GTTI	State Tech. and Theor. Lit. Press
IL	Foreign Lit. Press
ISN (Izd. Sov. Nauk)	Soviet Science Press
Izd. AN SSSR	Acad. Sci. USSR Press
Izd. MGU	Moscow State Univ. Press
LEIIZhT	Leningrad Power Inst. of Railroad Engineering
LET	Leningrad Elec. Engr. School
LETI	Leningrad Electrotechnical Inst.
LETIIZhT	Leningrad Electrical Engineering Research Inst. of Railroad Engr.
Mashgiz	State Sci.-Tech. Press for Machine Construction Lit.
MEP	Ministry of Electrical Industry
MES	Ministry of Electrical Power Plants
MESEP	Ministry of Electrical Power Plants and the Electrical Industry
MGU	Moscow State Univ.
MKhTI	Moscow Inst. Chem. Tech.
MOPI	Moscow Regional Pedagogical Inst.
MSP	Ministry of Industrial Construction
NII ZVUKSZAPIOI	Scientific Research Inst. of Sound Recording
NIKFI	Sci. Inst. of Modern Motion Picture Photography
ONTI	United Sci.-Tech. Press
OTI	Division of Technical Information
OTN	Div. Tech. Sci.
Stroiizdat	Construction Press
TOE	Association of Power Engineers
TsKTI	Central Research Inst. for Boilers and Turbines
TsNIEL	Central Scientific Research Elec. Engr. Lab.
TsNIEL-MES	Central Scientific Research Elec. Engr. Lab.–Ministry of Electric Power Plants
TsVTI	Central Office of Economic Information
UF	Ural Branch
VIESKh	All-Union Inst. of Rural Elec. Power Stations
VNIIM	All-Union Scientific Research Inst. of Meteorology
VNIIZhDT	All-Union Scientific Research Inst. of Railroad Engineering
VTI	All-Union Thermotech. Inst.
VZEI	All-Union Power Correspondence Inst.

Note: Abbreviations not on this list and not explained in the translation have been transliterated, no further information about their significance being available to us. – Publisher.

ELECTRON-DIFFRACTION INVESTIGATION OF THE STRUCTURE OF THE CHLOROPRENE MOLECULE

P. A. Akishin, L. V. Vilkov, and V. M. Tatevskii

(Presented by Academician N. N. Semenov, January 3, 1957)

The structure of butadiene and of its derivatives which are the fundamental constituents of natural and synthetic rubbers is of great interest in the theory of the structure of organic compounds and has been widely discussed in the literature.

The chief problems which require elucidation are the state of the single C—C bonds situated between two double bonds and rotational isomerism around this bond. The widespread view that molecules containing a system of conjugated double bonds have a planar configuration has been confirmed only in the case of certain simple compounds; in general, molecules of dienes and of their derivatives can exist in the form of rotational isomers with a nonplanar,conjugated double-bond system. Little investigation has been done on the rotational isomerism of compounds containing conjugated double bonds as well as on the problem of the form of the potential barrier which restricts rotation about the central C—C bond. The determination of the structure, the ratio of the concentrations and of the heats of interconversion of the various isomers is necessary for the understanding of the mechanism of chemical transformations as well as for the calculation of thermodynamic functions of these compounds. The necessary data may be obtained experimentally by means of various physical and physicochemical methods in addition to purely chemical ones.

The object of the present investigation was to determine the spatial configuration and the geometrical parameters of the chloroprene molecule by means of diffraction experiments of fast electrons in a stream of the vapor of the compound.* The electron-diffraction photographs were recorded with the apparatus described earlier [1]. Seven series of electron-diffraction photographs were recorded (3 photographs in each series) for electron wavelengths from 0.0520 to 0.0540 A, the distance from the vaporizer nozzle to the film being 117 mm. In these electron-diffraction photographs we have determined 8 maxima and 7 minima and evaluated their intensity by the visual method. On the basis of the experimental data (Table 1) we have constructed the radial distribution curve (Fig. 1) by the method of Walter and Beach [2].

The calculations which were carried out for varying intensities of the extrema, have confirmed the reliability of the radial distribution curve. We have carried out the following correlations of the peaks of the curve with interatomic distances in the chloroprene molecule** (see Fig. 2):

1) 1.34 A: composite of $5r(C-H)$, $2r(C=C)$ and $r(C-C)$;

2) 1.71 A: $r(C-Cl)$;

3) 2.02 A: very small, composite of $5r(C_2 \ldots H_1)$ and $r(C_2 \ldots H_3)$;

4) 2.67 A: very high, composite of $r(C_1 \ldots C_3)$, $r(C_2 \ldots C_4)$, $r(Cl \ldots C_3)$, $r(Cl \ldots C_1)$;

---

* Chloroprene is a colorless mobile liquid, b. p. 59°, with a pungent odor; it polymerizes easily even in the absence of light. To inhibit polymerization, hydroquinone was added to the ampoule containing the chloroprene.

** Of the symbols used to denote interatomic distances the line denotes the actual chemical bond while distances between atoms not linked directly are denoted by dots.

TABLE 1

Evaluation of Electron-Diffraction Patterns of Chloroprene Vapor

Maxima	Minima	$I_{(s)}$	s_{exptl}	$s_{\text{theor}}/s_{\text{exptl.}}$	$s_{\text{theor}}/s_{\text{exptl.}}$
1		+ 1	2.91	—	—
	1	−12	4.07	—	—
2		+10	5.05	(1.034)	(1.034)
	2	− 7	6.54	0.998	0.998
3		+ 5	7.33	—	—
	3	− 3	9.11	(1.026)	(1.026)
4		+ 4	10.44	0.991	0.994
	4	− 4	11.47	0.994	0.994
5		+ 4.5	12.46	1.002	1.004
	5	− 5	13.75	0.989	0.985
6		+ 5	14.78	1.008	1.007
	6	− 0.5	15.99	1.010	1.010
7		+ 0.5	16.86	1.005	1.002
	7	− 0.6	18.03	0.993	0.992
8		+ 6	19.19	0.999	0.998
		Mean		0.999	0.998
		Mean deviation		±0.006	±0.006

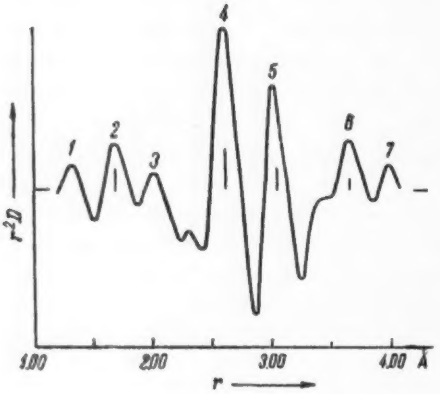

Fig. 1. Radial distribution curve plotted from the Walter-Beach equation [2] for the chloroprene molecule.

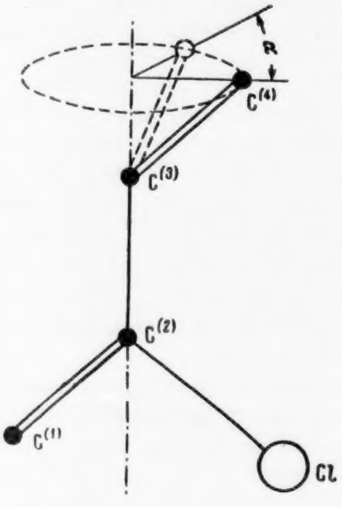

Fig. 2. Model of the chloroprene molecule.

5) 3.06 A − r(Cl . . . C_4) and 6) 3.70 A − r(C_1 . . . C_4) with the double bonds in the trans-position;

7) 4.02 A − small, may be ascribed to r(Cl . . . C_4) in the cis-configuration. If it is taken into account that the peak at 4.02 A also appears on the radial distribution curve plotted with data taken from the theoretical curve No. 5 which corresponds to the rotated trans-isomer (see below), it is necessary to refrain from allocating this peak to the cis-isomer.

Using the method of successive approximations we have subsequently plotted theoretical intensity curves for several chloroprene molecule models whose structural parameters are shown in Table 2; these curves are compared with the intensity curves plotted from actual experimental data (Fig. 3). The distances C−H, C=C and C_2-C_3 which have not been accounted for separately on the radial distribution curve have been taken to be equal

TABLE 2

Structural Parameters of Different Models of the Chloroprene Molecule

Model	r (C=C)	r (C—C)	r (C—Cl)	$\angle C_1C_2Cl = \angle C_1C_2C_3$	$\angle C_2C_3C_4$	α *
1 plane, trans	1.36	1.46	1.70	122°	122°	0°
2 plane, cis	1.36	1.46	1.70	122°	122°	180°
3 rotated	1.36	1.46	1.70	122°	122°	90°
4 plane, trans	1.36	1.46	1.70	122°	127°	0°
5 rotated	1.36	1.46	1.70	122°	122°	32°
6 "	1.36	1.50	1.70	122°	122°	32°
7 "	1.36	1.46	1.70	122°	122°	42°
8 "	1.36	1.46	1.70	122°	122°	22°

---

* α is the angle between the planes of the vinyl groups.

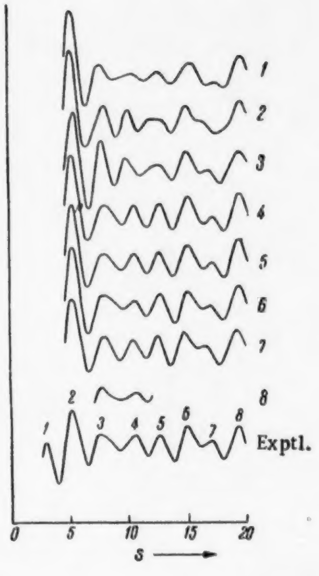

Fig. 3. Theoretical intensity curves of electron-diffraction patterns for models 1-8 of the chloroprene molecule, and the actual experimental curve.

to the corresponding distances in butadiene [4]; the distance C—Cl has been taken as 1.70 A, in agreement with the value given by the radial distribution curve; the hydrogen atoms have been accounted for in the way described in [5].

The theoretical intensity curves 1, 2 and 3 differ from the experimental intensity curve of the diffracted electrons. Curve 1 (plane trans-isomer) does not reproduce the distinct asymmetry of maximum 3, while the intensities of maxima 5 and 4 are very much lower. Curve 2 (plane cis-isomer) does not show the asymmetry of maximum 3 and does not reproduce the shape of maximum 5; it also lacks maximum 7. Curve 3 (rotated isomer, the angle of rotation of the vinyl groups about the C_2-C_3 bond being 90°) does not reproduce the asymmetry of maximum 3; also, its minimum 4 and maximum 5 are both small. The best agreement with the experimental curve is observed in the case of curves 4 and 5. Curve 4 corresponds to the plane model with the double bonds in the trans-position and with angles ClC_2C_3 and $C_2C_3C_4$ differing by 5°. Curve 5 corresponds to a nonpolar model in which the vinyl groups are rotated about the C_2-C_3 bond through 32° from the trans-position, angles $C_1C_2C_3$ and $C_2C_3C_4$ being equal.

The fundamental parameters for models 4 and 5 are in good agreement with the values of interatomic distances obtained from the radial distribution curve. Curves 6, 7 and 8 were calculated with a view of determining the possible variations in the length of the C_2-C_3 bond and in the distance Cl . . . C_4, which were found to be equal to ± 0.04 and ± 0.06 A, respectively. Thus, our experimental data on the geometry of the chloroprene molecule, obtained by the electron-diffraction method, correspond to the following two most probable structures:

1) a planar molecule with the double bonds in the trans-position and the following interatomic distances and valence-bond angles:

$$r\,(C=C) = 1.36\ \text{Å (adopted)};\quad r\,(C-C) = 1.46 \pm 0.04\ \text{Å};\quad r(C-Cl) = \\ = 1.70 \pm 0.02\ \text{Å};$$

$$\angle\, C_1C_2Cl = \angle\, C_1C_2C_3 = 122^\circ\ \text{(adopted) and}\ \angle\, C_2C_3C_4 = 127^\circ \pm 3^\circ.$$

2) a nonplanar molecule with the vinyl groups rotated about the single C_2-C_3 bond through an angle of 30 ± 10° from the trans-position, and with the following interatomic distances and valence-bond angles:

$$r(C=C)=1.36\ \text{A (adopted)};\quad r(C-C)=1.46\pm0.04\ \text{A}\cdot\quad r(C-Cl)=$$
$$=1.70\pm0.02\ \text{A}\cdot$$

$$\angle C_1C_2Cl=C_1C_2C_3=\angle\ 122^\circ\ \text{(adopted)}.$$

The ambiguity arising in the interpretation of the experimental data is due to the fact that the theoretical intensity curves do not show sufficiently accurately the variations in the distances $C_4 \ldots Cl$ and $C_4 \ldots C_2$ in the different models of the chloroprene molecule.

The results of our investigation show that the carbon-carbon double bonds in the chloroprene molecule are in the trans-position or in one close to it; this is in agreement with data obtained from infrared and ultraviolet spectra of chloroprene [6-8]. The trans-configuration of chloroprene also finds confirmation in the structure of its polymer, neoprene, which consists of repeating units with the methylene groups situated trans- with respect to the C−C bonds [9]. It is interesting to note that the trans-configuration of the double bonds is characteristic for most of the simple compounds known which contain a doubly conjugated system (for example, butadiene, glyoxal, dimethylglyoxal, acrolein, etc.). In considering the results of this investigation of the geometry of the chloroprene molecule we have to direct our attention to the distance $Cl \ldots C_4$, which is equal to 3.05 A and is much less than the sum of the intermolecular radii of the CH_2-group and the chlorine atom which equals 3.70 A. In attempting to explain this difference we cannot take recourse to the notion of inductive interaction of the chlorine atom with the CH_2-group since in allyl chloride [10, 11] the corresponding distance is unchanged and equal to 3.70 A.

LITERATURE CITED

[1] A. V. Frost and P. A. Akishin, Bull. Moscow State Univ. No. 12,.85 (1953).

[2] J. Walter and J. Beach, J. Chem. Phys. 8, 601 (1940).

[3] L. Pauling and L. Brockway, J. Chem. Phys. 2, 867 (1934).

[4] P. Allen and L. Sutton, Acta Cryst. 3, 46 (1950).

[5] R. Spurr and V. Schomaker, J. Am. Chem. Soc. 64, 2693 (1942).

[6] G. Szasz and N. Sheppard, Trans. Farad. Soc. 49, 358 (1953).

[7] W. Price and A. Walsh, Proc. Roy. Soc. A 179, 201 (1941).

[8] R. Mulliken, Rev. Mod. Phys. 14, 265 (1942).

[9] J. Maynard and W. Mochel, J. Polym. Sci. 13, 251 (1954).

[10] H. Bowen, A. Gilchrist, and L. Sutton, Trans. Farad. Soc. 51, 1341 (1955).

[11] P. A. Akishin, L. V. Vilkov, and V. M. Tatevskii, Bull. Moscow State Univ. No. 1, 143 (1957).

Received December 29, 1956

M. V. Lomonosov State University, Moscow

THE INFLUENCE OF ASSOCIATION OF ORGANIC ACIDS ON THEIR ADSORPTION FROM NONPOLAR SOLVENTS

N. N. Griazev

(Presented by Academician M. M. Dubinin, July 1, 1957)

Several authors have shown that when molecules of organic acids are adsorbed from solutions they orient themselves perpendicularly to the surface of the adsorbent. However, recently new hypotheses have been put forward with regard to the orientation of molecules of organic acids and of a number of other oxygen-containing organic compounds. Thus, Blackburn and Kipling [1], on the basis of investigations of the adsorption of organic acids from aqueous solutions on carbon black, have pointed out that molecules of organic acids may be adsorbed in the form of their dimers as well as mono- and dihydrates. Kiselev and Shikalova [2] have shown that phenol molecules may take up different positions with respect to the adsorbent surface.

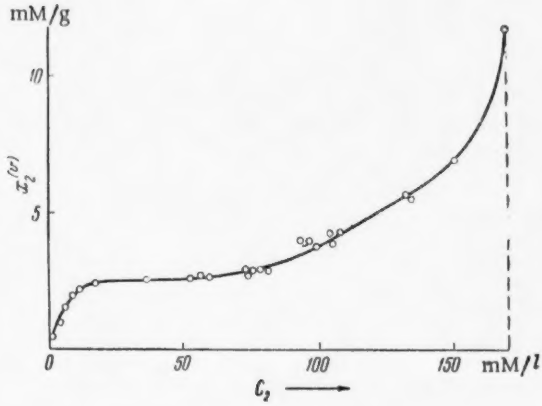

Fig. 1. Adsorption isotherm of formic acid on marl No. 120 from cetane solution at 60°.

The present investigation is devoted to the study of the effect of association of some organic acids on the nature of their adsorption from cetane and α-methylnaphthalene on natural and synthetic adsorbents. The adsorbents used were a highly active Volga marl (No. 120, from the region of Kamennyi Iar, Stalingrad) and an industrial specimen of silica gel KSK. The activity of these adsorbents has been studied by us in connection with certain technological processes [3-6]. The specific surface was determined from the adsorption of methanol vapor in a gravimetric adsorption apparatus. In the case of marl No. 120 the specific surface was 150 m^2/g, and for silica gel it was 285 m^2/g.

Cetane and α-methylnaphthalene were submitted to the requisite purification and, after being left in contact with the marl and silica gel, had the following constants: cetane, b. p. 152-153° (12 mm), m. p. 16-18°, d_4^{20}=0.7734, n_D^{20} = 1.4350; α-methylnaphthalene, b. p. 243-245° (760 mm), b. p. 130-132° (30 mm), n_D^{20} = 1.6131. Anhydrous formic acid was prepared from its 85% solution by prolonged drying over anhydrous copper sulfate, b. p. 100.5-101.5°, d_4^{20} = 1.2320, n_D^{20} = 1.3712. Anhydrous acetic acid was obtained from acetic anhydride and acetic acid, b. p. 118-118.5°, m. p. 16°, d_4^{20} = 1.0478, n_D^{20} = 1.3721. The adsorption experiments were carried out by the method adopted in the Laboratory of Adsorption of Moscow University [2], at a temperature of 60° and in some cases at 20°. Concentration of the acids was determined by means of interferometer ITR-2.

In Figs. 1 and 2 are plotted adsorption isotherms of formic acid from cetane. The solubility of formic acid in cetane is limited ($C_{s(HCOOH)}$ = 170 mM/l). Because of this the isotherm is S-shaped, a feature which is characteristic of adsorption from systems of limited mutual solubilities [7]. Calculation for point B gives the area occupied by a molecule of formic acid on the surface of marl, ω_{exp} = 10.4 A^2. Such a small area cannot be taken up by the molecule of HCOOH in any position with respect to the surface of marl. This discrepancy may be explained if we assume that the surface is covered by a monolayer of dimeric molecules of HCOOH oriented on the surface in the manner indicated below:

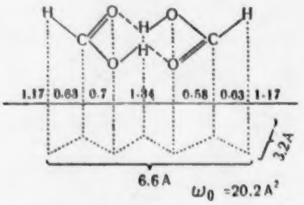

The bond lengths and atomic radii shown are taken from the literature [1, 8, 9]. In the case of this mode of orientation the value of 20.2 A^2 calculated is in good agreement with the value of 20.8 A^2 $(2 \cdot 10.4)$ obtained. For other positions of the dimer of formic acid on the surface the differences between the calculated and experimental values, ω_0 and ω_{exp}, are larger.

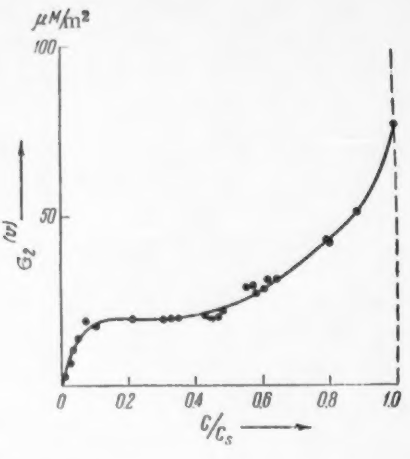

Fig. 2. Absolute adsorption isotherm of formic acid on marl No. 120 from cetane solution at 60°.

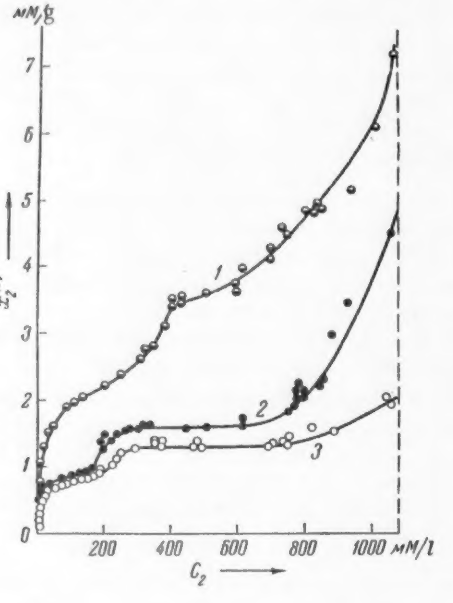

Fig. 3. Adsorption isotherm of acetic acid from cetane solutions on silica gel KSK at 20° (1) and on marl No. 120 at 20° (2) and at 60° (3).

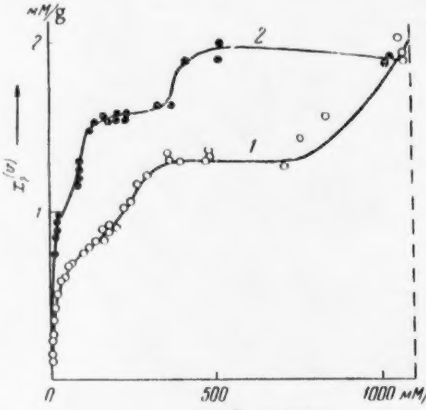

Fig. 4. Adsorption isotherm of acetic acid from cetane (1) and from α-methylnaphthalene (2) on marl No. 120 at 60°.

In Fig. 3 are plotted adsorption isotherms of acetic acid on marl No. 120 and silica gel KSK from cetane solution. The solubility of acetic acid in cetane is limited ($C_{s(CH_2COOH)}$ = 1080 mM/l). The isotherms appear wave-like. Each of the three isotherms has two inflections which are particularly sharply defined in the case of marl No. 120. The first inflection corresponds to coverage of the adsorbent surface with monomeric molecules of acetic acid which are evidently oriented parallel to the surface (ω_0 = 25.5 A^2; ω_{exp} = 33.3 A^2). If the molecules were oriented perpendicularly to the surface the area occupied by one molecule would be equal to 20.5 A^2. The second horizontal portion of the isotherm corresponds to coverage with dimeric molecules. The plane of the octahedron of the dimer, as also that of the dimer of formic acid, is perpendicular or inclined at an angle to the surface of the adsorbent, which position is, apparently, due to the distribution of neighboring rings. The experimental values obtained are in good agreement with those calculated (ω_{exp} = 31.2 A^2 and ω_0 = 31.5 A^2, respectively). The absence of the second horizontal portion on the adsorption isotherm of formic acid is due to the greater tendency of this acid towards association as compared with acetic acid.

In Fig. 4 are plotted the adsorption isotherms of acetic acid from cetane and from α-methylnaphthalene at 60°. Acetic acid is infinitely soluble in α-methylnaphthalene. The value of $x_2^{(v)}$ increases at first and thereafter decreases linearly. In Fig. 4 is shown only the initial portion of the isotherms up to $C_2 \approx 1000$ mM/l. At low equilibrium concentrations, $C_{2(CH_3COOH)}$, each curve has two inflections.

On the basis of the above results we suggest the following adsorption pattern for acetic acid from high molecular weight paraffinic and aromatic hydrocarbons on the surface of natural and synthetic silica adsorbents:

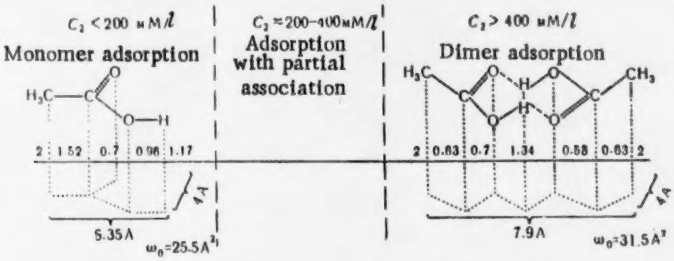

Thus, in view of the above results, which show that organic acids may undergo association during adsorption from nonpolar solvents and that this phenomenon affects the form of the adsorption isotherms, it is to be expected that similar association during adsorption may occur also with other compounds capable of forming dimeric and more complex molecules as a result of hydrogen bonding.

The author wishes to thank Prof. A. V. Kiselev for valuable advice and assistance in the present investigation.

LITERATURE CITED

[1] A. Blackburn and J. J. Kipling, J. Chem. Soc. 1955, 58, 496.

[2] A. V. Kiselev and I. V. Shikalova, J. Phys. Chem. 30, 94 (1956).

[3] N. N. Griazev, S. M. Rakhovskaia and B. N. Trakhtman, Electric Power Stations 12, 33 (1954).

[4] N. N. Griazev, S. M. Rakhovskaia, and B. N. Trakhtman, Trans. Road Res. Inst., Saratov, Vol. 2, 33 (1955).

[5] N. N. Griazev and S. M. Rakhovskaia, Sci. Annual Saratov State Univ. 1954, 570 (1955).

[6] N. N. Griazev and S. M. Rakhovskaia, Proc. 3rd Conf. on Adsorption at Moscow State Univ. 1957, p. 196.

[7] O. M. Dzhigit, A. V. Kiselev and K. G. Krasil'nikov, Proc. Acad. Sci. USSR 58, 413 (1947).

[8] J. D. Morrison and J. M. Robertson, J. Chem. Soc. 1949, 980, 987, 993, 1001.

[9] A. I. Kitaigorodskii, Crystallography of Organic Compounds, 1955.

Received June 29, 1957

M. V. Lomonosov State University, Moscow

ON THE INTERACTION OF OZONE WITH METHYL HYDROPEROXIDE

N. A. Kleimenov and A. B. Nalbandian

(Presented by Academician V. N. Kondrat'ev, July 6, 1957)

In our investigation of the oxidation of methane with atomic oxygen formed during thermal decomposition of ozone [1] we have shown that the ozone molecule does not react directly with methane prior to reaching its decomposition temperature. In the course of the investigation mentioned we found that in the scrubber where the intermediate reaction products were absorbed in distilled water, interaction took place between undecomposed ozone and methyl hydroperoxide, which at low temperatures is one of the main products of reaction. Other experimental conditions being equal, the yield of methyl hydroperoxide per 1 cc of the original reaction mixture was found to decrease continuously with extending duration of the experiment. The curve giving the yield of the hydroperoxide as a function of the duration of the experiment is illustrated in Fig. 1. As will be seen, after eight hours the yield of the peroxide decreased to less than $^1/_3$ of the initial concentration. The disappearance of methyl hydroperoxide in the solution was ascribed to the reaction

$$CH_3OOH + O_3 \rightarrow CH_3OH + 2O_2, \qquad (1)$$

which is analogous to the reaction of hydrogen peroxide with ozone [2], which leads to the formation of a molecule of water and two molecules of oxygen according to the over-all equation

$$H_2O_2 + O_3 \rightarrow H_2O + 2O_2. \qquad (2)$$

At the time of our investigation methyl alcohol, which is assumed to be the product of the interaction according to Eq. (1), was not identified. It was to be expected that similar interaction between the hydroperoxide and ozone would take place not only in the liquid but also in the vapor phase. Methyl hydroperoxide was prepared by methylation of hydrogen peroxide with dimethyl sulfate in alkaline solution [3]. In this way an approximately 80% aqueous solution of methyl hydroperoxide was obtained. The solution did not contain any hydrogen peroxide, as confirmed with tetravalent titanium.

The experimental procedure was as follows. Into the suction flask of 8.5 liter capacity, placed in a thermostat at the given temperature, was passed rapidly the given amount of the hydroperoxide followed by ozonized oxygen. In all experiments the concentration of ozone was 5-6 times as great as the concentration of hydroperoxide. In order to inhibit further interaction between the reagents, the gas, after determined reaction times, was passed rapidly into a second flask placed in melting ice. In order to separate unreacted peroxide from ozone the mixture was pumped slowly from the second flask through two successive traps at temperatures of −100° and of liquid nitrogen, respectively. In control experiments it was established that by this method separation of the hydroperoxide from ozone was quantitative.

The results of the experiments are plotted in Fig. 2. The points on curves 1, 2, 3, 4, and 5 represent experimentally determined concentrations of methyl hydroperoxide as functions of reaction time at temperatures of 25, 34, 43, 52, and 64°, respectively. The actual curves have been plotted by calculation on the assumption that in the presence of a large excess of ozone in the mixture the decrease in concentration of methyl hydroperoxide with time is expressed by the equation for a unimolecular reaction. As will be seen from Fig. 2, the experimental points fall, within the limits of experimental error, sufficiently close to the corresponding curves.

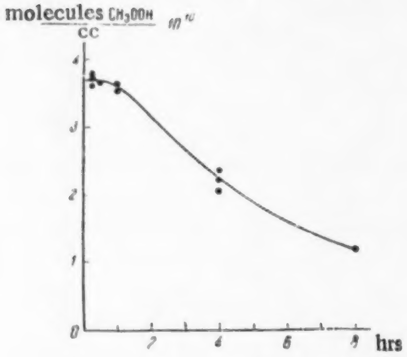

Fig. 1. Decrease in concentration of methyl hydroperoxide in solution, calculated on 1 cc of the reacted gas, as a function of the duration of the experiment.

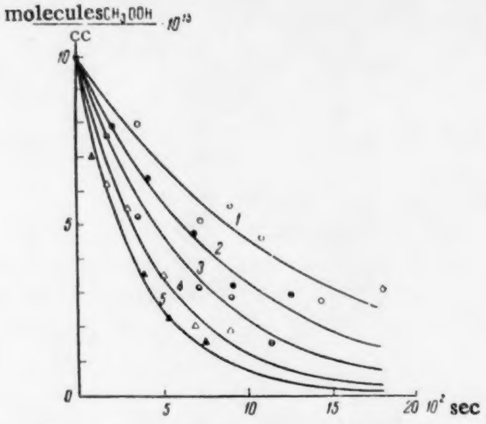

Fig. 2. Kinetics of the decrease in concentration of methyl hydroperoxide at different temperatures. 1) 25°, 2) 34°, 3) 43°, 4) 52°, 5) 64°.

From the kinetic curves in Fig. 2 we have calculated the following reaction velocity constants.

T, °C	K, sec
25	$7.7 \cdot 10^{-4}$
34	$1.12 \cdot 10^{-3}$
43	$1.5 \cdot 10^{-3}$
52	$2.12 \cdot 10^{-3}$
64	$2.8 \cdot 10^{-3}$

From the temperature dependence of the reaction velocity constant we have calculated the activation energy for the interaction of ozone with methyl hydroperoxide.

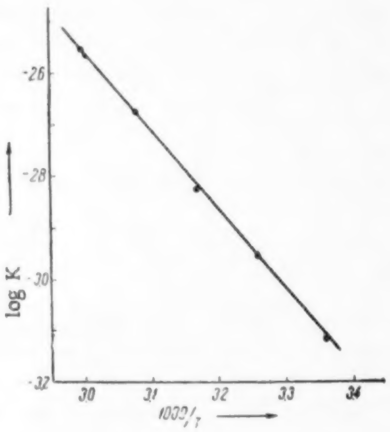

Fig. 3.

In Fig. 3 is shown the dependence of log K on 1/T. It will be seen that the experimental points come to lie close to the straight line, from the slope of which we have calculated a value of E = 7000 cal/mole for the activation energy.

From the set of kinetic curves illustrated in Fig. 2 it will be seen that while at a temperature of 25° a reaction time of 15 min is necessary in order to reduce the concentration of the peroxide by half, the corresponding time is only 2.5 min at 64°, while after 25 min practically all of the peroxide has reacted with ozone.

In addition to the experiments described we have also carried out a special investigation with the object of determining the main products of reaction between ozone and methyl hydroperoxide. Analysis of the reaction products has shown that the hydroperoxide is converted by ozone mainly to methyl alcohol, in agreement with the hypothesis expressed above. In the reaction products we have detected about 80% of methyl alcohol and about 6% formaldehyde. No other products were tested for. The alcohol was determined by the modified method of Guliaeva [4] based on esterification of methyl alcohol with nitrous acid. The formaldehyde was determined polarographically.

Schubert and Pease [5] have recently published a series of papers in which they described results of investigations of ozone-initiated oxidation of a number of hydrocarbons. The experiments were carried out either in static conditions with reaction times of many tens of minutes, or under flow conditions with fairly long contact times. The authors found that over the temperature range investigated (25-270°) the main reaction products were the corresponding alcohols which, in their view, are formed by the direct interaction of the ozone molecule with the hydrocarbon according to the following chain mechanism:

$$RH + O_3 \rightarrow RO + HO_2,$$
$$RO + RH \rightarrow ROH + R,$$
$$R + O_2 \rightarrow RO_2.$$

In the opinion of the authors, at low temperatures the radicals HO_2 and RO_2 decay without reacting further with the hydrocarbons. In the light of investigations described in our present communication, as well as on the basis of the paper [1] which was concerned with the oxidation of methane with atomic oxygen formed on thermal decomposition of ozone, the results obtained by Schubert and Pease may be interpreted in a different way.

The primary products of the oxidation of hydrocarbons in the presence of slowly decomposing ozone are the hydroperoxides of the corresponding hydrocarbons. However, the latter escape detection because during the comparatively long reaction time they are completely transformed into alcohols by the action of undecomposed ozone.

Comparison of the velocity constant of consumption of methyl hydroperoxide in its interaction with ozone with the velocity constant of consumption of ozone in its reaction with methane shows that the former constant is considerably higher.

The authors wish to express their sincere thanks to A. M. Markevich and L. F. Filippova for assistance in the experimental work.

LITERATURE CITED

[1] N. A. Kleimenov, I. N. Antonova, A. M. Markevich, and A. B. Nalbandian, J. Phys. Chem. 30, 794 (1956); J. Chim. Phys. No. 2392, 321 (1957).

[2] Abel, Monatsh. f. Chem. 86, 193 (1955).

[3] A. Rieche and F. Hitz, Ber. No. 8, 2485 (1929).

[4] A. I. Guliaeva et al., Analysis of the Products of Manufacture of Divinyl from Ethyl Alcohol by the S. V. Lebedev Method, 1950.*

[5] C. C. Schubert and R. N. Pease, J. Am. Chem. Soc. 78, 10, 2044 (1956); J. Chem. Phys. 24, 919 (1956); J. Am. Chem. Soc. 78, 21, 5553 (1956).

Received June 26, 1957

Institute of Chemical Physics, Academy of Sciences
of the USSR

---

* In Russian.

INVESTIGATION OF THE MECHANISM OF ELECTROLYTIC FORMATION AND DECOMPOSITION OF PERCARBONATE, PERBORATE AND PERPHOSPHATE BY THE ISOTOPE METHOD

I. F. Franchuk and A. I. Brodskii, Corresponding Member, Academy of Sciences, USSR

Earlier we have shown [1] that hydrogen peroxide does not take part in the anodic formation of persulfate and is not an intermediate product in the process, and also that during hydrolysis of persulfate,oxygen of the water does not take part in the formation of the hydrogen peroxide resulting from the decomposition. In the present work we have used heavy oxygen, O^{18}, to study the mechanism of anodic formation, hydrolysis and thermal decomposition of percarbonate, perborate and perphosphate.

Potassium percarbonate, $K_2C_2O_6$, was prepared [2] by electrolysis of a solution of 20-30 g of K_2CO_3 in 50 ml of H_2O^{18} with a current of 1.2-2 amp between platinum electrodes, at a cell temperature of from -10 to $-14°$. Samples of 1-2 ml were withdrawn periodicattly, degassed in vacuo and mixed with 1 : 3 sulfuric acid, also in vacuo. After removal of the CO_2 evolved, $KMnO_4$ was added to liberate peroxide oxygen. The content of O^{18} in the CO_2 and O_2 formed was determined by means of mass spectrograph MS-2. In control experiments it was established that no exchange reaction between the CO_2 and the electrolyte took place,and that under the given conditions oxygen of the $KMnO_4$ did not participate in the formation of the O_2 which was evolved. The results of one of these experiments as well as the results obtained in the electrolysis of $K_2CO_3^{18}$ (prepared by exchange reaction between K_2CO_3 and H_2O^{18}) in ordinary water are given in Table 1. The content of isotopic oxygen in CO_2 and O_2 is close to that in the original carbonate. This eliminates the participation of water in the formation of the percarbonate. The slow increase in O^{18} content in the course of electrolysis is due to exchange between water and carbonate under conditions of local overheating of electrolyte layers close to the electrode: when the current was switched off, the O^{18} content in peroxide oxygen did not change, while in CO_2 it increased by 0.05% in 4-6 hrs at $-6°$ and remained unchanged at $-15°$. The O^{18} content of CO_2 was always slightly higher than in O_2. This is due to the fact that in carbonate the exchange reaction proceeds throughout the duration of the experiment,whereas the isotopic oxygen content in the percarbonate is fixed at the moment of the formation of the latter, after

TABLE 1

Preparation of Potassium Percarbonate

Time, min	Electrolysis of K_2CO_3 in H_2O^{18} (1.100% O^{18})		Electrolysis: $K_2CO_3^{18}$ (0.714% O^{18}) in H_2O	
	Content of O^{18} in %			
	in K_2CO_3	in $K_2C_2O_6$	in K_2CO_3	in KC_2O_6
30	0.213	0.194	0.699	0.683
60	0.249	0.204	0.665	0.674
90	0.259	0.223	0.635	—
120	0.303	—	0.593	0.605
150	0.308	0.258		

which no further exchange takes place. If oxygen of the water were taking part in the formation of the percarbonate, the O^{18} content in the peracidic oxygen could not be lower than in CO_2. Exchange of oxygen between H_2O_2 and percarbonate proceeds very rapidly as a result of hydrolysis: the process is complete as soon as the solutions are mixed and a portion of the H_2O_2 is extracted with ether for isotope analysis. This made it impossible to apply the isotope dilution method used previously with the persulfate [1] to check the mechanism proposed by Glasstone and Hickling [3] involving the intermediate formation of H_2O_2. Haissinsky has shown [4] that this mechanism of anodic formation of percarbonate and perborate is doubtful. On the basis of all the evidence quoted it may be concluded that formation of percarbonate proceeds according to the equation $2CO_3^{2-} \longrightarrow C_2O_6^{2-} + 2e$.

Electrolytic formation of perborate in reasonable yields is possible only in the presence of percarbonate. It has been suggested [5] that the perborate is either formed directly at the anode, or that a percarbonate is formed first which then splits off H_2O_2 and passes it on to the borate [6]. In order to throw light on this problem we have carried out several electrolyses of a solution of 4 g of $Na_2B_4O_7^{18}$ and 12 g of Na_2CO_3 in 100 ml of H_2O^{18} (as well as of solutions of mixtures of $Na_2B_4O_7$ and $Na_2CO_3^{18}$ in ordinary water) at a temperature of +10 to +14° with a current of 2-3 amp between a platinum anode (1.9 cm^2) and a tin cathode (15 cm^2), with periodic determinations of isotopic oxygen content in the CO_2 from the carbonate and in peroxide oxygen. In addition we also determined the O^{18} content of the perborate, which precipitated on warming and was washed with water and dried. The results of two such experiments are given in Table 2. In interpreting these results it is necessary to bear in mind that isotopic oxygen content of the borax (or metaborate) is the same as that of water, due to very rapid exchange between the two. In all experiments the CO_2 and O_2 from the electrolyte and the O_2 from the perborate had similar O^{18} content (that of the CO_2 being somewhat higher) which, however, was much lower than that of water. This eliminates the participation of the oxygen of water in the formation of the perborate. The accumulation of O^{18} in CO_2 and in O_2 during electrolysis is not due to the presence of the borax; this was confirmed by the observation that in an experiment carried out under identical conditions, but without borax, accumulation of O^{18} proceeded to the same extent. As before, in the preparation of percarbonate, this phenomenon is due to exchange between water and carbonate, which in this case proceeded much faster because of the considerably higher temperature at which electrolysis was conducted. All this evidence leads us to conclude that formation of percarbonate is, in this case, the primary electrode process. It also follows from this that the electrolytic perborate obtained is the adduct of H_2O_2 to the borate and not a salt of the true peracid, since in the latter case the O^{18} content in the peroxide oxygen would be intermediate between that in water and that in the percarbonate: the structure of the adduct is, therefore, $NaBO_2 \cdot H_2O_2 \cdot 3H_2O$ and not $NaBO_3 \cdot 4H_2O$.

TABLE 2

Preparation of Sodium Perborate

Time, min	Electrolysis of a mixture of $Na_2B_4O_7^{18}$ (1.100% O^{18}) + + Na_2CO_3 in H_2O^{18} (1.100% O^{18})			Electrolysis of a mixture of $Na_2CO_3^{18}$ (0.983% O^{18}) + $Na_2B_4O_7$ in H_2O	
	Content of O^{18} in %				
	in Na_2CO_3	in peracidic oxygen	in solid perborate	in Na_2CO_3	in peracidic oxygen
30	0.363	—	—	0.831	0.881
60	0.521	0.410	—	0.758	0.799
90	0.645	—	—	0.697	0.723
120	0.719	0.640	—	0.620	0.630
150	0.758	0.712	0.688		

Potassium perphosphate, $K_4P_2O_8$, was prepared [7] by electrolysis of a mixture of 30 g of KH_2PO_4, 20 g of KOH, 0.036 g K_2CrO_4 and 12 g of KF in 100 ml of H_2O^{18} with a current of 4 amp at +10 to +14° during 2 hrs between a Pt-anode (1.9 cm^2) and a Sn-cathode (145 cm^2). The perphosphate was isolated by evaporation and was recrystallized from water and dried in vacuo. No O^{18} exchange between it and water was observed after 5 days at 20° or after 6 hrs at 100°. Heating the perphosphate gave oxygen with a normal isotope content (0.199-0.204% O^{18}), the O^{18} content of the water being 1.10%. Therefore, reaction mechanisms involving the participation of water [7] are out of question in this case. The formation of the perphosphate obviously proceeds in accordance with the equation $2PO_4^{3-} \rightarrow P_2O_8^{4-} + 2e$.

TABLE 3

Hydrolysis of Salts of Peracids

Salt	Content of O^{18} in %		
	in the salt	in water	in H_2O_2
Potassium percarbonate	0.591	0.204	0.586
The same	0.204	1.100	0.194
Sodium perborate	0.204	1.100	0.199
" "	0.654	0.204	0.660
Potassium perphosphate	0.204	1.100	0.199

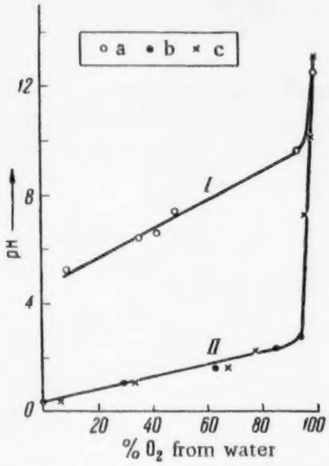

Fig. 1. Dependence on pH of O^{18} content of oxygen obtained by decomposition of perphosphate and persulfate in H_2O^{18}. I) Our results for perphosphate at 120° (a), II) results of Kolthoff and Miller for persulfate at 50° (b) and 90° (c).

Hydrolysis of percarbonate and perborate was effected at 20-30° in H_2O^{18} with dilute sulfuric acid. We have also carried out the hydrolysis of the "heavy" salts, obtained electrolytically, in ordinary water: $K_2CO_3^{18}$ and $Na_2CO_3^{18} + Na_2B_4O_7^{18}$. Hydrolysis of perphosphate was effected at 60° in a saturated solution in H_2O^{18} to which $^1/_4$ by volume of H_2SO_4 was added. The H_2O_2 formed was removed under vacuum. In all hydrolysis experiments (Table 3) the O^{18} content of the oxygen in the hydrogen peroxide was the same as that in the peroxide oxygen in the salt, irrespective of the O^{18} content of the water. Thus, during hydrolysis of the percarbonate, perborate and perphosphate the peroxide group O—O passes without disruption into the H_2O_2 formed, as has already been shown earlier [1] in the case of the hydrolysis of persulfate. These results point to the following mechanism

$$^{-}OC(O)O-O\,\boxed{C(O)O^{-}+H\overset{*}{O}}\,H \rightarrow$$

$$\rightarrow {}^{-}OC(O)O-O^{-}+HC\overset{*}{O}_3+H^{+}$$

$$H\,\boxed{\overset{*}{O}H+{}^{-}OC(O)}\,O-O^{-}+H^{+}\rightarrow H_2O_2+HC\overset{*}{O}{}_3^{-}$$

for the percarbonate and to a similar one for the perphosphate. In the case of the perborate it would be more correct to speak not of hydrolysis but of the splitting off of H_2O_2 attached as a molecular entity. This process takes place very rapidly since perborate exchanges oxygen with H_2O_2 extremely rapidly.

Thermal decomposition of percarbonate and perborate in H_2O^{18} gives oxygen of normal isotope content. This was to be expected since both salts split off free H_2O_2 in solution; as is well known from investigations of other workers, oxygen of this hydrogen peroxide does not contain oxygen originating from the water. A different course is followed in the decomposition in H_2O^{18} of perphosphate, which undergoes hydrolysis at a much slower rate. In this case the oxygen obtained has a composition which depends on the pH of the solution. Decomposition of 0.01 molar solution of $K_4P_2O_8$ in H_2O^{18} with varying amounts of H_3PO_4 or KOH was carried out in sealed ampoules at 120° after previous removal of dissolved gases by evacuation. The liberated oxygen was analyzed by means of the mass-spectrograph. The pH was measured by means of the glass electrode. The dependence of the composition of the oxygen on pH is represented by curve I in Fig. 1. At a pH of 5.2, 81% of it originates from the perphosphate (0.283% of O^{18}, with 1.11% of O^{18} in water), while at a pH of 12.4 it originates entirely from the water (1.09%). The curve has the same shape as that obtained by Kolthoff and Miller [8] for thermal decomposition of persulfate at 50° and 90° (Fig. 1, curve II), but is displaced by several pH units. The similarity of the curves leads us to assume an identical mechanism of decomposition, although the mechanism proposed by the authors in the case of the persulfate is inapplicable to the perphosphate. According to that mechanism, decomposition of persulfate proceeds along two parallel lines: in one case it is independent of pH, [$S_2O_8^{2-} \xrightarrow{k_1} 2SO_4^{\cdot -}$ (slow)] and in the other it is catalyzed, [$S_2O_8^{2-} + H^+ \xrightarrow{k_2} SO_4 + HSO_4^-$ (slow)], from which it follows that the ratio of persulfate oxygen to that originating from the water is equal to $k_2[H^+]/k_1$. Our data for the persulfate show that the ratio k_2/k_1 changes, within the pH range investigated, by two orders of magnitude, instead of remaining constant.

We found that at room temperature no oxygen exchange took place after 8 hrs between perphosphate and $H_2O_2^{18}$, in contrast to the very rapid exchange between the latter and percarbonate and perborate.

LITERATURE CITED

[1] A. I. Brodskii, I. F. Franchuk, and V. A. Lunenok-Burmakina, Proc. Acad. Sci. USSR 115, 5 (1957).*

[2] E. J. Constam and A. Hansen, Zs. f. Elektrochem. 3, 137 (1896).

[3] S. Glasstone and A. Hickling, Electrolytic Oxidation and Reduction, London, 1935.

[4] M. Haissinsky, Trans. Farad. Soc., Discussion,No. 1, 254 (1947).

[5] K. Arndt and E. Hantge, Zs. f. Elektrochem. 28, 263 (1922).

[6] F. Fichter and W. Bladergroen, Helv. Chim. Acta 10, 566 (1927); F. Foerster, Zs. angew. Chem. 34, 354 (1921).

[7] F. Fichter and E. Gutzwiller, Helv. Chim. Acta 11, 323 (1928); F. Fichter and A. R. Mira, Helv. Chim. Acta 2, 3 (1919).

[8] I. M. Kolthoff and I. K. Miller, J. Am. Chem. Soc. 73, 3055 (1951).

Received August 12, 1957

L. V. Pisarzhevskii Institute of Physical Chemistry,
Academy of Sciences of the Ukrainian SSR

---

* See C. B. translation.

THE FREE ENERGY, HEAT AND ENTROPY OF THE ADSORPTIONAL DISPLACEMENT OF ALCOHOLS BY WATER FROM THE SURFACE OF AN OXIDE CATALYST

Academician A. A. Balandin, O. K. Bogdanova, and A. P. Shcheglova

For a number of alcohols, the kinetics of dehydrogenation on a mixed oxide catalyst have been studied in the papers of [1]. It was shown that dehydrogenation proceeded on the catalyst without a detectable formation of products from the decomposition and dehydration of the alcohols. Relative adsorption coefficients for the reaction products were determined. It was also found that the relative adsorption coefficient of hydrogen was essentially equal to zero whereas the relative adsorption coefficients of the aldehydes were functions of the temperature and diminished as the temperature increased.

TABLE 1

The Dehydrogenation of Binary Alcohol–Water Mixtures

Expt. no.	Temperature, °C	Amount of H_2 at STP in ml/5 min	Gas analysis (% by volume)		
			CO_2	C_nH_{2n}	H_2
n-Propyl alcohol – water					
534	307	10.9	nil	nil	99.9
535	320	19.4	0.4	0.2	99.4
538	326	20.7	0.4	0.2	99.4
536	342	36.1	1.2	0.2	98.6
537	357	52.2	1.4	0.2	98.4
n-Butyl alcohol – water					
539	302	8.6	nil	nil	99.9
540	322	15.5	0.4	nil	99.6
541	340	30.5	0.8	0.2	99.0
542	360	51.0	0.8	0.6	98.6
n-Hexyl alcohol – water					
550	302	11.5	nil	nil	100
547	320.5	26.0	0.6	"	99.4
548	340	52.0	0.8	"	99.2
549	360	83.0	0.8	0.2	99.0

The present work is a study of the kinetics of the dehydrogenation on this same oxide catalyst of binary mixtures of water and primary alcohols of normal structure. In this study it was proposed to determine values of the relative adsorption coefficient of water and to investigate the dependence of this quantity on the length of the carbon chain in the alcohol. The investigation of these adsorption coefficients is of interest in connection with the surface orientation of the molecules. n-Propyl, n-butyl and n-hexyl alcohols were selected for this work. Prior to experiment, these alcohols were dried with magnesium methylate [2] and distilled in a fractionating column. These alcohols had the following constants: n-propyl alcohol; b. p. 97-97.2°, d_4^{20} 0.8044, n_D^{20} 1.3858; n-butyl alcohol; b. p. 117-117.5°, d_4^{20} 0.8098, n_D^{20} 1.3992; n-hexyl alcohol, b. p. 155.1-155.8°, d_4^{20} 0.8196, n_D^{20} 1.4188.

The initial alcohol–water mixtures were obtained by adding water to weighed amounts of the alcohols. In the preparation of these mixtures, a limit was placed on the selection of concentrations by the limited intersolubility of the components. In the experiments with n-propyl and n-butyl alcohols, the mixtures contained 34.2 mole% of water, and in the experiments with n-hexyl alcohol, 17.1 mole%. The experiments were carried out by a flow method and under the same conditions as in [1]. The reaction rate was determined from the evolution of hydrogen, which proceeded at constant velocity; analysis showed that the evolved gas contained small quantities of CO_2 and unidentified hydrocarbons in an amount not exceeding 2% (Table 1). Experiments were carried out over the temperature interval 300-360° at an introduction rate amounting to 1.05 ml per 5 min for mixtures containing propyl and butyl alcohols and to 1.4 ml per 5 min for mixtures of the hexyl alcohol. The resulting data are presented in Table 1, the arrangement being in order of increasing temperatures. In Table 2, values are shown for the relative adsorption coefficients of water, z_4, these having been calculated from the experimental data through the equation [3]:

TABLE 2

The Dehydrogenation of Binary Alcohol − Water Mixtures. Relative Adsorption Coefficients of Water, Calculated from Equation (1)

Mixture	Temperature, °C	m_0 ($p = 100$) mole%	m ($p = 65.8$) mole%	z	$-\Delta F$, $\frac{\text{cal}}{\text{mole}}$	$-\Delta H$, $\frac{\text{kcal}}{\text{mole}}$	$-\Delta S$, $\frac{\text{cal}}{\text{deg} \cdot \text{mole}}$
n-Propyl alcohol−H_2O	307	31	10.9	3.5	1440	16.2	26.0
	326	45	20.7	2.25	960		
	342	60	36.1	1.27	290		
	357	77	52.2	0.9	130		
n-Butyl alcohol−H_2O	302	25	8.6	3.6	1460	16.4	26.0
	320	35	15.5	2.42	1040		
	341	52	30.5	1.34	360		
	360	75	51.0	0.9	130		
			$p = 82.9$ mole%				
n-Hexyl alcohol−H_2O	302	28	14.5	3.7	1490	16.4	26.1
	320.5	43	26.0	2.48	1070		
	340	70	52.0	1.36	370		
	360	102	83.0	0.9	140		

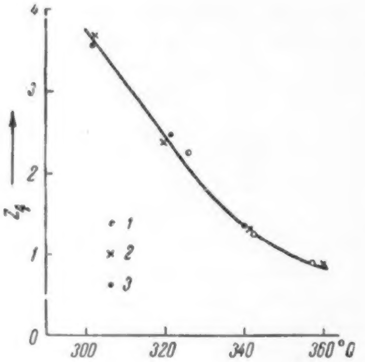

Fig. 1. The temperature dependence of values of z_4 for mixtures of various alcohols with water: 1) n-propyl alcohol; 2) n-butyl alcohol; 3) n-hexyl alcohol.

$$z_4 = \left(\frac{m_0}{m} - z\right) \Big/ \left(\frac{100}{p} - 1\right). \tag{1}$$

From the data which have been presented it is to be seen that the relative adsorption coefficient for water depends on the temperature, its value dimishing as the temperature rises. At fixed temperature, a comparison of the rates of alcohol dehydrogenation as observed with alcohol−water mixtures and with pure alcohols (m and m_0, Table 2) shows that the rate of dehydrogenation at 320° is decreased by more than 45% by the addition of water. This retarding action of the water gradually diminishes with increasing temperature. It can thus be concluded that water vapors are adsorbed by the catalyst and that this adsorption is more pronounced, the lower the temperature. Over the investigated temperature interval, the values of the adsorption coefficients of water on the active catalyst centers prove to be 1.3-3.5 times larger than those for alcohol. Figure 1 shows the values of z_4 for the investigated alcohols at various temperatures. It is to be seen from Table 2 that the values of the relative adsorption coefficient of water are approximately the same when calculated from the experimental data on n-propyl, n-butyl and n-hexyl alcohols. Applying the earlier derived equation [4, 5],

$$\Delta F = -RT \ln z_4, \tag{2}$$

to the experimental data, we find the free energy change for the adsorptional displacement by water of the alcohol on the active surface of the catalyst (see Table 2). In a plot of log z_4 vs 1/T (Fig. 2), the experimental points fall on a straight line. From this there were calculated the change in heat content, ΔH, and in entropy, ΔS, for the adsorptional displacement by water vapor of alcohols on the active catalyst surface (see Table 2).

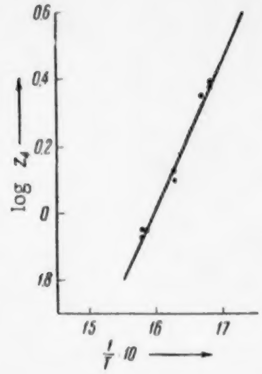

Fig. 2. The dependence of log z_4 on the reciprocal absolute temperature.

Since

$$z_4 = \frac{a_w}{a_{al_1}} = \frac{a_w}{a_{al_2}}, \tag{3}$$

where a_w, a_{al_1} and a_{al_2} are the constants for the adsorption equilibria of water and of the first and the second alcohols, respectively, it follows that

$$\frac{a_{al_2}}{a_{al_1}} = 1, \tag{4}$$

and thus in this case the adsorption coefficients of the alcohols are identical. In its turn, this identity of the adsorption coefficients points to an identical orientation of the molecules of the investigated alcohols with respect to the active centers on the catalyst surface.

On the basis of our experimental data it can be concluded that the dehydrogenation of alcohols on an oxide catalyst is to a considerable degree retarded by water; the absolute adsorption coefficients of water—alcohols for primary alcohols of normal structure are functions of temperature and do not depend on the length of the alcohol carbon chain.

LITERATURE CITED

[1] O. K. Bogdanova, A. A. Balandin, and A. P. Shcheglova, Bull. Acad. Sci. USSR, Div. Chem. Sci. 1957,* 788, 795.

[2] H. Lund and J. Bjerrum, Ber. 64, 210 (1931); 56, 894 (1923).

[3] O. K. Bogdanova, A. A. Balandin, and A. P. Shcheglova, Bull. Acad. Sci. USSR, Div. Chem. Sci. 1946, 497.

[4] O. K. Bogdanova, A. A. Balandin, and A. P. Shcheglova, Bull. Acad. Sci. USSR, Div. Chem. Sci. 1955,* 723.

[5] A. A. Balandin, Proc. Acad. Sci. USSR 63, 33 (1948).

Received October 23, 1957

The N. D. Zelinski Institute of Organic Chemistry
of the Academy of Sciences of the USSR

---

* Original Russian pagination. See C. B. translation.

THE ISOTOPIC EXCHANGE BETWEEN GASEOUS HYDROGEN AND SOLID POLYMERS UNDER THE ACTION OF NUCLEAR RADIATIONS

Ia. M. Varshavskii, G. Ia. Vasil'ev, V. L. Karpov,
Iu. S. Lazurkin, and I. Ia. Petrov

(Presented by Academician V. A. Kargin, June 24, 1957)

It is known [1] that the irradiation of polymeric hydrocarbons is accompanied by the evolution of gaseous products containing hydrogen as the principal constituent. Interest attaches to the question of the reversibility of these processes, i. e., to the possibility of the intrusion of hydrogen from the gaseous phase into the polymer molecules during irradiation. We have made the attempt to elucidate this question, following the method of tagged atoms and using deuterium. The isotopic exchange between gaseous deuterium and various solid polymers was studied in the radiation field of the nuclear reactor.

TABLE 1

Substance	Dose, M_{rad}	Conc. of deuterium in polymer (mole%)
Polyethylene	400	0.18
Polypropylene	400	0.18
Polystyrol	800	0.07
Divinyl rubber	400	0.06
Polymethylmethacrylate	50	0.02

The following polymers of the vinyl series were studied: 1) Polyethylene; nonplasticized; a film of 0.1 mm thickness. 2) Polypropylene; obtained by catalytic polymerization; plasticizing temperature, 110-130°; powder. 3) Polystyrene; obtained by emulsion polymerization; flow temperature, 175°; powder. 4) Divinyl rubber; obtained by unit polymerization; without addition of an anti-ager; small pieces (2-3 mm). 5) Polymethylmethacrylate; obtained by emulsion polymerization; powder.

The charge of test polymer (~ 0.6 g) was introduced into a glass ampule of 50-70 ml volume, after which the ampule was evacuated, filled with gaseous deuterium (~ 99.6%), cooled in liquid air and sealed (the cooling being aimed at increasing the amount of deuterium in the ampule). The loaded ampules were placed in a cage of thin aluminum wire and were subjected to irradiation in a water cooled, water modulated reactor. In order to diminish radiational heating, the canal was filled with water to the level of the active zone. At the maximum differential dosage, the temperature of the water in the canal did not exceed 60°.

Under the experimental conditions, the theoretical equilibrium concentration of deuterium in the polymer (i. e., the concentration calculated on the supposition that isotopic exchange proceeds to equilibrium and that the coefficient of distribution of deuterium between the C—H and H—H bonds is approximately equal to 3 [2]) amounts to approximately 5-7 mole%. In Table 1 there are shown the deuterium concentrations of each of the polymers as actually measured after irradiation.

Following the falling drop method, the deuterium concentration of the polymer was determined by burning it in an atmosphere of oxygen and measuring the deuterium content of the water resulting from the combustion. For each substance four combustions were carried out. The results of these parallel measurements did not differ by more than 0.02%. Mean values are shown in Table 1. Over the investigated range of deuterium concentrations (0.02-0.2 mole%), the absolute precision of the falling drop method of isotopic analysis amounts to ± 0.01-0 02%.

For each polymer separately it was proven that the intrusion of deuterium was not related to the adsorption of the gaseous material. Control experiments which were set up for this purpose showed that in the absence of irradiation, deuterium could not be detected in the polymer. In order to establish that irradiation did not activate the adsorption of deuterium on the polymer surface and that the penetration of deuterium was caused by the isotopic exchange, separate charges of each irradiated material were desorbed prior to combustion by being pumped out in high vacuum at 100-150° for 10-20 hours. The percentage of deuterium in the polymer did not change as a result of such treatment.

The observed effects obviously result from chemical interaction between the polymer molecules and the molecules of deuterium; furthermore this reaction must take place under the action of the radiation since it is known that without irradiation isotopic hydrogen exchange does not occur under the indicated conditions.

Of the investigated polymers, the largest amounts of deuterium intruded into polyethylene and polypropylene. A somewhat slower exchange occurred with polybutadiene and polystyrene, and with polymethylmethacrylate it was impossible to detect any sign of exchange. All four of the polymers for which there was a detectable exchange belong to the class of substances in which cross-linkages arise under the action of radiation. For polyethylene there is presently accepted a mechanism according to which this process precedes through free radicals; thus

$$R - CH_2 - R_1 \rightsquigarrow R - \dot{C}H - R_1 + H\cdot$$

It is quite likely that in our case the intrusion of deuterium into a polymer occurred as the result of a reaction between the polymer radicals and molecular deuterium:

$$\dot{R} + D_2 \longrightarrow RD + D, \qquad (I)$$

$$RH + D \longrightarrow \dot{R} + HD \qquad (II)$$

etc. In the polymer the equilibrium concentration of dissolved deuterium is of the order of 10^{-6} moles/g [4]. Thus a mechanism in which the initial step would be the reaction $D_2 \rightarrow D + D$ is less likely than is the mechanism represented by (I) and (II). It should be noted that these experiments were carried out under heterogeneous conditions so that the quantity of deuterium in the polymer could not serve as a factor uniquely characterizing the probability of the processes (I) and (II). To a first approximation, however, such a relationship can be assumed and certain qualitative conclusions may then be drawn.

The possibility is not to be excluded that the observed intrusion of deuterium into the polymer molecules resulted in some measure from isotopic exchange between the gaseous deuterium and free radicals. This type of exchange in the gaseous phase has been studied by Voevodskii and his collaborators [5].

A comparison of the amounts of deuterium which intruded into polyethylene and polybutadiene shows that combination of hydrogen does not take place at the double bonds. The comparatively weak exchange in the case of polystyrene can be explained by the high radiational stability of this substance, i. e., by the low yield of radicals.

The absence of exchange in polymethylmethacrylate could be related to the fact that the radicals which are formed cannot participate in Reaction (I) because of steric hindrances, although it is not impossible that it resulted from an inadequate radiational dosage.

LITERATURE CITED

[1] a) V. L. Karpov, Session of Acad. Sci. USSR on Peaceful Applications of Atomic Energy, July 1-5, 1955, Sec. Chem. Sci., Acad. Sci. USSR Press, 1955, p. 11; b) I. Ia. Petrov and V. L. Karpov, Trans. 1st Conference on Radiation Chemistry, Acad. Sci. USSR Press (in press).

[2] Ia. M. Varshavskii and S. E. Vaisberg, Proc. Acad. Sci. USSR 100, 97 (1955); J. Phys. Chem. 29, 523 (1955).

[3] A. I. Shatenshtein and Ia. M. Varshavskii, J. Anal. Chem. 11, 746 (1956).*

[4] R. M. Barrer, Trans. Farad. Soc. 35, 628, 644 (1939).

[5] V. V. Voevodskii, Free Radicals in Gaseous Chain Reactions (in Russian), Doctoral Dissertation, Inst. Chem. Phys., Acad. Sci. USSR, Moscow, 1955.

Received June 24, 1957

---

* Original Russian pagination. See C.B. Translation.

ADSORPTION FROM THREE-COMPONENT SOLUTIONS

N. N. Griazev

(Presented by Academician M. M. Dubinin, July 1, 1957)

There is in the literature a large amount of work devoted to the study of adsorption from binary solutions of certain organic materials onto various adsorbents. The study of the ternary systems is considerably more involved. The few published investigations present only isolated points and these are for the most part at low, uniform concentrations [1-3]. Here the concentration of one of the components of the mixture has been held essentially constant.

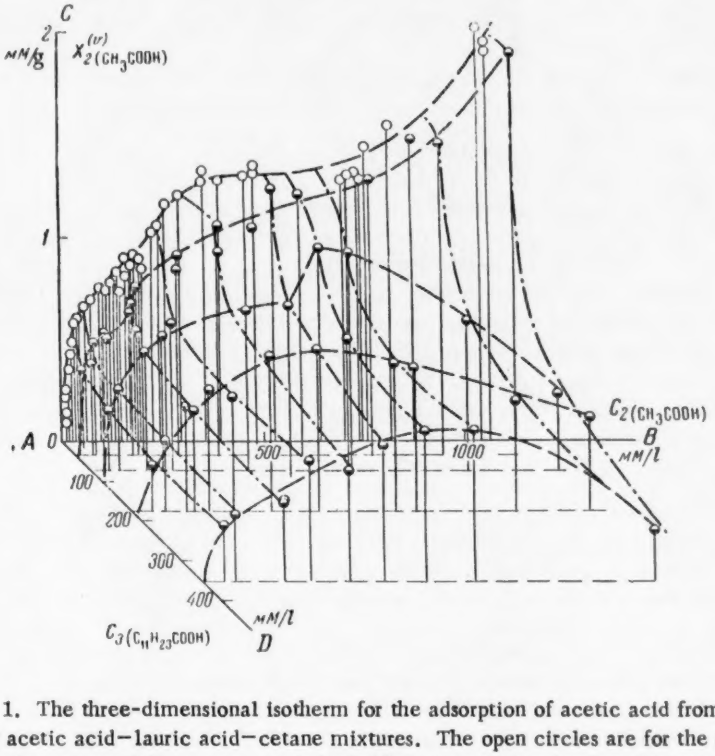

Fig. 1. The three-dimensional isotherm for the adsorption of acetic acid from ternary acetic acid–lauric acid–cetane mixtures. The open circles are for the adsorption of acetic acid from cetane and the half-shaded circles, for the adsorption of acetic acid from ternary mixtures.

Working over a wide interval of concentrations, we have developed adsorption isotherms for ternary systems and have constructed three-dimensional adsorption isotherms for them. In this work there are presented results on adsorption from the three component system acetic acid–lauric acid–cetane. One of the most active of the Volga diatomites (No. 120, from the neighborhood of the village of Kamennyi Iar, Stalingrad Oblast) [3] was used as the adsorbent. Its surface, determined gravimetrically from the adsorption of methanol vapors, proved to be equal to 150 m^2/g. The cetane and acetic acid were subjected to purification (see [4]). The lauric acid had a

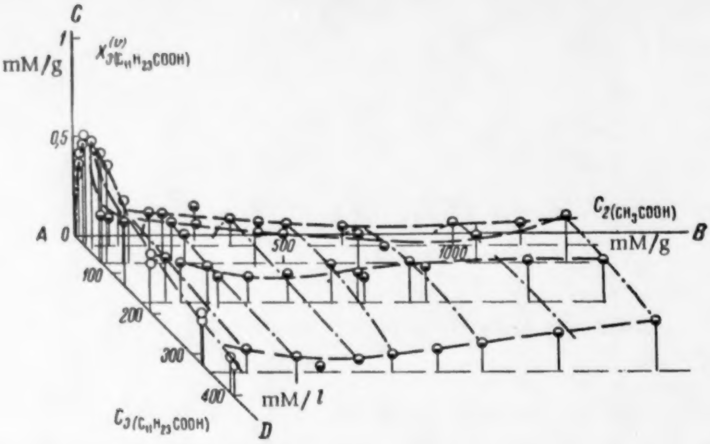

Fig. 2. The three-dimensional isotherm for the adsorption of lauric acid from ternary mixtures. The open circles are for the adsorption of lauric acid from cetane and the half-shaded circles, for the adsorption of lauric acid from ternary mixtures.

melting temperature of 43-44°. These adsorption experiments were carried out according to the technique which has been adopted in the Adsorption Laboratory of the Moscow State University [5].

Much attention was given to the analysis of the three component mixtures. In view of the fact that only binary mixtures can be analyzed with the aid of the interferometer, a special technique was developed for the analysis of these ternary mixtures. In this development use was made of differences in the solubilities of the components in water. Acetic acid passes completely into an aqueous layer, whereas the solubility of cetane and lauric acid in water is so infinitesimal as to be practically without influence on the recording of even such a sensitive instrument as the interferometer. The tests which were carried out confirmed that over the interval of concentrations which is of interest to us, neither cetane nor lauric acid will dissolve in an aqueous solution of acetic acid. After a number of refinements, the analyses were finally performed in the following manner. To 5 ml of the mixture which was under investigation there was added 25 ml of distilled water. The resulting mixture was shaken on a mechanical agitator at room temperature for 30 min. The aqueous layer was then separated, centrifuged and its content of acetic acid determined on an ITR-2 interferometer. The amount of lauric acid remaining in the cetane after centrifuging was also determined on the interferometer.

In Fig. 1 there is shown a three-dimensional isotherm for the adsorption of acetic acid from ternary acetic acid—lauric acid—cetane mixtures. On the CAB plane there is sketched the isotherm for the adsorption of acetic acid from cetane (in the absence of lauric acid). The wave form of this curve has been interpreted by us in a preceding work [4]. The presence of the lauric acid has a pronounced effect on both the magnitude of the adsorption and the form of the isotherm (at C_2 = const and C_3 = const). The points which are distributed over the space bounded by the coordinates ABCD indicate the magnitude of the adsorption, $X_2^{(v)}$, of acetic acid from ternary mixtures. In the adsorption of CH_3COOH alone from cetane or in the presence of low concentrations of $C_{11}H_{23}COOH$ ($C_3 <$ < 100 mmoles/liter), the isotherms are S-shaped (system of limited solubility). At higher values of C_3, the system under study becomes infinitely soluble and an isotherm with C_3 = const passes through a maximum. As the equivalent concentration of the lauric acid is increased, the adsorption diminishes, falling quite markedly when $C_3 \approx 100\text{-}200$ mmoles/liter.

In Fig. 2 there are presented values of $X_3^{(v)}$ for these same ternary mixtures. On the plane CAD there is plotted the isotherm for the adsorption of lauric acid from cetane (in the absence of acetic acid). Since lauric acid is infinitely soluble in cetane, this isotherm passes through a maximum and then gradually falls. The points which are distributed in the region bounded by the coordinates ABCD indicate the magnitude of the adsorption, $X_3^{(v)}$, of lauric acid from ternary mixtures. At small values of C_2 and C_3, the adsorption of lauric acid falls rather rapidly, but then increases with increasing C_2 (at C_3 = const), as a result of the diminution of the adsorption of

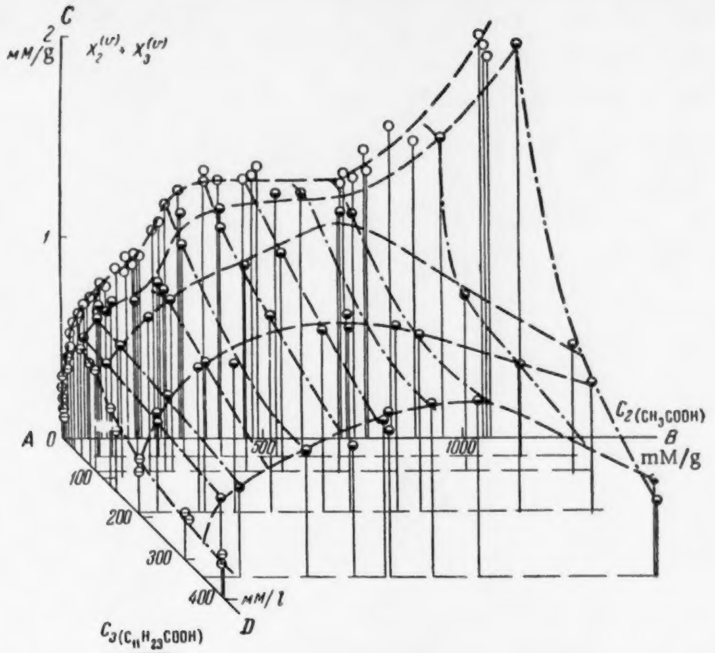

Fig. 3. The three-dimensional isotherm for the adsorption of acetic and lauric acids from ternary mixtures. The open circles are for the adsorption of acetic acid from cetane, the divided circles, for the adsorption of lauric acid from cetane and the half-shaded circles for the adsorption of acetic and lauric acids from cetane.

acetic acid (see Fig. 1). With C_2 = const, $X^{(v)}$ passes through a maximum and the character of the adsorption isotherm is the same as in the absence of acetic acid. On each of these isotherms, the maximum falls lower than is the case in the adsorption of lauric acid alone.

In Fig. 3 there is shown the isotherm for the adsorption of both acids from ternary mixtures. On the axis AC there is plotted the sum of $X_2^{(v)}$ and $X_3^{(v)}$. On the planes CAB and CAD, respectively, there have been plotted the isotherms for the adsorption of acetic acid and of lauric acid out of binary mixtures with cetane. Qualitatively, the general character of the adsorption isotherms for C_2 = const or C_3 = const remains the same as in Fig. 1. This is to be explained by the fact that the adsorption of lauric acid. An analogous alteration is to be observed in the character of the isotherms with C_3 = const., these changing from S-shaped curves (system of limited solubility) over to curves passing through maxima (system of unlimited solubility).

Thus adsorption from three component solutions has been studied over a wide interval of equivalent concentrations and it has been shown that mutual limitations on the adsorption of all of the components in a mixture exert an influence on both the magnitude of the adsorption and the character of the adsorption isotherms.

The author expresses his indebtedness for the valuable advice and assistance which Prof. A. V. Kiselev has given him in this work.

LITERATURE CITED

[1] N. F. Ermolenko, Bull. Acad. Sci. USSR 3, 229 (1949).

[2] G. Papps and D. F. Othmer, Ind. and Eng. Chem. 5, 430 (1944).

[3] N. N. Griazev and S. M. Rakhovskaia, Symposium, Conference on Adsorption at Moscow State University, 1957, p. 196.

[4] N. N. Griazev, Proc. Acad. Sci. USSR 118, 1 (1958).*

[5] A. V. Kiselev and I. V. Shikalova, J. Phys. Chem. 30, 94 (1956).

Received June 29, 1957

The M. V. Lomonosov State University, Moscow

---

* See C. B. translation.

THE INFLUENCE OF THE ADDITION OF ACIDS ON THE KINETICS OF ACYLATION OF AN AROMATIC AMINE IN AN INERT SOLVENT

L. M. Litvinenko and D. M. Aleksandrova

(Presented by Academician V. N. Kondrat'ev, August 16, 1957)

A study of the kinetics of the acylation of a number of aromatic amines, undertaken by one of the authors of the present work with a view to explaining the influence of spatial factors [1-5] on the amine reactivity, showed this reaction to be sensitive to the medium in which it takes place. Considering this detail to be of interest for the theory and practice of organic chemistry, and taking into account the fact that, in so far as is known to us, the acylation reaction has not been studied from this point of view, we have undertaken an investigation of this problem. In the present communication there are outlined the results of a study of the influence of small additions of benzoic acid on the rate of acylation of aniline by benzoyl chloride and by benzoic anhydride in benzene solution. The experimental technique has been described in [1].

It has been established that the acylation of aromatic amines by acid chlorides and anhydrides of organic acids proceeds according to the two following equations:

$$\mathrm{RCOCl} + 2\mathrm{ArNH_2} \longrightarrow \mathrm{RCONHAr} + \mathrm{ArNH_2 \cdot HCl} \qquad \text{(A)}$$

$$\mathrm{(RCO)_2O} + \mathrm{ArNH_2} \longrightarrow \mathrm{RCONHAr} + \mathrm{RCOOH}. \qquad \text{(B)}$$

Ebel [6] and Hinshelwood and his collaborators [7-10] have shown that when the acylation of aniline and its simplest derivatives by an acid chloride is carried out in an inert solvent, the molecule of HCl which is evolved in the initial step of the reaction immediately unites with a second molecule of the amine to form a completely insoluble salt which is totally unreactive in comparison with the acylating agent. In order to be convinced that the loss in reactivity results here from the formation of the salt and not from the poor solubility of this latter in benzene, we studied the kinetics of the acylation of 4-amino-4'-nitro-2,2'-diisopropoxybiphenyl [4] and its acid chloride, a compound which is readily soluble in benzene. It turned out that the velocity constant for the acylation of the salt (by n-nitrobenzoylchloride) is only about $^1/_{20}$ as large as that for the amine itself, the values of k_{25} being 0.0024 and 0.0451 liter/mole · sec. Thus hydrochloric acid serves to deactivate the aromatic amine for acylation.

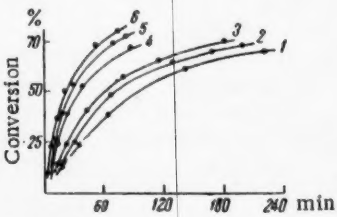

Fig. 1. Kinetic curves for the reaction of aniline with benzoyl chloride at various values of m: 0 (1); 0.0025 (2); 0.005 (3); 0.025 (4); 0.05 (5); 0.1 (6); a = = 0.00125; b = 0.0025; t = 25°.

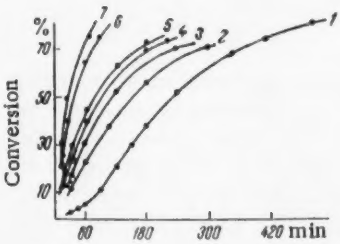

Fig. 2. Kinetic curves for the reaction of aniline with benzoic anhydride at various values of m: 0 (1); 0.001 (2); 0.0025 (3); 0.005 (4); 0.01 (5); 0.05 (6); 0.1 (7). a = b = 0.01; t = 25°

In Figs. 1 and 2 it was shown* that the rate of acylation of aniline, both by benzoyl acid chloride and by benzoic anhydride, is considerable increased through the action of additions of benzoic acid. It follows from Reaction B that benzoic acid is liberated during acylation by benzoic anhydride. In pure benzene this reaction must therefore be autocatalytic. And in actuality, curve 1 of Fig. 2 has that S-form which is characteristic of autocatalysis. In the initial step of the acylation, the presence of even small amounts of benzoic acid leads to a suppression of the autocatalysis,** as is clearly illustrated by the other curves of Fig. 2.

According to our opinion, the cause for this difference in the effects of hydrochloric and benzoic acids on the rate of acylation is in all likelihood to be found in the fact that in benzene solution these acids interact differently with the amine. Whereas hydrochloric acid converts the amine into a cation which is of low reactivity in comparison with the acylating agent, benzoic acid does not form an ionic compound with the amine, the nitrogen of the amino group of the latter is not carried over into the tetracovalent positive state and high reactivity of the amine results. Confirmation of the fact that the aromatic amines form compounds of fundamentally different types with hydrochloric acid and with organic carboxylic acids can be found in the works of P. P. Shorygin and A.Kh. Khalilov [11] (see [12]).

It is of interest to develop the quantitative relation between the rate of acylation and the concentration of the acid catalyst in solution. For the case of acylation by benzoyl chloride in benzene containing benzoic acid, it is simplest to assume that the reaction rate is described by the following equation:

$$-\frac{d\,[\mathrm{ArCOCl}]}{dt} = k_0\,[\mathrm{ArCOCl}]\,[\mathrm{ArNH_2}] + k_c\,[\mathrm{ArCOCl}]\,[\mathrm{ArNH_2}]\,[\mathrm{ArCOOH}], \qquad (1)$$

where k_0 and k_c are, respectively, the velocity constants for the uncatalyzed and the autocatalyzed reactions. From this it follows that the observed velocity constant for the over-all process should be equal to:

$$k = k_0 + k_c m, \qquad (2)$$

$\underline{m}$ being the analytic concentration of the benzoic acid. It is clear that when the value of $\underline{m}$ becomes sufficiently large, Eq. (2) will also be valid for acylation by benzoic anhydride.

According to (2), a linear relation should be observed between the velocity constant for the acylation and the concentration of the benzoic acid, but this is not confirmed by experiment. There is every reason to believe that in this case the absence of a linear relation is the result of the fact that the carboxylic acids possess the property of associating into dimers. Supposing that the benzoic acid exerts its catalytic effect chiefly through its monomeric form, we, in Fig.3, have sketched the relation between the velocity constants for acylation by benzoyl chloride and by benzoic anhydride and the concentration of the monomers in benzene solution, this concentration being equal to $m\alpha$, where α is the degree of dissociation of the dimers into monomers.*** In both cases the experimental points fall in a quite satisfactory manner on a straight line. Thus in order that Eq. (2) be valid for the acylation of aniline by benzoyl chloride and by benzoic anhydride, it is necessary that in it the analytic concentration of benzoic acid be replaced by the concentration of the monomeric form, i. e.,

$$k = k_0 + k_c m\alpha. \qquad (3)$$

---

* The following symbolism has been employed in Figs. 1-4; $\underline{a}$, $\underline{b}$, and $\underline{m}$, are respectively, the initial concentrations of the acylating agent, the amine and the benzoic acid, in moles/liter, and $\underline{t}$ is the temperature in °C.

** The rate of acylation by benzoyl chloride, both in pure benzene and in the presence of dissolved benzoic acid, nicely follows a bimolecular law. The same is also true for the acylation by benzoic anhydride once the autocatalysis has been depressed by a sufficient amount of benzoic acid, which is to say, after the concentration of the acid has become equal to about 0.005 moles/liter.

*** The values of α have been calculated from the constant for the dissociation of the dimers of benzoic acid into monomers, in benzene solution [13].

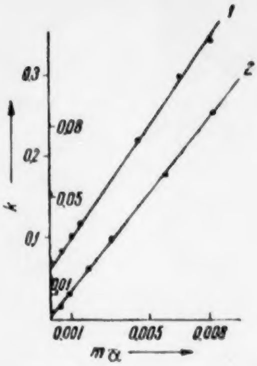

Fig. 3. The dependence of k on mα in the acylation of aniline by benzoyl chloride (1) and by benzoic anhydride (2), t = 25°. The figures to the left of the axis of ordinates are the values of k for 1, those to the right, the values of k for 2.

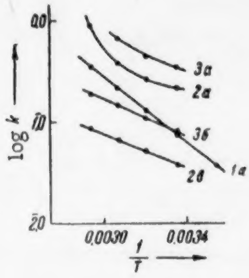

Fig. 4. The dependence of log k on 1/T for the acylation of aniline by benzoyl chloride (a) and by benzoic anhydride (b) at various values of m: 0 (1); 0.025 (2); 0.1 (3).

In Fig. 3, the lengths of the segments cut by the straight lines on the axis of ordinates should correspond numerically to the values of the velocity constants of the uncatalyzed reactions. This is well illustrated by the data for the acylation by benzoyl chloride (curve 1) since the velocity constant for the uncatalyzed reaction was here measured directly (k_{25}° = = 0.0700 liter/mole·sec). Because of autocatalysis, it is impossible to directly determine the velocity constant for the uncatalyzed reaction of acylation by benzoic anhydride, but with the aid of curve 2 its value is easily found to be equal to 0.000816 liter/mole·sec. From the slopes of the straight lines in this same Fig. 3 values of the velocity constants can be calculated for the autocatalytic reaction. For acylation by benzoyl chloride and by benzoic anhydride the respective values of this quantity are 22.3 and 9.86 liter^2·moles^2·sec.

From Fig. 4 it is to be seen that the temperature dependence of the velocity constant for the acylation of aniline by benzoyl chloride is rigorously covered by the Arrhenius Equation, when the reaction takes place in pure benzene.* On the other hand, a linear relation does not exist between log k and 1/T when the solvent contains benzoic acid. This last fact is not difficult to explain. We will write Eq. (3) somewhat differently as:

$$k = A_0 e^{-E_0/RT} + (A_c e^{-E_c/RT})\, m\alpha, \qquad (4)$$

A_0, E_0 and A_c, E_c being the Arrhenius parameters for the uncatalyzed and for the catalyzed reactions, respectively. Since the right side of Eq. (4) cannot be represented as one simple function of the form $Ae^{-E/RT}$, a linear log k vs 1/T relation can be observed only when it is possible to neglect one of the right-hand terms. Here two limiting cases are possible: 1) the value of mα is sufficiently small so that the magnitude of k is essentially fixed by the first member and the experimentally determined energy of activation is approximately equal to E_0; 2) the value of mα is sufficiently large so that k is essentially fixed by the second member and, consequently, the experimental energy of activation is approximately E_c. Naturally these limiting values of mα, beyond which one of the members becomes negligibly small in comparison with the other, also depend on the ratio of k_0 to k. In the case of the acylation of aniline by benzoyl chloride, the absence of a linear relation between log k and 1/T indicates that the velocities were measured in the region benzoic acid concentrations in which the two members of Eq. (4) are commensurable. Just as is to be expected, with increasing concentration of benzoic acid, the temperature curve for the velocity constant shows a marked tendency to approach a straight line. Because of the low solubility of the acid in benzene, rate measurements were not carried out at higher acid concentrations. However, in Fig. 4 at these same concentrations of benzoic acid straight lines are observed for the acylation of aniline by benzoic anhydride. Taking into account what has been said above, this can be easily understood, since in this case the value of k_0 is quite insignificant in comparision with k_c. Here the experimentally determined energy of activation is in the neighborhood of 4000 cal/mole and, over 0.005-0.1 moles/liter, is essentially independent of variations in the concentration of the benzoic acid.

---

* The energy of activation, the frequency factor and the entropy of activation for the acylation of aniline by benzoyl chloride in pure benzene are, respectively, equal to: 7700 cal/mole, $3.0 \cdot 10^4$ ml/mole·sec and −40.2 cal/deg·mole. Our value of E_0 is in good agreement with that determined by Hinshelwood and his collaborators (7350 [8] or 7600 [10]).

Later, after obtaining certain additional experimental data, we hope to express an opinion as to the mechanism of the influence of the acid on the kinetics of the acylation of aniline.

The authors are indebted to E. A. Shilov, Academician of the Academy of Sciences of the UkSSR, to N. A. Izmailov, Corresponding Member of the Academy of Sciences of the UkSSR, to Professor V. V. Voevodskii and to Lecturer V. A. Pal'm for consultation and for interpretation of the results of this work.

LITERATURE CITED

[1] L. M. Litvinenko and A. P. Grekov, J. Gen. Chem. 26, 3391 (1956).*

[2] L. M. Litvinenko and A. P. Grekov, J. Gen. Chem. 27, 234 (1957).*

[3] L. M. Litvinenko, R. S. Cheshko, and A. D. Gofman, J. Gen. Chem. 27, 758 (1957).*

[4] L. M. Litvinenko, S. V. Tsukerman, A. P. Grekov, and E. A. Slobodkina, Ukrain. Chem. J. 23, 223 (1957).

[5] L. M. Litvinenko and A. P. Grekov, Ukrain. Chem. J. 23, 228 (1957).

[6] F. Ebel, Ber. 60, 2079 (1927).

[7] G. Grant and C. Hinshelwood, J. Chem. Soc. 1933, 1351.

[8] E. Williams and C. Hinshelwood, J. Chem. Soc. 1934, 1079.

[9] W. Newling, L. Staveley, and C. Hinshelwood, Trans. Farad. Soc. 30, 597 (1934).

[10] F. Stubbs and C. Hinshelwood, J. Chem. Soc., Suppl. Issue No. 1, 71 (1949).

[11] P. P. Shorygin and A. Kh. Khalilov, J. Phys. Chem. 25, 1475 (1951).

[12] G. Barrow, J. Am. Chem. Soc. 78, 5802 (1956).

[13] F. Wall and F. Banes, J. Am. Chem. Soc. 67, 898 (1945).

Received July 30, 1957

The A. M. Gor'khii State University, Kharkov

---

* Original Russian pagination. See C. B. translation.

THE ELECTRON MICROSCOPIC INVESTIGATION OF OBJECTS IN A GASEOUS MEDIUM

I. G. Stoianova

(Presented by Academician P. A. Rebinder, June 4, 1957)

In order to carry out investigations with the electron microscope, it is necessary that the object be held in vacuum. At the same time, the study of many objects and processes must be conducted in presence of a gas. Begining with the appearance of the first model of the electron microscope, a technique has been sought which would make possible electron microscopic investigations of objects in air or gases [1-7]. A closed gas camera has been developed into which an object can be placed without preliminary drying [7],and an open camera permitting the observation of objects in gaseous atmospheres at pressures of 10-20 mm Hg has appeared [4-6]. Any further increase of the pressure in the region of the object is accompanied by an impairment of the vacuum in the microscope column and by a reduction in the stability of the image.

Since the electron microscopic study of an object in a gaseous medium requires that the pressure in the immediate neighborhood of the object exceed by several orders the pressure in the microscope column, the elements of the camera containing this object must have high mechanical strength in order to withstand such a considerable pressure difference, they must be sufficiently gas-tight so that the passage of gas from the camera into the microscope column is prevented,and in the zone of action of the ray they must, at the same time,be thin enough to avoid any considerable scattering of the electrons which have passed through the object.

The experiments which we have carried out made it possible to develop an open microcamera which satisfied these requirements [9]. This camera differed from those presently in use insofar as the gas pressure in it could be varied from 0 to 700 mm Hg without disturbing the working conditions of the microscope or interrupting the observation of the image. Gas-tightness was assured in this camera by gaskets and by protective films deposited on the diaphragms bounding the camera on two sides. These protective films were of collodion covered with thin layers of graphite.

Alteration of the pressure of gas in the camera was carried out by joining it to a balloon containing the requisite gas. The gas pressure in the zone of the object was measured by a U-shaped mercury manometer; the pressure in the microscope, by an ionization gauge. Experiments indicated that the camera was well sealed: on varying the pressure in it up to 600-700 mm Hg, the vacuum in the microscope column fell by no more than 5-10%.

The effect of the gas and the protective films on the quality of the image in the electron microscope. The presence of the gas and the protective films above the object led to an increase in the total thickness of the layer traversed by the electrons which form the image, and, because of chromatic error, there was a resulting deterioration in the resolution. Making use of an empirical equation which expresses the relation between the thickness of the object and the chromatic error in a form showing that the resolved interval cannot be smaller than $^1/_{10}$ of the object thickness, a resolving power of 50 A was found for our case (at extreme working conditions).

With an increase in the thickness of the scattering layer, there was a rise in the number of electrons which were scattered at such large angles as to be for the most part intercepted by the objective aperture. This led to a diminution of the intensity of the image. To restore the initial intensity, the charge on the object had to be raised.

Investigation showed that with a potential of 80 kv the two graphite-collodion films of the microcamera scattered up to 30% of the incident electrons beyond the limits of the aperture angle of $8 \cdot 10^{-3}$ radians. Increasing the pressure in the gas camera resulted in a diminution in the intensity of the image which at pressures close to atmospheric amounted to 70% with a 0.1 mm, and to 20% with a 0.03 mm height of gas layer. This diminution in intensity was accompanied by a considerable diminution in the contrast of the image. In order to select the optimal conditions of contrast, the dependence of the intensity distribution in the image [8] on the objective aperture and the acelerating potential was determined by a photographic method and from this the optimal aperture was fixed. Its value proved to be equal to $8 \cdot 10^{-3}$ radians. It turned out that up to an angle of $8 \cdot 10^{-3}$ radians, the magnitude of the minimum contrast depended only weakly on the objective aperture and increased considerably when this angle went above 10^{-2} radians. From the point of view of adequacy of image intensity, an aperture of $8 \cdot 10^{-3}$ radians could be looked on as satisfactory. Considering 0.2 to be the limiting contrast for the image of a particle, we found that in the gas microcamera it was possible to detect gold particles of 3A diameter and particles of organic origin of ~ 50 A diameter.

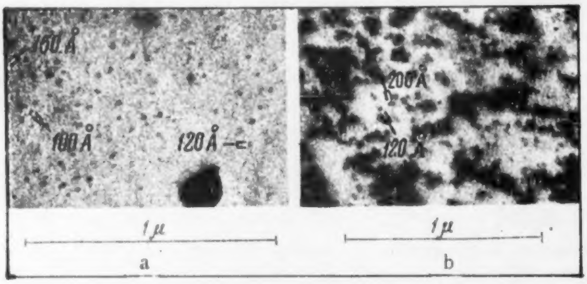

Fig. 1. Colloidal gold in the microcamera; V = 80 kv, a—p = 170 mm Hg, b—p = 520 mm Hg.

The resolution of the electron microscopic image was determined from particles of colloidal gold deposited on one of the protective films. With a pressure of 120-170 mm Hg in the microcamera the resolution was 80 A-100 A and with a pressure of 520 mm Hg it was 120 A (Fig. 1).

The observation of a chemical reaction in the electron microscope. The results obtained pointed up the possibility of carrying out electron microscopic investigations of objects in a gaseous medium as well as observations on chemical reactions between gaseous and solid phases.

By way of example we selected the reaction of silver and gaseous hydrogen sulfide in the presence of oxygen. By vaporization in vacuum, silver was deposited on the film of one of the diaphragms of the camera. These experiments were carried out with well sealed microcameras.

Before initiating the reaction, the structure of the initial layer was checked with the electron microscope and by electron diffraction. The external appearance of this initial silver layer and its electron diffraction pattern are presented in Figs. 2a, a'. Into the camera there was passed a mixture of gaseous hydrogen sulfide (p^{H_2S} = = 30 mm Hg) and oxygen (p^{O_2} = 10 mm Hg) and the changes in the structure of the initial layer were followed. Two minutes after the introduction of the gas, particle movement began on the section under observation (Figs. 2b, b'). Because of the high rate of migration, it was impossible to obtain at this point a sharp photograph of 1-2 sec exposure. From the electron diffraction pattern it was determined that this point corresponded to the beginning of chemical reaction; here there appeared not only the lines of silver but those of Ag_2S (Fig. 2b'). On the observed section, full conversion of silver to Ag_2S was completed within 3-4 min (Figs. $2c_0$, c, c').

Further investigation proved that this rapid conversion of Ag into Ag_2S occurred only on that section which was exposed to the electrons. On neighboring sections which were screened from the radiation, the initial structure was retained (Fig. 2d).

Control experiments, carried out in a tube under the same conditions as in the gaseous microcamera, showed that rapid (in the course of 2-3 min) conversion of Ag into Ag_2S takes place at a temperature of 95-100°. At temperatures lower than 80° no essential change in the silver structure is to be observed over this brief time interval. Thus the beam exerted a thermal action on the object and accelerated the reaction.

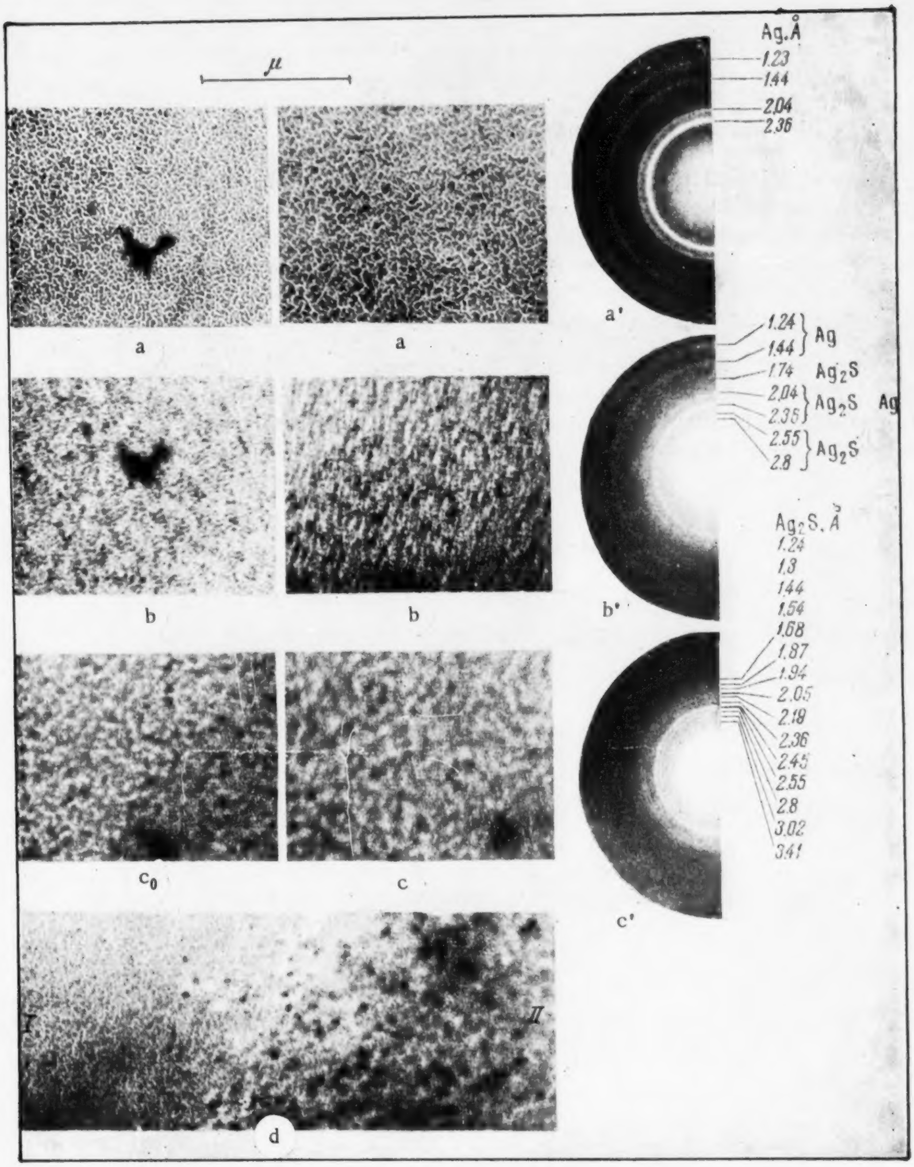
μ
a
a
b
b
c0
c
d
I
II
a'
b'
c'
Ag.Å
1.23
1.44
2.04
2.36
1.24
1.44
Ag
1.74
Ag2S
2.04
2.35
Ag2S
Ag
2.55
2.8
Ag2S
Ag2S.Å
1.24
1.3
1.44
1.54
1.68
1.87
1.94
2.05
2.18
2.36
2.45
2.55
2.8
3.02
3.41

Fig. 2. Images in the electron microscope (a, b, c, c_0, d) and electron diffraction patterns (a', b', c') of the structure of the silver layer during the reaction with hydrogen sulfide and oxygen; V = 80 kv; a, a') initial layer; b, b') layer 2 min after the beginning of the reaction; c_0, c, c') layer 3 and 4 min after the beginning of reaction; d) a section adjacent to the exposure; I) far removed from the exposure, II) bounding on the exposure.

In a number of cases, electron microscopic investigation of reaction processes showed a diminution of the amount of material on the exposed section and an increase of it on adjacent sections (Fig. 2d). This is clearly the result of a marked temperature drop on the radiated and unradiated sections.

In addition to this positive effect of the electrons which favored a higher rate of reaction, there was also observed a negative effect expressed in the formation of a film on the object, the thickness of this film increasing in proportion to the time and intensity of irradiation. The appearance of this film led to a considerable decrease in the contrast of the image. When reaction proceeded more rapidly than the process of film formation, it was possible to observe all the reaction steps. In the opposite case, the reaction ceased in one of its initial stages. It is necessary to take this detail into account in selecting the working conditions for the reaction.

By observing in the electron microscope the reaction between silver and hydrogen sulfide in the presence of oxygen it was possible to follow the conversion of silver into silver sulfide; at the same time it was revealed that the silver layer formed by evaporation in vacuum consisted of agglomerates which were not individual structural units, but aggregates of several such units. It was not the entire agglomerate which entered into reaction, but each structural unit separately, with a subsequent aggregation resulting from coagulation of the particles during the conversion of silver into silver sulfide.

Thus the technique which has been developed shows the possibility of an electron microscope investigation of objects in a gaseous medium, the resolution being not less than 120 A at pressures close to atmospheric. The application of this technique to the study of chemical processes makes it possible to follow in the electron microscope the various steps which are involved in reactions between gaseous and solid phases.

LITERATURE CITED

[1] R. Rudenberg, Österr. Patenschrift No. 137611 (1934).

[2] F. Krause, Naturwiss. 25, 817 (1937); Schwed. Patent 101576 (1938).

[3] M. V. Ardenne and D. Beischer, Zs. Elektrochem. 46, 270 (1940).

[4] E. Ruska, Koll. Zs. 100, 212 (1942).

[5] M. V. Ardenne, Zs. techn. Phys. 8, 239 (1939); Zs. Phys. Chem. 51, 61 (1942).

[6] L. Morton, Bull. Cl. Sci. Acad. Roy. Belg. 7, 553 (1935).

[7] J. M. Abrams and I. W. McBain, J. Appl. Phys. 15, 607 (1944); Science 100, 273 (1944).

[8] I. G. Stoianova and A. I. Frimer, Proc. Acad. Sci. USSR 94, 459 (1954).

[9] I. G. Stoianova, P. V. Zaitsev, and S. V. Bezlepkin, Patent (Russian) No. 584676 /26 of Oct. 16, 1957.

Received June 1, 1957

CATALYSIS ON SEMICONDUCTORS IN THE REGION OF INTRINSIC CONDUCTIVITY

O. V. Krylov and S. Z. Roginskii, Corresponding Member of the Academy of Sciences, USSR

In works dealing with the electronic mechanism of catalysis on semiconductors, the catalyst has, up to the present time, been considered to be an extrinsic semiconductor in which the current carriers participating in catalysis (electrons and electron holes) are formed with the direct participation of the impurity levels [1-4]. In actuality, many catalyzed oxidation-reduction reactions occur at temperatures which place the semiconducting catalyst in the region of intrinsic conductivity. The oxide of chromium, Cr_2O_3, is, for example, commercially employed for dehydration at 500-600° [5], i. e., in the region if intrinsic conductivity [6]. It is very likely that intrinsic conductivity predominates in the Cu_2O which is used to catalyze the oxidation of propylene to acrolein at a temperature of approximately 300°. Elementary germanium, a dehydrogenating catalyst at 200-300° according to the data of V. M. Frolov and the present authors [7], also functions in the region of intrinsic conductivity. The predominance of intrinsic conductivity is obvious in all cases of high temperature catalysis, and especially in the deep oxidation of hydrocarbons, the conversion of methane, etc.

Even with similar mechanisms for the initial step in the interaction of the catalyst with the substratum, catalysis in the region of intrinsic conductivity must differ, in many respects, from catalysis in the region of impurity conductivity and a number of propositions which are valid for the latter cast must then lose their significance. For catalysis in the region of intrinsic conductivity it is characteristic that:

1) the catalytic activity depends only weakly on the "structurally sensitive" properties: the amount and character of the additive and the previous history of the specimen;

2) the catalytic properties are related to the fundamental, rather than the impurity characteristics, this relation involving in the first instance the energy levels of the valence electrons of the atoms and the dimensions of the ions and thus the positions which the elements forming the catalyst occupy in the Mendeleev Periodic System;

3) there is a definite relation between the catalytic properties and the width of the forbidden band, U, of the semiconductor, the quantity $\exp(-U/2kT)$ being introduced into the equation for the catalytic reaction rate as an essential multiplying factor;

4) the term multiplying the exponential has high values;

5) there is a leveling out of differences between the n- and p-semiconductors, this fact making it unlikely that there are in this region materials which are specific in their catalytic activity. It is to be noted that according to the present concepts [8,9], materials with covalent bonds and, in particular, atomic semiconductors such as Ge, Si, etc., must have a minimum value of U and a maximum intrinsic conductivity at low temperatures. In binary compounds the width of the forbidden zone is the narrower the smaller the difference between the electronegativities of the elements which enter into the binary solid body. There is also an empirical relation, $U \cdot \epsilon^2 = \text{const}$, between the width of the forbidden zone and the dielectric permeability, ϵ, a factor which is known [10] to be classed among the fundamental characteristics of semiconductors.

Experiments on the catalytic decomposition of isopropyl alcohol on the binary compounds ZnO, ZnS, ZnSe and ZnTe which the authors have carried out with E. A. Fokina [11-13] have made it possible to follow the alteration in the catalytic properties which accompanies a variation of the physical characteristics in this group of related substances. Table 1 presents our catalytic data and the electronic characteristics of these compounds as reported in the literature [14-16].

TABLE 1

The Variation of Properties in the Series ZnO—ZnTe

	ZnO	ZnS	ZnSe	ZnTe
Energy of activation for dehydrogenation, kcal/mole	25-46	18-41	15-22	–
Energy of activation for dehydration, kcal/mole	14-16	23-24	–	–
Temperature interval over which the decomposition of the alcohol was studied, °C	120-125	100-170	20-140	20-100
Difference in electronegativities, Δx	2.1	1.1	1.0	0.7
Width of the forbidden band, U, ev	3.2	3.7	2.6	0.6
Dielectric permeability, ϵ	8.22	9.7	–	18.6
M —X distance, A	1.968	2.34 (Wurtzite) 2.36 (Sphalerite)	2.45	2.63

The data which have been obtained point to a sharply increased catalytic activity in the dehydrogenation of isopropyl alcohol on passing from ZnO to ZnTe. At the same time there is a decrease in the activation energy for dehydrogenation, a factor which is strongly dependent on the degree of coverage, and in the temperature interval over which the reaction has been studied. Because of rapid surface poisoning, it has not been possible to measure the energy of activation for the dehydrogenation of the alcohol on ZnTe. For the reaction on ZnTe the velocity constant proved to be at least 600 times greater than the constant for ZnSe when evaluated per unit surface at a single temperature (20°). On all of these catalysts the degree of dehydration was low, the percentage dehydration diminishing on passing from ZnO to ZnTe.

By studying the variation of other properties in the sequence ZnO → ZnTe, it is possible to see that an increase in catalytic activity is accompanied by a rise in the dielectric permeability, ϵ, a decrease in the difference between the electronegativities, Δx, calculated according to Pauling [17], and a decrease in the width of the forbidden band, U. An exception is ZnO, in which the value of U, 3.2 ev, is less than in ZnS, a fact which can be related to its crystallization in the Wurtzite rather than in the zinc blend lattice around which the remaining three compounds crystallize.* Catalysis proceeds in a temperature region which locates at least three of these binary compounds, ZnS, ZnSe and ZnTe, in the region of intrinsic conductivity.**

At the same time, the increased activity in dehydrogenation is accompanied by an increase in the lattice parameter of the compound ZnS, this change being, however, in the opposite direction to that which A. M. Rubinshtein, S. G. Kulikov, A. A. Dulov and N. A. Pribytkova have postulated [18] for the dehydrogenation of alcohols on the basis of the multiplet theory.

Thus, in these binary compounds a simple correlation is observed between the width of the forbidden band and the catalytic activity. It is desirable to carry out similar comparisons for other groups of compounds.

We note in conclusion that the existence of a relationship between the catalytic activity of semiconductors and the positions of their constituent elements in the Mendeleev Periodic System cannot be considered as entirely excluded even in the region of impurity conductivity. For elementary semiconductors with homopolar bonding, the depth of the impurity level, ΔE_{imp}, is determined by the equation [10]:

$$\Delta E_{\text{imp}} = \frac{13.53}{\epsilon^2} \cdot \frac{m^*}{m} - \alpha \sqrt[3]{N},$$

---

* Arguments as to the regular changes in semiconducting properties resulting from alteration of one of the elements in a compound are strictly applicable only to materials with uniform crystal structures.

** According to the data of [19], ZnO in the region 0-200° also approaches intrinsic conductivity as the dispersion is increased.

m being the effective mass of the electron; N, the concentration of impurity and α, a constant; i. e., for small values of N, the direction of change in the catalytic properties of a series of compounds which differ in the value of ϵ should be the same as for the case of intrinsic conductivity. However, ΔE_{imp} proves to be very small for the common homopolar semiconductors and for semiconductors with partial ionic bonding the applicability of this equation is not clear.

LITERATURE CITED

[1] S. Z. Roginskii and F. F. Vol'kenshtein, Symposium, Catalysis [in Russian], Proc. Kiev Conference on Catalysis, 1948 (Kiev, 1950), p. 9.

[2] S. Z. Roginskii, Chem. and Ind. 2, 138 (1957).

[3] F. F. Vol'kenshtein, Progr. Phys. 60, 249 (1956).

[4] H. J. Engell and K. Hauffe, Z. Elektrochem. 57, 762 (1953).

[5] M. A. Dalin and A. Z. Shikhmamedbekova, Trans. Acad. Sci. Azerbaijan SSR 15, 84 (1956).

[6] G. Bush, Progr. Phys. 47, 258 (1952).

[7] O. V. Krylov, S. Z. Roginskii, and V. M. Frolov, Proc. Acad. Sci. USSR 111, 623 (1956).*

[8] H. Welker, Z. Naturforsch. 7a, 744 (1952).

[9] E. Mooser and W. B. Pearson, Phys. Rev. 101, 1608 (1956).

[10] A. F. Ioffe, Semiconductors in Contemporary Physics [in Russian] (Acad. Sci. USSR Press, 1954).

[11] O. V. Krylov, S. Z. Roginskii and E. A. Fokina, Bull. Acad. Sci. USSR, Div. Chem. Sci. 1957, No. 4, 422.*

[12] O. V. Krylov and E. A. Fokina, Bull. Acad. Sci. USSR, Div. Chem. Sci. (in press).

[13] O. V. Krylov, M. Ia. Kushnerev and E. A. Fokina, Bull. Acad. Sci. USSR, Div. Chem. Sci. (in press).

[14] S. S. Shalyt, The Electrical Conductivity of Semiconductors [in Russian] (Leningrad, 1956).

[15] W. W. Piper and F. F. Williams, Phys. Rev. 84, 659 (1952).

[16] Z. I. Kir'iashkina, F. M. Popov, D. I. Bilenko, and V. M. Kir'iashkin, J. Tech. Phys. 27, 85 (1957).

[17] L. Pauling, The Nature of the Chemical Bond (Moscow, 1947), p. 71.**

[18] A. M. Rubinshtein, S. G. Kulikov, A. A. Dulov and N. A. Pribytkova, Bull. Acad. Sci. USSR, Div. Chem. Sci. 956, p. 596.*

[19] W. Ruppel, H. J. Gerritsen, and A. Rose, Helv. Phys. Acta 30, 495 (1957).

Received September 9, 1957

The Institute of Physical Chemistry of the Academy
of Sciences, USSR

---

* Original Russian pagination. See C. B. Translation.

** Russian translation.

A STUDY OF THE PHASE COMPOSITION AND ADSORPTIVE PROPERTIES OF IRON–CARBON CATALYST

S. M. Samoilov, A. A. Slinkin, and A. M. Rubinshtein

(Presented by Academician B. A. Kazanskii, July 22, 1957)

An iron–carbon catalyst, consisting of activated carbon or generator dust impregnated in turn with solutions of FeS_4 and NaOH,* is used for the destructive hydrogenation of aromatic hydrocarbons, tars and oil residues [1-10]. Until now the phase composition and adsorptive properties of this catalyst have not been studied. In the present work data have been obtained characterizing two unused specimens of iron–carbon catalyst prepared as described in [5]: specimen 1 contained 5.6% Fe on activated carbon; specimen 2 contained 10.5% Fe on generator dust.** Their activities were estimated by hydrogenating 20 g phenol in an autoclave with 2.5 g catalyst present for 3 hrs at 480° and an initial H_2 pressure of 114 atm as was described in [12]. In addition, specimen 1 was studied, using magnetic and x-ray structural methods, after H_2 had been adsorbed upon it. The experimental results are given in Figs. 1-3 and Table 1.

TABLE 1

The Specific Surface S, Pore Volume U, Activity in Phenol Hydrogenation Under Pressure, and the Magnetic Susceptibility χ at 20°, for Iron–Carbon Catalysts

Catalyst	$S \cdot m^2/g$		V, cc/g by N_2 adsorption	Degree of phenol conversion, %	H_2 consumption mole per mole	$\chi \cdot 10^6$	$\chi \cdot 10^6$ per 1 g Fe
	by toluene adsorption	by N_2 adsorption					
Specimen No. 1	440	622	0.334	85	2.7	330	5900
Specimen No. 2	185			75	2.7	57	540
Reduced specimen No. 1						1600	29,000

The x-ray phase structural analysis was carried out using standard powder cameras with Cu K-radiation (Ni filter) and Co K_α-radiation (Fe filter). Almost no difference was observed in the diffraction patterns of the specimens studied. The observed interplanar distances were close to the interplanar distances in the following individual compounds: Na_2SO_4, α-Fe_2O_3, γ-Fe_2O_3, Fe_3O_4, β-$Fe_2O_3 \cdot H_2O$ [13, 14]. It seemed impossible to establish which of the Fe oxides were actually present in the specimens under study, since, as a result of their high dispersion, the patterns were incomplete and did not contain a sufficient number of lines for an exact identification, while each of the lines present in the x-ray diagrams for the oxides and hydroxide of Fe could be with equal justification related to two or more of the above-mentioned Fe compounds. Together with the oxides of Fe (and possibly β-$Fe_2O_3 \cdot H_2O$) crystalline Na_2SO_4 was also shown to be present by the x-ray structural method.

---

* This catalyst is often designated No. 10927 in the literature.

** The Fe content was determined by Hillebrand's method [11].

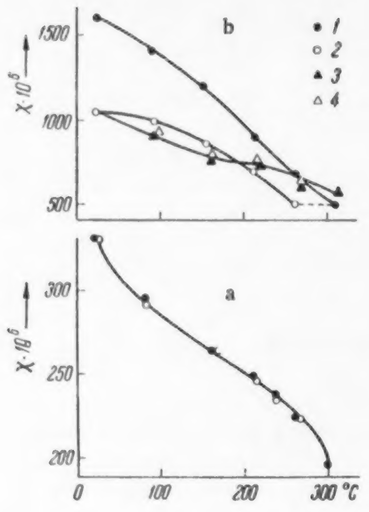

Fig. 1. Thermomagnetic curves for the iron–carbon catalyst: a) specimen 1; b) reduced specimen 1. 1) Heating, 2) cooling, 3) second heating, 4) second cooling.

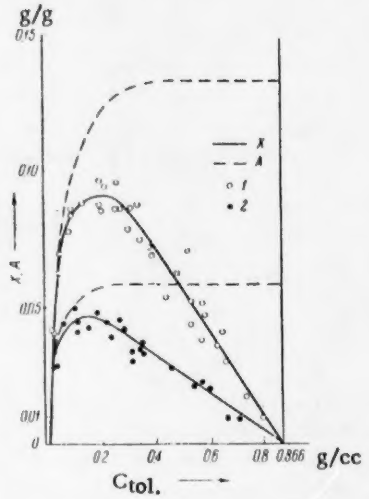

Fig. 2. Isotherms for the adsorption of toluene from solution in isooctane onto iron–carbon catalysts at room temperature. 1) On specimen 1, 2) on specimen 2.

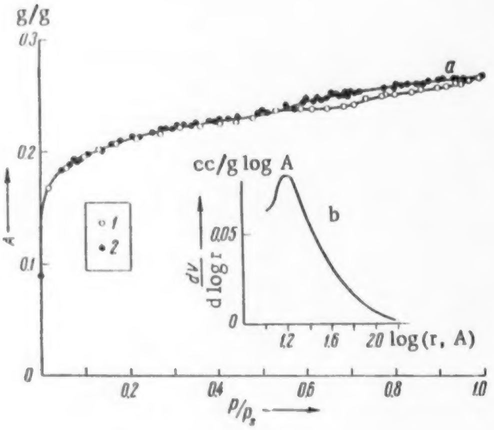

Fig. 3. Isotherm (a) for the adsorption of N_2 vapor at −196° on iron–carbon catalyst (specimen 1) [1) adsorption, 2) desorption] and the distribution of pore volume (b) of specimen 1 according to effective radii, as calculated from the adsorption isotherm.

This conclusion is in good agreement with the results of the measurements of the magnetic susceptibility χ (Table 1), which were made as described in [15].

The data from Table 1 should be compared with the tabulated data on the magnetic susceptibility χ of those compounds of Fe whose presence in the form of a separate phase was possible from the data obtained in the x-ray structural analysis, namely: a) the ferromagnetic γ-Fe_2O_3 and Fe_3O_4, for which, with a field intensity H = 2000 oersted, $\chi \cdot 10^6 = 47{,}500$, and, calculated on 1 g of Fe, 68,000 and 67,500, respectively, and b) the paramagnetic α-Fe_2O_3 with $\chi \cdot 10^6 = 20$, together with FeO and β-$Fe_2O_3 \cdot H_2O$ (for which no exact values of χ are given in the literature). The measurements have shown that the values of χ for specimens 1 and 2, calculated on 1 g Fe, lie between the corresponding values for γ-Fe_2O_3 and Fe_3O_4 and for α-Fe_2O_3, FeO, β-$Fe_2O_3 \cdot H_2O$. From the fact that the thermomagnetic curve for specimen 1 is completely reversible, it follows that no metallic iron is present in the specimen, since on the application of heat this would be oxidized by the air, so that χ for the specimen would be changed.

1. This is confirmed by the fact that χ for the reduced specimen 1 is decreased by a factor of 1.5 when it is oxidized in air (see Fig. 1).

In this way, the results of the determinations of phase composition and magnetic properties which we have carried out disprove the statements made in certain works [1, 5] that the iron in an unused iron–carbon catalyst is present in the form of only one compound: $Fe(OH)_3$ or $Fe(OH)_2$. The unused catalyst contains a mixture of paramagnetic and ferromagnetic oxides of iron, and possibly β-$Fe_2O_3 \cdot H_2O$. Under hydrogenation conditions (480°, 300-700 atmos H_2), of course, in the absence of sulfur compounds, the Fe oxides should be reduced to the metal; when sulfur compounds are present in the raw material, the formation of Fe sulfides should take place.

The isotherms for the adsorption of toluene from solution in isooctane (X) and the toluene content in the adsorption volume of the catalysts (A) (Fig. 2) were measured at room temperature as described in [16]. The specific surface S was calculated (Table 1) from the molecular area ω_0 for toluene (50 A^2). The isotherm for the adsorption of N_2 vapor at the temperature of liquid N_2 was measured on specimen 1 as described in [17], and is shown in Fig. 3 together with the distribution of pore volume for this specimen according to effective radii. A comparison of the adsorptive properties of the catalysts with the results of the phenol hydrogenation shows that from the degree of conversion, the more active catalyst was specimen 1, for which S, determined from the adsorption of toluene (whose molecular dimensions are close to the molecular dimensions of phenol), is 2.4 times greater than S for specimen 2. Since it has been shown [2] that the activity of an iron–carbon catalyst increases with increasing Fe content only up to 4-5%, after which further increases in the Fe content has no effect, the differences in the activities of specimens 1 and 2 are not dependent on differences in their Fe contents.

The selectivity of action of catalysts 1 and 2 was the same for both, as can be seen from the H_2 consumption. It is seen that it considerably (by 2.7 times) exceeds the H_2 consumption required for the reduction of phenol in benzene, which indicates that in the presence of the iron–carbon catalyst, not only aromatic hydrocarbons, but also hydrocarbons richer in hydrogen, are formed. These results are of interest in connection with the contradictory literature data [7, 10] on the selectivity of action of the iron–carbon catalyst in the hydrogenation of phenol. It may also be noted that the results obtained in the present work confirm and supplement the results of work [2] (in which S for the catalysts was not determined) on the influence of the magnitude of the specific surface of the carrier on the activity of the catalyst under discussion. S for specimen 1, determined from the adsorption of toluene, is less than the value obtained from the adsorption of N_2, since in this catalyst a considerable volume is occupied by ultra-fine pores (see Fig. 3).

The adsorption of H_2 was studied in a series of successive experiments on the same sample of specimen 1 at 400° and constant H_2 pressure of 740 mm Hg, until complete saturation had been achieved, using an apparatus similar to that described in [18]. Before each experiment the catalyst was degassed at 400° in high vacuum. In the first experiment the catalyst absorbed 15.9 cc/g (NTP) H_2 and in the subsequent experiments, which showed good reproducibility, 4.8 cc/g (NTP).

Taking ω_0 for the H atom at 400° as equal to 6.1 A^2 [19], we find that the surface area of catalyst 1, active to the reversible chemisorption of H_2 at 400°, is equal to 16 m^2/g, which makes up approximately 3% of S for this specimen, as determined from the low-temperature adsorption of N_2 vapor.

LITERATURE CITED

[1] I. B. Rapoport, Synthetic Liquid Fuel (Moscow, 1955).*

[2] J. Zogala, Freiberg. Forsch. A, 36, 31 (1955).

[3] W. Krönig, Katalytische Drukchydrierung, Berlin, 1950.

[4] S. V. Tatarskii, K. K. Papok, and E. G. Semenido, Oil Industry 24, 2, 52 (1946).

[5] A. Ia. Vavul and E. I. Sil'chenko, Works of the VNIGI 3, 159 (1951).

[6] A. V. Lozovoi, S. A. Seniavin, and A. B. Vol'-Epshtein, J. Appl. Chem. 28, 175 (1955).

[7] B. K. Klimov and I. F. Bogdanov, Works of the IGI 3, 140 (1954); 3, 151 (1954).

[8] V. I. Karzhev and D. I. Orochko, Works of the VNIGI 3, 71 (1951).

[9] V. I. Karzhev, D. I. Orochko, and B. Ia. Rabinovich, Works of the VNIGI No. 6, 55 (1954).

[10] I. V. Kalechits and F. G. Salimgareeva, Works of the Eastern Siberian Section of the USSR Acad. Sci. 3, 79 (1955); 4, 5 (1956); 4, 12 (1956).

---

* In Russian.

[11] V. F. Hillebrand et al., Practical Handbook of Inorganic Analysis (Moscow, 1957).* **

[12] S. M. Samoilov and A. M. Rubinshtein, Bull. Acad. Sci. USSR, Div. Chem. Sci. 1958 (in press).

[13] A. I. Kitaigorodskii, The X-ray Structural Analysis of Finely Crystalline and Amorphous Substances (Moscow-Leningrad, 1952).*

[14] V. B. Aleksovskii, Works of the Lensoviet Technol. Inst., Leningrad 35, 138 (1956).

[15] A. M. Rubinshtein and A. A. Slinkin, Bull. Acad. Sci. USSR, Div. Chem. Sci. 1958 (in press).

[16] S. M. Samoilov and A. M. Rubinshtein, Bull. Acad. Sci. USSR, Div. Chem. Sci. 1958 (in press).

[17] S. M. Samoilov and A. M. Rubinshtein, Bull. Acad. Sci. USSR, Div. Chem. Sci. 1957, 1158.**

[18] H. S. Taylor and C. O. Strother, J. Am. Chem. Soc. 56, 586 (1934).

[19] O. Beeck, Advances in Catalysis 2, 151-195 (1950) (quoted in Catalysis, Theoretical Problems and Methods of Study, Foreign Lit. Press, 1955).***

Received July 12, 1957

N. D. Zelinskii Institute of Organic Chemistry, USSR Academy of Sciences

---

* In Russian.

** See C. B. translation.

*** Russian translation.

THE KINETICS OF THE IONIZATION OF MOLECULAR CHLORINE

Academician A. N. Frumkin and G. A. Tedoradze

We have made a study of the kinetics of the electrolytic reduction of chlorine at a rotating platinum disc electrode. The electrode consisted of a platinum wire fixed in a brass rod and sealed into glass; when the end of the cylinder thus obtained had been ground off, the surface of the wire was revealed in the form of a disc. The surface of the electrode had an area of 0.78 mm^2. The chlorine was prepared by the electrolysis of 15% HCl and washed by passing through the solution under study; a platinum–rhodium wire was used as anode in the electrolyzer. The electrode under study was activated before use by repeatedly changing the potential from +1.8 to −0.1 v, relative to the normal hydrogen electrode, in a solution of 0.05 N HCl. Before each point on the polarization curve was recorded, the electrode was subjected to cathodic polarization up to the potential of hydrogen liberation for 3 sec. A potential of the required value was then applied to the electrode and maintained constant for 15 sec, after which the current strength was fixed. This method of working was made necessary by the fact that the current strength at a given potential did not remain constant with time, but decreased gradually as a result of electrode passivation. The overvoltage of the reaction of chlorine reduction η_c was determined relative to a platinum electrode in the same solution, used as an equilibrium chlorine electrode under atmospheric pressure of chlorine.

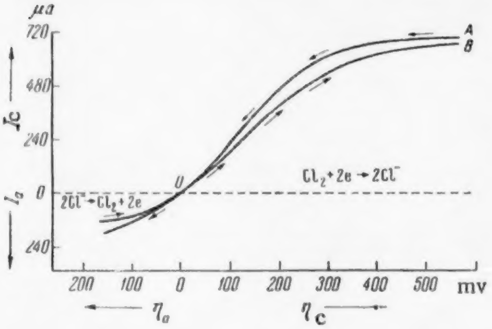

Fig. 1. Polarization curves for the ionization and liberation of chlorine from a solution of 0.023 N HCl+ + 0.6 N $HClO_4$. m = 1500 rpm. P_{Cl_2} = 1 atmos. η_c – Overvoltage of the cathodic process of chlorine ionization, η_a – overvoltage of the anodic process of Cl ion discharge.

It was found that at fairly low overvoltages the current strength of chlorine ionization depends on whether the voltage is changing from more anodic potentials to more cathodic, or in the reverse direction. When the change is from more anodic potentials to more cathodic, the course of the curve is lower than that of the curve recorded in the reverse direction, but at fairly high overvoltages both these curves converge (Fig. 1). With sufficiently high cathodic overvoltages, the reaction, even in the case of the less active electrode, is apparently accelerated to such an extent that the limiting factor becomes the diffusion of the chlorine to the electrode surface. In addition, when a sufficiently high cathodic overvoltage is reached, the adsorbed oxygen, which is responsible for the reduction in the activity of the platinum, is removed from the electrode surface, and this assists the diffusion current to reach its limiting value.

The value of the limiting current for the reaction of chlorine ionization, reached at high values of η_c, in accordance with V. G. Levich's equation [1], is proportional to $\sqrt{m}$, where m is the number of revolutions per sec. At fairly low overvoltages, however, for example, at η_c = 40 mv, the points showing the values of the current density i no longer lie on a straight line passing through the origin (Fig. 2). In these conditions, as has been shown in [2], it is possible, by extrapolating the relationship between $1/i$ and $1/\sqrt{m}$ to infinite values of m, to find the kinetic current i_∞, which expresses the rate of reaction when the concentration of the reacting substance is not changed by the passage of the current (section AC in Fig. 2). As was shown in the same work, it is possible to deduce the order of the electrode reaction from the value of the ratio AB/BC; here BC = i_{m_0} – the value of the

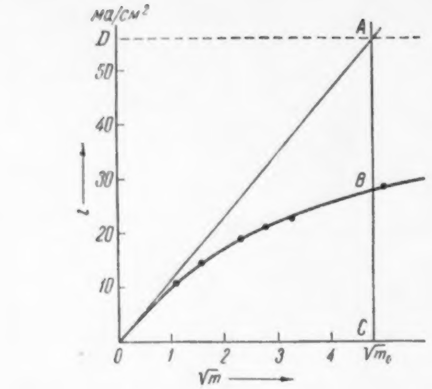

Fig. 2. Relationship between the current density of chlorine ionization and $\sqrt{m}$ at η_C = 40 mv. Solution composition: 0.1 N HCl + 1.9 N H_2SO_4.

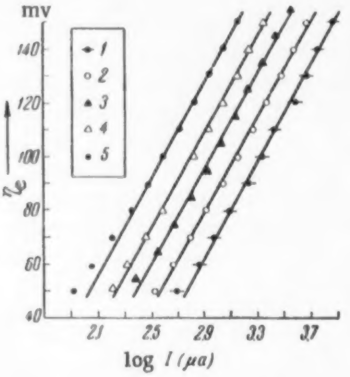

Fig. 3. The relationship between the logarithm of the current strength for chlorine ionization and the overvoltage η_C for different values of φ_r. 1) φ_r = = 1.073 v; 2) φ_r = 1.087 v; 3) φ_r = 1.102 v; 4) φ_r = = 1.115 v; 5) φ_r = 1.141 v (potentials relative to a saturated calomel electrode with no correction for diffusion potential). Support 2.2 N $HClO_4$.

current at $\underline{m} = m_0$, i. e., at the value of $\underline{m}$ at which the limiting diffusion current i_d becomes equal to i_∞. The values of i_d at any value of $\underline{m}$ may be found by drawing the tangent to the curve $\underline{i}$, $\sqrt{m}$ at the origin.

From the relationship $\frac{AB}{BC} = \frac{i_\infty - i_{m_0}}{i_{m_0}}$, denoting AB/BC by $\underline{x}$, it follows that:

$$x = \frac{C^p - C_s^p}{C_s^p}, \tag{1}$$

where $\underline{p}$ is the order of the reaction, C, the concentration in the bulk of the solution, C_s, the concentration at the electrode surface with current passing at $\underline{m} = m_0$. From (1) it follows that:

$$p = \frac{\log(x+1)}{\log\frac{C}{C_s}}. \tag{2}$$

According to the equation for diffusion kinetics

$$\frac{C}{C_s} = \frac{i_d}{i_d - i_{m_0}} = \frac{i_\infty}{i_\infty - i_{m_0}} =$$

$$= \frac{AC}{AB} = 1 + \frac{1}{x}. \tag{3}$$

From (2) and (3) it follows that:

$$p = \frac{\log(x+1)}{\log(x+1) - \log x}. \tag{4}$$

The conclusion just presented is accurate only on the assumption that when $\underline{m} \geq m_0$, the rate of the reverse reaction may be neglected in comparison with the rate of the forward reaction, while at low values of $\underline{m}$, when the polarization is purely concentration polarization, the values of C established at a definite polarization at the electrode surface is small compared with the original concentration. These assumptions may be realized only if η_C is not too small. As can be seen from Fig. 2, for the case of the reaction of chlorine ionization, the ratio $\underline{x}$ = AB/BC is close to unity, so that in accordance with Eq. (4), the reaction of chlorine ionization is a reaction of the first order relative to the chlorine.

The first order of the reaction relative to chlorine was also confirmed by a determination of the relationship between the cathode current i_∞ and the chlorine concentration at constant potential.

The electrode process of chlorine ionization may be broken down into successive stages, for example, as follows:

$$Cl_2 \rightleftarrows 2Cl_{ads} \tag{a}$$

$$2Cl_{ads} + 2e \rightleftarrows 2Cl^- \tag{b}$$

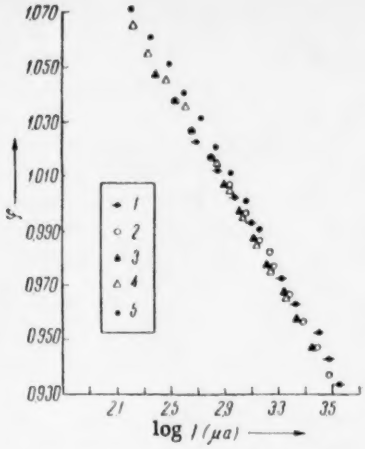

Fig. 4. The relationship between the logarithm of the current strength for chlorine ionization and the potential at different values of φ_r. The symbols are the same as those used in Fig. 3.

If the first stage is slow and the second reversible, then for the process of chlorine ionization, assuming uniformity and low degree of covering of the electrode surface by chlorine, it should be possible to apply an equation analogous to the equation, derived with similar assumptions, for the process of hydrogen ionization:

$$\eta_c = -\frac{RT}{2F}\ln\left(1 - \frac{i}{i_0}\right). \tag{5}$$

It follows from (5) that the value of i cannot exceed the value of the exchange current for stage (a) i_0; consequently, there should be a limiting current for the ionization, whose value is determined by the rate of dissociation of the chlorine molecule. In addition, there is no linear relationship between the overvoltage and the logarithm of the cathode current.

If, however, the overvoltage values are taken as ordinates and the logarithm of the cathode current strength, obtained by extrapolating the experimental data to m = ∞, i. e., corresponding to an unchanging chlorine concentration in the solution, is taken as abscissa, then a linear relationship is observed between log i and η_c at $\eta_c > 50$ mv, with angular coefficient 85 mm, this relationship being observed up to $\eta_c = 150$ mv.

It follows from (5) that the cathode current density at a given overvoltage should not be dependent on the chlorine ion concentration [Cl⁻], since the exchange current i_0 is completely determined by the chlorine concentration. If the equilibrium potential of the electrode is altered by changing [Cl⁻] while the chlorine concentration is kept constant, then all the points giving the current density at a definite overvoltage and different values of [Cl⁻] should coincide. As can be seen from Fig. 3, experiment does not confirm this conclusion, which is reached assuming retardation of the first stage, and, which is more important, is reached independently of further assumptions regarding the state of the electrode surface.

If it is assumed that the limiting stage is the process by which the adsorbed chlorine atoms are converted to chloride ions, while stage (a) is reversible, then according to the theory of retarded discharge, the following equation should be true for the cathode process at a sufficiently high value of η_c and constant chlorine concentration:

$$\varphi = \text{const} - \frac{RT}{\alpha F}\ln i, \tag{6}$$

where φ is the potential of the electrode. Since $\eta_c = \varphi_r - \varphi$, where φ_r is the equilibrium potential of the electrode, we have:

$$\eta_c = \text{const} + \varphi_r + \frac{RT}{\alpha F}\ln i. \tag{7}$$

It follows from (6) and (7) that if the second assumption is correct, a linear relationship should exist between the logarithm of the current density and the potential or overvoltage. As has been pointed out above, experiment confirms this conclusion. It also follows from (6) and (7) that with change in φ_r and constant chlorine concentration, the polarization curves should converge if the potential of the electrode is taken as ordinate, and diverge if the overvoltage is taken instead of the potential. As can be seen from Figs. 3 and 4, experiment also confirms this conclusion, which is equally accurate no matter what assumptions are made regarding the state of the electrode surface.

The fact that the current density for a given value of φ is independent of [Cl^-] proves that the actual ionization stage is irreversible, but from the assumption that the stage (a) is irreversible it follows, at least for a uniform surface covered only to a small extent, that the reaction is of half order relative to Cl_2, whereas experiment shows a first order reaction, as already mentioned above. We may make an attempt, still preserving the conclusions reached regarding the irreversibility of stage (b), to regard stage (a) as also irreversible, or to reject the assumption that the surface is uniform and covered only to a small extent. However, as a more detailed analysis shows, it is difficult, within the framework of these assumptions, to explain simultaneously the first order of the reaction relative to chlorine, the absence of a limiting cathode current and the absence of a relationship between i and [Cl^-]. The experimental data may be readily fitted into the framework of the theory if it is assumed that the process of Cl_2 ionization, in addition to the Cl_2 diffusion stage, takes place via the following two stages:

$$Cl_2 + e \rightleftarrows Cl_{ads} + Cl^- \tag{c}$$

$$Cl_{ads} + e \rightleftarrows Cl^- \tag{d}$$

of which the first is irreversible at fairly high values of η_c. From the theory of retarded discharge, with these assumptions, and taking the concentration of $C_{ads}[Cl_a]$ as small, it follows that:

$$i_\infty = 2k_1 [Cl_2] e^{\frac{-\alpha_1 F}{RT} \varphi} \tag{8}$$

where k_1 is the rate constant for reaction (c).

Equation (8) expresses accurately the relationship between i and φ, the first order of the reaction relative to Cl_2 and the absence of a relationship between i_∞ and [Cl^-]. No conclusions can be reached regarding the nature of the stage (d) on the basis of the data obtained at fairly high values of η_c. From observations made on the kinetics of the oxidation of Cl^- ions on a Pt electrode [3], and from the value of the so-called stoichiometric number [4] $\nu = \frac{2F}{RT} i_0 \left(\frac{\partial \eta_c}{\partial i_\infty}\right)_{\eta=0}$, which in the present case is close to 2 (i_0 is the exchange current, which is found by extrapolation of the right-hand part of Eq. (8) to the value of $\varphi = \varphi_r$), it follows that the stage (d) at fairly high overvoltages should also be irreversible, while the exchange currents of the stages (c) and (d) should have values of the same order.

LITERATURE CITED

[1] V. G. Levich, Physicochemical Hydrodynamics (Moscow, 1949).*

[2] A. N. Frumkin and E. A. Aikazian, Proc. Acad. Sci. USSR 100, 315 (1955); Bull. Acad. Sci. USSR, Div. Chem. Sci. (in press); E. A. Aikazian, Thesis, Moscow State University, 1955.

[3] G. Tedoradze , J. Phys. Chem. (in press).

[4] A. N. Frumkin, Proc. Acad. Sci. USSR (in press).

Received September 25, 1957

Electrochemistry Department, M. V. Lomonosov State
University, Moscow

---

* In Russian.

THE CHEMICALLY NONUNIFORM STRUCTURE OF SODIUM BOROSILICATE GLASSES

N. S. Andreev and E. A. Porai-Koshits

(Presented by Academician A. A. Lebedev, July 27, 1957)

That structural uniformity of complex glasses which is postulated in the Zachariasen-Warren disordered lattice hypothesis [1, 2] has been repeatedly criticized in recent years [3-8]. Especially convincing data pointing to the chemical nonuniformity of such structures have been obtained for certain sodium borosilicate glasses. The major portion of this data is, however, of an indirect character and the experiments underlying it can also be interpreted from the standpoint of the disordered lattice hypothesis. In particular, the sharpest objections have been raised against attempts to establish and particularize the chemically nonuniform structure of sodium borosilicate glasses on the basis of a study of the submicroscopic structure of the porous products resulting from leaching. For example, N. V. Belov has asserted that by the action of acids on chemically uniform glasses, pores are formed which "even according to their geometry, were not marked out in the initial glass" [15, 16]. Fundamental interest thus attaches to any direct structural method for detecting chemical nonuniformity in a glass structure.

For this purpose there was employed the method of x-ray scattering at small angles. A new vacuum camera, based on the principle of the "frame camera" proposed by Kratky [17], was constructed. With the aid of this camera a clear and reproducible small-angle diffraction was obtained from a glass containing Na_2O, 7; B_2O_3, 23 and SiO_2, 70 mole% which had not been subjected to any chemical treatment.

Because of the insignificant difference between the electron densities in the region of nonuniformity, the intensity of the small-angle scattering by unleached glasses is very low, and attempts to record it by x-ray photography from powdered glass specimens were without results because of pure surface effects at the glass grains, these effects having no relation to the internal structure of the object under investigation. This scattering was almost independent of the composition and thermal treatment of the glass but depended strongly on the degree of powder dispersion. With grains of 0.1 mm diameter, for example, a marked scattering in a region very close to the primary ray was observed with a 2-hr exposure. In this connection it should be noted that such an effect could introduce a considerable distortion into the results of Hoffman and Statton who, investigating specimens in powder form [18], have recently obtained small-angle scattering of x-rays from glassy silica and from sodium magnosilicate glass.

We have, therefore, employed glass specimens which were in the form of polished plates of approximately 0.2 mm thickness, the absence of a surface effect being controlled by varying the specimen thickness. X-ray analysis was carried out with filtered copper radiation (from a BSVI tube; working conditions, 10 ma, 30 kv) the distance from specimen to film being 350 mm. Small-angle scattering was obtained for 9 specimens of glass which had been subjected to various types of thermal treatment. The initial glass was specimen No. 1 which had been annealed at approximately 500°; the remaining specimens were heated at 600 and 650° for various periods of time (ranging from 1 to 8 hrs) and cooled in air. Depending on the dimensions of the regions of nonuniformity, exposure varied from 15 hrs (for a specimen which had been heated at 650° for 6 hrs) to 100 hrs (for specimen No. 1). The glasses which were annealed at 600° remained transparent, as did specimen No. 1; those which were annealed at 650° showed various degrees of opalescence and this opalescence increased with the duration of the annealing. The intensity of scattering of visible light (λ = 5400 A) was measured with a special apparatus using a FEU-19 photomultiplier and direct current amplification.

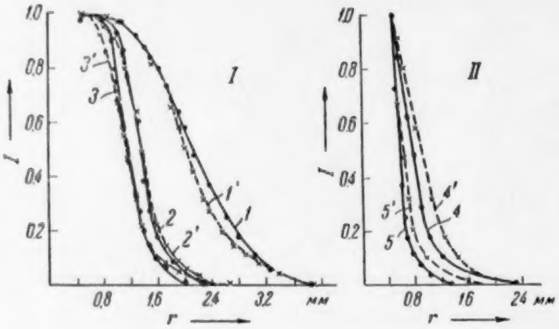

Fig. 1. Curves which show the intensity of small-angle scattering by unleached (full curves) and by porous (dotted curves) glasses and reflect the influence of annealing at 600° (I) and at 650° (II), r being the distance, in mm, from the center of the primary ray.

At the same time there were investigated the porous glasses resulting from these same specimens by treatment with HCl and KOH under conditions which have been described earlier in [11]. These materials were studied in powdered form. Assurance that the surface effect was without significance in this case was found in the shortness of the exposures (of the order of several min) and in the dependence of the diffraction pattern on the thermal treatment of the parent glass rather than on the degree of dispersion of the powder.

In Fig. 1, I, the full lines represent the intensity curves for the parent glass, No. 1, and for glasses which had been annealed for 4 and for 8 hrs at 600° (glasses No. 2 and No. 3, respectively). The presence of maxima on these curves indicates the existence of scattering regions of fairly uniform dimensions and essentially continuous distribution. The intensity at the maxima has been chosen as unity. An increase in the annealing time is accompanied by a displacement of the curves which points to a rise in the dimensions of these regions. The dotted lines in this same figure represent the intensity curves for the porous glasses obtained from these same specimens. These curves are very close to the corresponding curves for the parent glasses, a fact which serves as convincing proof of the close similarity between the forms and dimensions of the regions of nonuniformity in the parent glasses and the forms and dimensions of the pores which are formed during leaching. Evaluation of the radii of the nonuniformities was carried out on the basis of the positions of the interference maxima, a collimation correction being made at the terminal height of the primary ray (R_m) and also by the "method of tangents" (R), the results for specimen No. 1 being: $R_m = 105$ A, $R = 113$ A for the parent glass and $R_m = 113$ A, $R = 99$ A, for the porous glass. In specimen No. 3, the radius increased to 180 A. The intensity of scattering of visible light increased correspondingly by 3-4-fold.

In Fig. 1, II, intensity curves are shown for parent and leached glass from specimens which had been annealed at 650° for 1 hr (No. 4) and for 6 hrs (No. 5). The intensity at the minimum scattering angle (at a distance of 0.05 mm from the edge of the primary ray, i. e., at a scattering angle of ≅ 30") has been taken as unity. In the region of accessible angles, interference maxima were not observed. The somewhat greater discordance in this case between the curves for the parent and the porous glasses is explained by differences in the conditions of the x-ray analyses: the parent glasses were analyzed at 30 kv and the porous at 15 kv and the more intense shortwave portion of the continuous spectra passed through the filter to cause a displacement of the intensity curves for the parent glasses toward small scattering angles. This detail was confirmed by special experiments. Thus even here it is possible to consider that the forms and dimensions of the regions of nonuniformity in the parent glasses are close to the forms and dimensions of the pores in the leached glasses. In regard to the influence of the thermal treatment, it can be said that it is the same here as for the specimens which were annealed at 600° but that the dimensions of the region of nonuniformity are considerably greater at 650°.

A calculation which was carried out by the method of tangents (without the introduction of a collimation correction at the terminal width of the ray) showed that in comparison with specimen No. 1, the mean radius of the regions of nonuniformity in specimen No. 4 had increased to 380 A (the intensity of scattering of visible light rising at the same time by approximately 30-fold) and in specimen No. 5, to 610 A (the intensity of scattering of the visible light increasing by more than 3 orders).

Thus on applying the method of small angles to unleached sodium borosilicate glasses which had been heated at various temperatures over various periods of time, there appeared those same regularities as are met in the study of porous glasses [12]. This convincingly supports the earlier supposition of the existence of submicroscopic regions of nonuniformity in the parent glasses. The growth of such regions during heating can be accompanied by an increased degree of ordering (crystallites), as is indicated by preliminary results from an investigation of these glasses by the usual method of x-ray analysis. At the present time, the role of this crystallization of the borate "components" of these glasses in the scattering of visible light and small-angle x-rays is clear. The problem of the chemically inhomogeneous structure of the sodium borosilicate glasses should be considered as completely solved.

LITERATURE CITED

[1] W. H. Zachariasen, J. Am. Chem. Soc. 54, 3841 (1932).

[2] B. E. Warren, Z. Krist. 86, 349 (1933).

[3] W. A. Weyl, J. Soc. Glass Techn. 35, 421 448, 462, 469 (1951).

[4] A. G. Smekal, J. Soc. Glass Techn. 35, 411 (1951).

[5] N. J. Kreidl, Glass Ind. 31, 573 (1950).

[6] J. M. Stevels, Philips Techn. Rund. 13, 350 (1952).

[7] E. A. Porai-Koshits, Symposium, The Structure of Glass (Acad. Sci. USSR Press, 1953), p. 30.*

[8] K. Grjotheim, J. Krogh-Moe. Glass 33, 465 (1956).

[9] T. Abe, J. Am. Ceram. Soc. 35, 284 (1952).

[10] V. L. Indenbom, Proc. Acad. Sci. USSR 89, 509 (1953).

[11] D. I. Levin, S. P. Zhdanov, and E. A. Porai-Koshits, Bull. Acad. Sci. USSR, Div. Chem. Sci. 1955,* 31, 197, 395.

[12] E. A. Porai-Koshits, D. I. Levin, and N. S. Andreev, Bull. Acad. Sci. USSR, Div. Chem. Sci. 1956,* 287.

[13] F. Oberlies, Naturwiss. 43, 224 (1956).

[14] D. P. Dobychin and N. N. Kiseleva, Proc. Acad. Sci. USSR 113, 372 (1957).*

[15] N. V. Belov, Symposium, The Structure of Glass (Acad. Sci. USSR Press, 1955), p. 334.*

[16] N. V. Belov, Symposium in Minerology, Lvov Geological Soc. No. 8, 13 (1956).

[17] O. Kratky, Z. Elektrochem. 58, 49 (1954).

[18] L. C. Hoffman and W. O. Statton, Nature 176, 4481, 561 (1955).

Received July 15, 1957

The Institute of Silicate Chemistry of the Academy
of Sciences of the USSR

---

* Original Russian pagination. See C. B. translation.

THE EFFECT OF OXYGEN ON THE PARAMAGNETIC RESONANCE ABSORPTION IN αα-DIPHENYL-β-PICRYLHYDRAZYL

N. S. Garif'ianov and B. M. Kozyrev

(Presented by Academician B. A. Arbuzov, July 8, 1957)

Proceeding according to the method which has been described in [1], we have discovered that oxygen strongly effects the paramagnetic resonance absorption at 127 megacycles in freshly ground, finely crystalline powders of αα-diphenyl-β-picrylhydrazyl (DPhPH). Diminishing the air pressure above a specimen increased the intensity of this absorption line and diminished its half-width. Raising the pressure back to its starting value led to the re-establishment of the original absorption line.

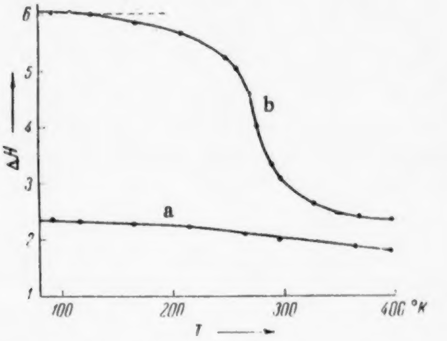

Fig. 1. The dependence of ΔH on the temperature at pressures of $9 \cdot 10^{-4}$ mm Hg (a) and 760 mm Hg (b).

The influence of oxygen on the intensity, width and form of this line appeared with special clarity on cooling a specimen of DPhPH. The relation between the half-width, ΔH, of the absorption line and the temperature in specimens maintained under air pressures of $9 \cdot 10^{-4}$ mm and 760 mm is shown in Fig. 1, and photographs of certain of the resulting lines in Fig. 2.

From Fig. 1 it is clear that there was only a very gradual diminution of ΔH on warming the DPhPH from 77 to 395°K in the absence of oxygen (curve a), this change being, in all likelihood, related to the decreased effectiveness of the local magnetic fields which results from the thermal movement [2].

A specimen of DPhPH which was held in contact with air (Fig. 1, b) behaved quite differently; in this case the ΔH(T) curve lay higher and a sharp increase in the line width was observed in the temperature interval from ~ 300 to ~250°K. Identical results were obtained in numerous repetitions of these experiments with a single specimen. At an air pressure of 760 mm, the various specimens differed somewhat from one another, the line broadening being the stronger, the smaller the dimensions of the DPhPH particles. Thus in specimens prepared by pulverizing DPhPH with sugar, it was possible to obtain a line whose width was ~ 3 gauss at 295°K and approximately 10 gauss at 77°K. In this case the effect of temperature on ΔH was reversible. With a coarsely crystalline specimen which had a small surface for contact with the oxygen of the air, the course of the ΔH(T) curve was close to that for a specimen held in vacuum.

An especially pronounced change in the absorption line was observed when a finely pulverized DPhPH specimen was held in direct contact with liquid oxygen. If, on the other hand, this specimen was brought into contact with liquid nitrogen, the ΔH(T) relation proved to be approximately the same as for the specimen in vacuum and the line width did not change even if the specimen was brought into direct contact with liquid oxygen immediately after immersion in the liquid nitrogen.

These experiments showed that the variation in line width was entirely due to molecular oxygen adsorbed on the DPhPH surface. Line broadening of DPhPH was also observed in an NO_2 atmosphere. Thus it turned out that adsorbed paramagnetic gases considerably reduce that time, T_2, which determines the line width in DPhPH, just as in the case of charcoal [2].

The sharp change in the line width in the neighborhood of 275°K is most noteworthy. This could result from either a pronounced change in the adsorption of O_2 on DPhPH (arising, for example, from the formation of a second adsorption layer of O_2 molecules at temperatures $<$ 275°K) or an alteration in the character of the movement of the O_2 molecules on the DPhPH surface. The latter explanation seems the more likely. It can be supposed that adsorbed oxygen possesses considerable freedom of movement on a DPhPH surface at temperatures above 275°K, and forms as it were, a two-dimensional gas or liquid, the movement reducing the effectiveness of the local magnetic fields which arise from the molecules of O_2; at temperatures below ~ 275°K this movement of the adsorbed molecules is "frozen out."

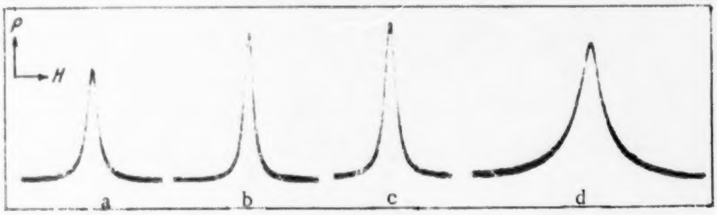

Fig. 2. Curves showing the paramagnetic resonance absorption in DPhPH. a) 760 mm Hg, T = 295°K; b) $9 \cdot 10^{-4}$ mm, 295°K; c) $9 \cdot 10^{-4}$ mm, 77°K; d) 760 mm, 77°K.

The adsorption of oxygen on the DPhPH surface is the first step in the oxidation of this free radical, the oxidation itself proceeding slowly; the paramagnetic resonance completely disappears only after several days, even in a highly dispersed sample held in air.

It should be noted that rather contradictory data are to be found in the literature on the line width for paramagnetic resonance in DPhPH [3-6]. The reported temperature dependence of ΔH in DPhPH also varies from author to author [5, 7-9]. It seems likely that these divergencies can be explained by the fact that the investigated specimens of DPhPH differed in their age and degree of dispersion and that, as a result, the oxygen effects in them were not identical.

In conclusion the authors wish to express their deep appreciation to F. G. Valitova for the preparation of the αα-diphenyl-β-picrylhydrazyl.

LITERATURE CITED

[1] N. S. Garif'ianov and B. M. Kozyrev, J. Exptl.-Theoret. Phys. 38, 272 (1956).

[2] L. S. Singer and W. J. Spry, Bull. Am. Phys. Soc. 1, 214 (1956).

[3] R. S. Codrington, J. D. Olds, and H. C. Torrey, Phys. Rev. 95, 607 (1954).

[4] M. A. Garstens, L. S. Singer, and A. H. Ryan, Phys. Rev. 96, 53 (1954).

[5] F. Bruin and M. Bruin, Physica 22, 129 (1956).

[6] M. R. Gabrillard and J. A. Martin, Compt. rend. 238, 2307 (1954).

[7] L. Van Gerven, A. Van Itterbeek, and E. De Wolf, J. Phys. Radium 17, 140 (1956).

[8] L. S. Singer and E. G. Spenser, J. Chem. Phys. 21, 939 (1953).

[9] H. J. Garritsen, R. Okkes, H. M. Gijsman, and J. Vanden Handel, Physica 20, 13 (1954).

Received July 4, 1957

The Physico-Technical Institute of the Kazan Branch
of the Academy of Sciences of the USSR

THE DETERMINATION OF REACTION ORDER FROM ACIDITY

A. I. Gel'bshtein and M. I. Temkin

(Presented by Academician A. N. Frumkin, July 23, 1957)

In catalysis by concentrated acids, the degree of conversion of the substrate, B, into the protonized form, BH^+, is determined by the acidity of the medium, i. e., by its ability to furnish protons, and by the basicity of the substrate itself:

$$\frac{C_{BH^+}}{C_B} = Kh_0. \tag{1}$$

Here h_0 is the acidity of the medium and K is the equilibrium constant for the reaction

$$B + H^+ \rightleftarrows BH^+, \tag{2}$$

expressed in terms of the activity characterizing the basicity of B.

According to Hammett [1], the observed velocity constant, k, is proportional to h_0 when the degree of protonization is low ($C_{BH^+} \ll C_B$), provided that the establishment of the Equilibrium (2) is the first step in the reaction and the rate is limited by the further monomolecular transformation of the protonized form, BH^+.

Cases are conceivable, however, in which the limiting step would be the establishment of the equilibrium

$$B + 2H^+ \rightleftarrows BH_2^{2+}. \tag{3}$$

Then k should be proportional to h_0^2 if h_+, the acidity expressed in terms of the uniformly positively charged base, is proportional to h_0, the acidity in terms of the uncharged base (for simplicity it is assumed in what follows that $h_+ = h_0$).

Thus the dependence of k on h_0 is represented by the equation

$$k = \text{const} \cdot h_0^n. \tag{4}$$

The exponent n is usually determined graphically by plotting log k against $H_0 = -\log h_0$, a function of the acidity.

Thus it was found that n = 2 for the decomposition of benzoylformate in sulfuric acid and the conclusion was drawn that this reaction involves the addition of two protons [2].

From the rates of decomposition of other carboxylic acids in sulfuric acid, values of n were obtained which in some cases were approximately 1, in other cases were approximately 2 and in still others were variable over the interval from 1 to 2 or even beyond, depending on the acid concentration, special hypotheses concerning reaction mechanisms having been advanced [2] to account for these results.

We have investigated the kinetics of the decomposition of formic acid into carbon monoxide and water [3] in the media: $H_2SO_4-H_2O$ (from 80.7 to 98.2% H_2SO_4) and $P_2O_5-H_2O$ (from 72.4 to 83.3% P_2O_5, i. e., in the region of the so-called strong phosphoric acids). For these same media measurements were carried out on H_0 and its temperature dependence [4].

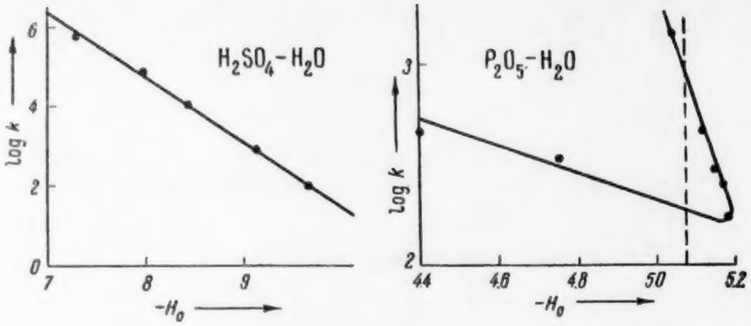

Fig. 1.

In distinction to the $H_2SO_4-H_2O$ system in which the acidity varies monotonically with composition [4], the acidity of the $P_2O_5-H_2O$ system passes through a maximum at a P_2O_5 concentration of 80%. This pecularity of the $P_2O_5-H_2O$ system permits a better understanding of the relation between the reaction velocity constant and the acidity.

In Fig. 1 values of log k, extrapolated to 20° through the Arrhenius Equation, are shown as functions of $-H_0$.

For decomposition in sulfuric acid, the slope of the straight line corresponds to $n = 1.6$, a fact which makes it impossible to choose between the mechanisms corresponding to $n = 1$ and to $n = 2$.

The curve for the $P_2O_5-H_2O$ system points up the inapplicability of Eq. (4). With a single acidity there are associated radically different values of the velocity constant. It should be considered [3] that the variation of the velocity constant with the composition of the medium is the result of the superposition of two effects, the one due to the acidity and the other to the nature of the solvent (Menshutkin effect).

Leaving unanswered the question as to the number of protons which unite with the reacting molecules and considering the limiting step to be the monomolecular transformation of the protonized form, it is easy in analogy with [3] to obtain the expression

$$k = Bh_0^n(x)\, e^{-A(x)/RT}. \tag{5}$$

Here $h_0(x)$ is the acidity expressed as a function of the acid concentration, x; n is the order of reaction in terms of acidity; $A(x)$ is the energy of activation expressed as a function of x so that $A(x) = A_1(x) + \Delta H^0$, $A_1(x)$ being the activation energy of the limiting step, and ΔH^0 is the standard change in heat content accompanying protonization.

TABLE 1

The $H_2SO_4-H_2O$ System

H_2SO_4, %	log β	H_2SO_4, %	log β
80	5.28	92	6.28
82	5.55	94	6.34
84	5.77	96	6.44
86	5.97	97	6.44
88	6.10	98	6.57
90	6.21	99	6.80

TABLE 2

The $P_2O_5-H_2O$ System

P_2O_5, %	log β	P_2O_5, %	log β
72.4	0.49	79.0	1.37
73.0	0.56	79.7	1.40
74.0	0.94	81.0	1.10
75.0	1.05	82.0	1.06
76.0	1.14	83.0	0.86
77.0	1.23	83.8	0.74
78.0	1.30	—	—

The coefficient of proportionality is given by the equation: $B = B_1 e \Delta S^0/R$, where B_1 is the multiple of the exponential term in the expression for the velocity constant of the limiting step and ΔS^0 is the standard entropy change for protonization. We shall suppose that B_1 is independent of *x*, and the same is then also true of B.

For the purpose of determining *n*, we shall represent h_0 by the equation

$$h_0 = \beta(x)\, e^{-\alpha(x)/RT}, \tag{6}$$

$\alpha(x)$ and $\beta(x)$ being certain functions of *x*.

The Equalities (5) and (6) give:

$$k = B\beta^n(x)\, e^{-[A(x)+n\alpha(x)]/RT} \tag{7}$$

Thus,

$$k = F(x)\, e^{-E(x)/RT}, \tag{8}$$

F(x) representing the observed multiple of the exponential term and E(x), the observed energy of activation, expressed as

$$F(x) = B\beta^n(x), \tag{9}$$

$$E(x) = A(x) + n\alpha(x). \tag{10}$$

In the determination of *n*, it is useful to employ the logarithmic form of Eq. (9):

$$\log F(x) = \log B + n \log \beta; \tag{11}$$

$\log \beta$ is evaluated from the function of the acidity and its temperature dependence, use being made of the equation

$$\log \beta = -H_0 - T\left(\frac{\partial H_0}{\partial T}\right)_x, \tag{12}$$

which follows from (6).

In Tables 1 and 2 there are given values of $\log \beta$ at 20° as calculated from the experimental data [4].

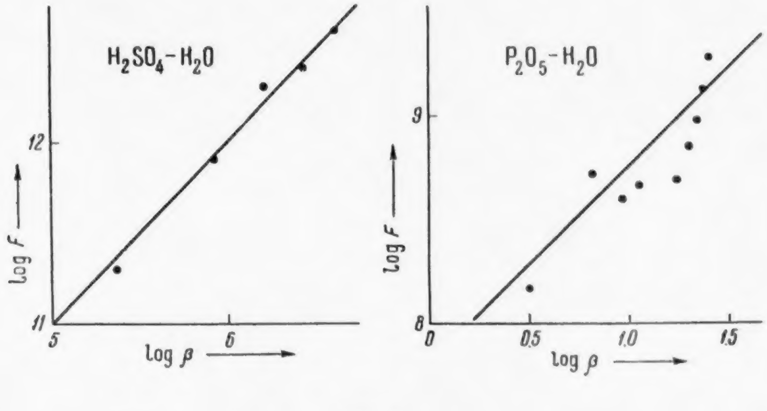

Fig. 2.

The values of log β are somewhat less exact than those of H_0. The determination of S from the kinetic data is also less precise than is the determination of $\underline{k}$. Thus the log F, log β graph shows a larger point spread than does the log k, H_0 graph.

The points in Fig. 2 correspond to the experimental data on the decomposition of formic acid [3]; the straight lines are those corresponding to $\underline{n} = 1$. In spite of the considerable spread of points in the case of the $P_2O_5-H_2O$ system, the conclusion can be drawn that reaction proceeds through reversible protonization, each of the reacting molecules uniting with a single proton. This conclusion is confirmed by the constancy of the values of B calculated at various values of $\underline{x}$ through Eq. (5) with n = 1 [3].

The cases in which there is a pronounced departure of $\underline{n}$ from 1, $\underline{n}$ being determined through Eq. (4), clearly result from failure to take into account the influence of the acid concentration on the activation energy for the reaction.

The evaluation of $\underline{n}$ from Eq. (11) is in principle more nearly correct than is its evaluation from Eq. (4) but imposes very high demands on the experimental data.

LITERATURE CITED

[1] L. P. Hammett and A. J. Deyrup, J. Am. Chem. Soc. 54, 2721 (1932); L. P. Hammett, Physical Organic Chemistry (London, 1940).

[2] W. Elliott and D. Hammick, J. Chem. Soc. 1951, 3402.

[3] A. I. Gel'bshtein, G. G. Shcheglova, and M. I. Temkin, J. Phys. Chem. 30, 2267 (1956).

[4] A. I. Gel'bshtein, G. G. Shcheglova, and M. I. Temkin, J. Inorg. Chem. 1, 282 (1956); Proc. Acad. Sci. USSR 107, 108 (1956).*

Received July 16, 1957

L. Ia. Karpov Physicochemical Scientific-Research Institute

---

* See C. B. translation.

THE ACTION OF TRIETHANOLAMINE ON PHOTOGRAPHIC EMULSIONS

A. P. Zhdanov, A. L. Kartuzhanskii, I. V. Ryshkova, and L. P. Shur

(Presented by Academician A. P. Vinogradov, July 13, 1957)

During the last ten years communications have appeared [1-3] reporting the use of triethanolamine (TEA) for increasing the sensitivity of nuclear photographic emulsions toward ionizing particles. Insofar as it is known to us, the mechanism of this action has not been investigated. There is even a lack of data on the effect of TEA on the sensitivity of photographic emulsions toward light. Thus it has seemed to us worthwhile to investigate the effect of TEA on sensitivity to light under various conditions of illumination and to apply the resulting data so as to interpret the mechanism of the sensitizing action of TEA in analogy with other types of sensitization. In view of the existence of a certain similarity between the photographic action of light (in particular light of high intensity) and the action of ionizing particles, a parallel investigation of the effect of such particles was carried out with these same emulsions.

The behavior of seven different emulsions was studied; two of these were "light" emulsions (a cinematographic emulsion of Type A and the aerophotographic emulsion, AS-1, of high sensitivity) and five were nuclear emulsions (one fine grained emulsion of Type II-9 [4] and four fine grained experimental emulsions, sensitive to protons of energies up to 15 mev, which had been synthesized in our laboratory ($\overline{d}$ = 0.25 μ). Exposure to light was carried out through a neutral gray step wedge with a constant of 0.17, use being made of a pulsed source having a flash duration of $1.2 \cdot 10^{-6}$ sec and a low voltage incandescent lamp, with exposure times ranging from 5 to 45 sec. Exposure to alpha- and beta rays was so carried out as to obtain gradations in blackening, the alpha particles of Po^{210} being employed in the one case and a beta radioactive sensitometer [5] in the other. In addition, there was exposure to the recoil electrons from a Ra + Be neutron source. Prior to exposure, the emulsions were immersed in an aqueous TEA solution in which the concentration varied from 1 to 5%, and in a number of cases to 20%, by weight, the immersion period amounting to 3 min for the light emulsions and to 10 min for the nuclear emulsions (of 50 μ thickness). Development was carried out under the conditions which were standard for each type of emulsion. The blackening was measured on a MF-2 photoelectric microphotometer.

In Fig. 1 there is shown the relation between the concentration of TEA and the sensitivity (evaluated for a density of blackening 0.5 above the background, the sensitivity of an emulsion which had not been treated with TEA being taken as a unit) of each of the investigated emulsions when exposed to light at exposure times of 5-45 sec. From these curves it is to be seen that the sensitivity increased in all of the emulsions, the increase being the larger, the smaller the initial sensitivity; for the various emulsions of low sensitivity this increase amounted to 1.5 orders. The characteristic curves for the emulsions (these are not shown here) indicate that the action of the TEA was always somewhat greater on the initial section, i. e., on the coarser emulsion crystals. It is precisely through this fact that certain differences in the effect of TEA on the nuclear emulsions can be explained. It is interesting to note that for increasing the light sensitivity the optimal concentration is of the order of 1-2%. A further rise in concentration leads to increased fogging without improving the sensitivity.

Special experiments have shown that no increase in sensitivity results from immersion in TEA after exposure, and the action of the TEA is accordingly unrelated to the development process.

In Fig. 2 there is shown the relation between the concentration of TEA and the sensitivity of one of the nuclear emulsions to various types of radiation. Here for the alpha and beta radiations, the sensitivity was again evaluated in terms of the exposure required for obtaining a density of blackening of $0.5 + D_0$; for protons the

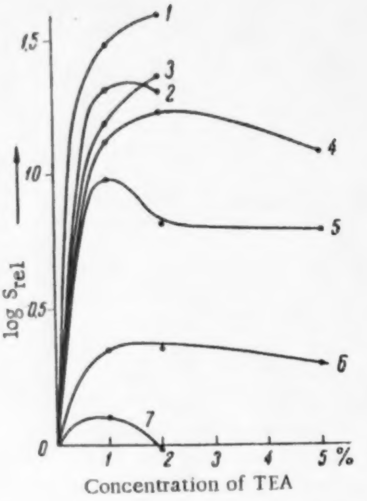

Fig. 1. The relation between the concentration of TEA and the sensitivity to light at long exposures. 1) f. e.* No. 110, 2) f. e.* No. 122, 3) f. e.* No. 124, 4) f. e.* No. 123; 5) special fine grained emulsion P-9, 6) movie film emulsion, type A, 7) aerophotographic emulsion, AS-1.

* f. e. designates a fine grained emulsion.

evaluation was in terms of the track density. The regularities of Fig. 2 are typical for the remaining test emulsions as well. In particular, the increase in sensitivity is always considerably greater for long exposures than for short impulses, this suggesting the hypersensitizing action of a preliminary short-time exposure. Another important detail of the curves of Fig. 2 is the fact that the optimal concentration for all types of radiation lies within the same limits as before, namely, 1 to 2%.

The similarity between the sensitizing action of TEA and a preliminary short-time exposure justifies the hypothesis that the role of TEA comes down to the formation of high-effective centers for fixing the conductivity electrons which arise in the emulsion crystals under the action of radiation. Earlier it could not be said whether these centers result from the growth of other centers which were already present or whether they arise through direct reaction between the TEA and the silver halide. From this point of view interest attaches to experiments in which there was studied the action of TEA on emulsion crystals from which the surface sensitivity centers had been removed. For this purpose the emulsions were treated with a relatively concentrated (5%) solution of chromic acid, H_2CrO_4. With these emulsions the following facts have been established:

1) Desensitization increases in proportion to the duration of the immersion in H_2CrO_4 and for all of the investigated emulsions with a 10-15 μ layer, passes through a maximum at a 3-5 min immersion. The decreased desensitization resulting from extended treatment with H_2CrO_4 should clearly be ascribed to the baring of the internal centers of sensitivity which accompanies the destruction of the crystal surface layers.

2) The action of TEA on an emulsion treated with H_2CrO_4 is in general considerably less than on an untreated emulsion. This is very clearly expressed with the high sensitivity emulsions (with the "light" emulsions in particular) whose crystal surfaces contain large sensitivity centers, and is much more weakly expressed with the low sensitivity emulsions in which these surface centers are small.

3) The regeneration of sensitivity which results from bathing, in TEA, emulsions which had been previously desensitized by H_2CrO_4 is considerably greater for the emulsions which have been subjected to long immersion in H_2CrO_4 than for those in which the immersion time was short. This detail is connected with the fact that the surface centers are to a considerable degree destroyed during short-time action by H_2CrO_4 and the internal centers not yet bared. Only with the baring of these internal centers does the sensitizing action of the TEA become pronounced and then in certain cases (for example, in the irradiation of a low sensitivity emulsion by electrons) it fully compensates, or even exceeds, the desensitizing action of H_2CrO_4.

4) For emulsions which have been previously desensitized with H_2CrO_4 the relation between the sensitizing action of TEA and its concentration also passes through a maximum at 1-2%, just as for emulsions which had not been subjected to treatment with H_2CrO_4.

The enumerated facts clearly show that the presence of sensitivity centers is required for the action of TEA and that the role of TEA consists in increasing the dimensions of these centers. This is also indicated by the rapid increase of fogging which is observed on increasing the concentration of TEA above the optimal value or on lengthening the time of immersion in TEA.

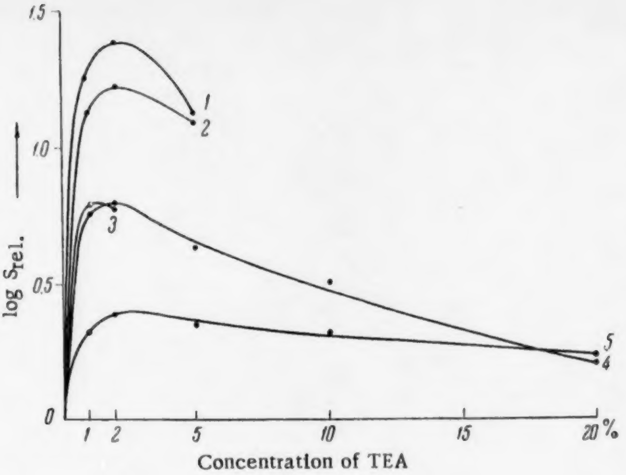

Fig. 2. The relation between the concentration of TEA and the sensitivity of the fine grained emulsion, No. 123, to various types of radiation. 1) β-Radiation from C^{14}, 2) extended exposure at low illumination (t = 45 sec), 3) brief exposure at high illumination ($t = 1.2 \cdot 10^{-6}$ sec), 4) α-radiation from Po^{210}, 5) recoil protons from a Ra + Be neutron source.

LITERATURE CITED

[1] P. Demers, Canad. J. Res. A25, 233 (1947).

[2] A. P. Zhdanov, L. I. Shur, and V. V. Volina, Trans. RIAN 7, vol. 1, 276 (1956).

[3] N. A. Perfilov, E. I. Prokof'eva and N. R. Novikova, Trans. RIAN 8 (1958).

[4] N. A. Perfilov, E. I. Prokof'eva, and N. R. Novikova, Trans. RIAN 7, vol. 1, 257, 261 (1956).

[5] A. L. Kartuzhanskii and B. P. Soltitskii, J. Scientific and Appl. Photog. and Cinematog. 2, 167 (1957).

Received July 11, 1957

THE PROBLEM OF THE REACTION PATH FOR CONTACT OXIDATION ON SEMICONDUCTING CATALYSTS

(THE EXAMPLE OF THE OXIDATION OF BENZENE)

I. I. Ioffe and F. F. Vol'kenshtein

(Presented by Academician P. A. Rebinder, July 8, 1957

In recent years the works of numerous authors [1-4] have shown that the vapor phase oxidation of hydrocarbons by molecular oxygen proceeds on semiconducting catalysts through a system of side reactions rather than through a series of successive transformations.

Actually, up to the present time there has been no attempt to explain theoretically the differences in the paths followed by the oxidation processes on the various semiconducting catalysts. It has seemed worthwhile to attempt an interpretation of these phenomena from the point of view of the electron theory of catalysis which has been developed by one of us [5-7]. The simplest aromatic hydrocarbons (benzene, naphthalene) are suitable materials for the development of the reaction mechanism, since with these substances clear-cut reaction paths have been marked out for the heterogeneous-catalytic and the homogeneous processes.

In the vapor-phase contact oxidation of benzene and naphthalene by molecular oxygen on the oxides of vanadium, tungsten, molybdenum and uranium, maleic and phthalic anhydrides, derivatives of furane, stable under the conditionsof oxidation, are, respectively, formed in considerable quantity.

On the other hand, by oxidizing benzene or naphthalene on copper (cuprous) oxide, it is comparatively easy to obtain complete oxidation of all of the hydrocarbon which enters into reaction. The oxides of manganese and nickel act similarly.

These various reactions embrace a wide range of temperatures beginning at relatively low values (approximately 200°) and going up to 400-600° (the region of additive conduction).

Since it is known that V_2O_5, WO_3, MoO_3 and UO_3 are, as a rule, electron semiconductors and that CuO, Cu_2O, NiO and, obviously, MnO_2 are hole semiconductors, it is probable that there is some relation between the catalytic action of these two groups of oxides and their electronic or hole properties. The present paper represents an attempted investigation in this direction.

The heterogeneous catalytic oxidation of benzene on copper oxide (copper lattice) is, to a certain extent, similar to the homogeneous oxidation, the latter proceeding according to a chain mechanism with rupture of the C—H bond and the initial formation of phenyl radicals [8, 9]. Phenol is found here among the reaction products and a considerable fraction of the benzene is oxidized to carbon monoxide. The formation of phenolic products during the oxidation of benzene on cuprous oxide has been noted by E. I. Orlov [10]. According to the observations of Ia. S. Levin, I. G. Kronich and one of the present authors, the oxidation of a mixture of benzene and water vapor by oxygen on a copper surface at 660° results in the formation of 0.3 mole% of phenol, 1.2 mole% of condensed materials containing diphenyl,and 6.4 mole% of the oxides of carbon.

In the catalytic oxidation of benzene on vanadium catalysts, maleic anhydride (1,4-dihydrofurandione) is the principal product, 1,4-benzoquinone being formed to a considerably smaller extent. The existence of different reaction paths on the two types of catalysts is also confirmed by other examples. During its oxidation on vanadium catalysts, naphthalene is converted with high yields into phthalic anhydride (2,3-phenylene-1,4-dihydrofurandione), neither naphthols nor reaction products from the naphthyl radicals (dinaphthols) being formed. According to the data of Grigor'ev and Borzenko [11], resorcin on copper and copper-chromium catalysts yields tetraoxydiphenyl, a product of the recombination of dioxyphenyl radicals; on vanadium catalyst, however, this reaction is not observed.

In conformity with these observations, we consider it permissible to advance certain hypotheses concerning the possible mechanisms of the oxidation of benzene on electron and on hole semiconductors as represented by vanadium pentoxide and copper (cuprous) oxide respectively.

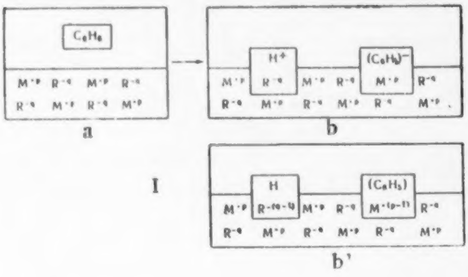

I

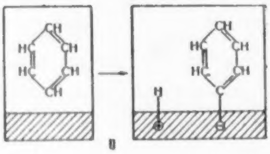

II

We start from the supposition that the adsorption of benzene results in the rupture of one of the bonds in the molecule, the resulting free valence being saturated by a free valence of the catalyst. There are two, and only two, possibilities here: the adsorption can lead to the rupture of either the C—H or the C—C bonds of the benzene molecule.

As an adsorbent we shall consider a crystal of the type M_mR_r (M being the symbol for the metal and R the symbol for the metalloid), which we shall imagine to be built up from the ions M^{+p} and R^{-q} ($pm = rq$). Most of the semiconductors which are used as catalysts (oxides, sulfides) can be supposed to have lattices of this type.

We shall first consider adsorption accompanied by the rupture of the C—H bond. In this case, adsorption leads to the dissociation of the benzene molecule into two ions, as is shown in Scheme I. We note that Scheme I, b could be replaced with the equivalent Scheme I, b'. In symbols of the electronic theory of catalysis, the mechanism represented by Scheme I could be described as by Scheme II. Here, the very act of adsorption presents us with the generation of two oppositely charged valences on the catalyst surface [7], i. e., with the formation of a pair, electron + hole, the electron fulfilling the function of a positive valence, and the hole — a negative valence. These valences bind to themselves the C_6H_5 and H radicals which thus are present on the surface as valence-saturated and, at the same time, electrically charged structures.

The mechanism for adsorption accompanied by the rupture of the C—H bond which is represented by Scheme II (or, what amounts to the same thing, by Scheme I) can apply to both electron and hole semiconductors. The difference between the electron and hole semiconductors appears in the following step. This subsequent step is the interaction of the resulting surface compounds with the free, stray valences of the catalyst. This is shown by Scheme III, a referring to the case of electron semiconduction, and b to hole semiconduction. Thus (and this is essential), the electrically neutral surface radical, which in Scheme III, b is shown inside of the dotted frame, is one that is produced on a hole semiconductor and is practically incapable of formation on the electron type of semiconductor.

We shall now consider that adsorption of the benzene molecules which is accompanied by the rupture, not of the C—H, but of the C—C bond. In the symbolism of the electronic theory, the mechanism of this type of adsorption is represented by Scheme IV. Here, as well as in the preceding case, the act of adsorption leads to the generation of positive and negative valences on the catalyst surface, the negative valence (a hole) remaining free and the positive valence (an electron) uniting with the benzene molecule to bind this latter onto the surface and at the same time convert it to an electrically charged surface radical (ion radical), as is shown in Scheme IV. In actuality, the C—C bond of the benzene molecule involves two paired electrons. Such a bond can be ruptured by a lattice electron (a positive valence of the catalyst) replacing the electron of one of the C atoms and pairing up with the electron of the other C atom. As a result, instead of the two C atoms being bound to one another, one of these C atoms is bound to the lattice and the benzene molecule thereby acquires a free valence. This type of adsorption mechanism with rupture of the C—C bond can apply to both electron and hole semiconductors. On

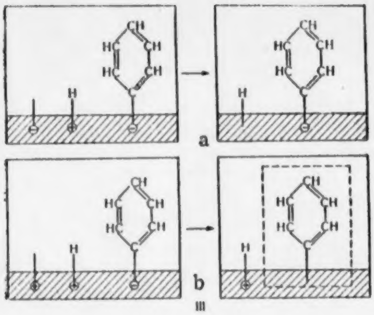

III

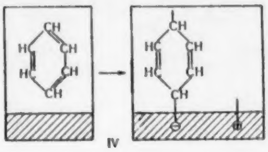

IV

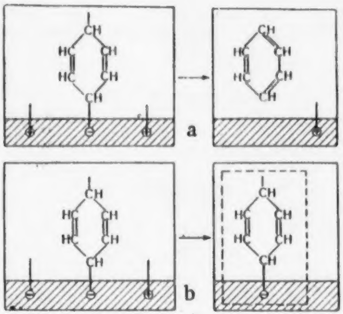

V

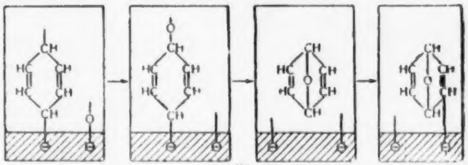

VI

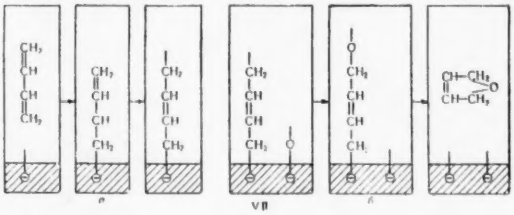

a VII б

a hole semiconductor, the resulting ion radical is, however, of low stability. As a result of its interaction with a free negative valence of the catalyst (i. e., with a free hole) such an ion radical is again desorbed as an electrically neutral benzene molecule, as is shown in Scheme V, a. On the other hand, such surface ion radicals prove to be stable in the case of electron semiconductors. In this instance interaction with a free valence of the catalyst does not lead (V, b), to the desorption of the ion radical, but to the annihilation of two oppositely charged valences of the catalyst.

Thus a surface ion radical such as is shown within the dotted frame of Scheme V, b is found almost exclusively on the electron, and not at all on the hole semiconductor. Radicals of the two different types shown inside the dotted frames of Schemes III,b and V, b lead to reaction in two different directions and the reaction path is thus the result of the electronic nature of the catalyst.

Phenyl radicals formed on the surface of a hole semiconductor (Scheme III, b) are capable of entering into all reactions in which they participate under homogeneous conditions [8]. In addition to the products of complete oxidation there are formed phenol, diphenyl and other condensation products which are observed in practice.

The sequence of reactions of the ion radicals which are formed on an electron semiconductor (Scheme V, b) is less clear since, up to the present time, the intermediate products in the chain of reactions leading to the formation of maleic anhydride have not been separated. As has been shown by one of us [8], it is very likely that the initial step involves formation of a dihydroendoxybenzene containing a furan cycle, as shown in Scheme VI. Further oxidation of this compound to maleic anhydride should proceed rather smoothly [12-13].

The hypothetical mechanisms which have been considered here are of course highly schematic. They merely indicate a path toward the understanding of the action of electron and hole semiconducting catalysts in the oxidation of benzene.

The idea that catalytic oxidation proceeds by the union of an oxygen atom at the double bond on electron semiconductors and by the rupture of the C—H bond on hole semiconductors can be used to explain certain facts from the practice of the catalytic oxidation of hydrocarbons. For example, the observation of Brenton [14] that butadiene, as compared with butane, is relatively easily oxidized to maleic anhydride on V_2O_5 becomes understandable from Scheme VII, which is impossible for butane. Likewise the oxidation of propylene into acrolein on a copper catalyst poisoned with selenium

[15], the formation of benzaldehyde during the oxidation of toluene on copper [10], and the low yield of phthalic anhydride in the oxidation of o-xylene on a vanadium catalyst [8] all become understandable.

LITERATURE CITED

[1] L. Ia. Margolis and O. M. Todes, J. Appl. Chem. 6, 1043 (1948); S. Z. Roginskii and L. Ia. Margolis, Bull. Acad. Sci. USSR, Div. Chem. Sci. 1955* 624.

[2] I. I. Ioffe and Iu. G. Sherman, J. Phys. Chem. 29, 4, 692 (1955).

[3] P. H. Calderbank, Ind. Chem. No. 7, 291 (1952).

[4] C. G. B. Hamar, Swensk. Kem. Tid. 64, 165 (1952).

[5] F. F. Vol'kenshtein, J. Phys. Chem. 26, 1462 (1952); 27, 159, 163 (1953); 28, 422 (1954); Bull. Acad. Sci. USSR, Div. Chem. Sci. 1953* 788, 972; Symposium, Problems of Kinetics and Catalysis 8 (1955), p. 79.

[6] F. F. Vol'kenshtein and S. Z. Roginskii, J. Phys. Chem. 29, 485 (1955).

[7] V. V. Voevodskii, F. F. Vol'kenshtein, and N. N. Semenov, Symposium, Problems of Chemical Kinetics, Catalysis and Reactivity 1955, p. 423.

[8] I. I. Ioffe, Ibid., p. 232.

[9] I. I. Ioffe, Ia. S. Levin et al., J. Phys. Chem. 28, 1386 (1954).

[10] E. I. Orlov, J. Russ. Phys.-Chem. Soc. 40, 1142, 1158 (1908).

[11] N. E. Grigor'ev and L. A. Borzenko, Bull. Kharkov Univ. 11, 127 (1954); Referat Zhur. Khim. No. 26, 45, 842 (1955).

[12] S. A. Giller and M. V. Tarvid, Bull. Acad. Sci. Latvian SSR No. 11, 89 (1952).

[13] S. A. Giller, M. V. Tarvid, and P. F. Kalnin', Bull. Acad. Sci. Latvian SSR No. 11, 57 (1952).

[14] R. H. Brenton, Wan Shen-Wu, and B. F. Dodge. Ind. and Eng. Chem. 44, 594 (1952).

[15] L. F. Marek, Ind. and Eng. Chem. 43, 9, 1991 (1951).

Received April 24, 1957

The Voroshilov Scientific-Research Institute for
Organic Intermediates and Dyestuffs and
The Institute of Physical Chemistry of the Academy
of Sciences of the USSR

---

* See C. B. translation.

CAPILLARY CONTRACTION DURING THE DRYING OF JELL FILMS AND DISPERSED POROUS BODIES

M. S. Ostrikov, G. D. Dibrov, and E. P. Danilova

(Presented by Academician P. A. Rebinder, July 18, 1957)

Modern concepts of the influence of a liquid medium on the properties of a solid body [1, 2] have been fruitfully employed for explaining the mechanism of the setting and hardening of cement and this, in turn, has led to the discovery of the possibility of regulating these processes [3-5].

The equally important phenomenon of concrete corrosion is analyzed at the present time in the light of these ideas. Under isothermal conditions and in the absence of chemically aggressive agents, adsorption and solvate layers have been shown to play a decisive role in this complex process. Their action appears with especial clarity in the results of rapidly altering the wetting and drying of cements and many similar natural and artificial materials.

The effect of water and of the materials dissolved in it on solid bodies is known as the adsorptional decrease of strength (Rebinder effect) [1]; it consists in a weakening of the intermolecular structural bonds and a swelling and disintegration of the structure itself as a result of interaction with the surrounding liquid medium. In the very transition from wetting to drying, capillary forces arise which act in the air—water interface and continually increase in magnitude. The action of these forces is directed toward a condensation (compression) of the hydrophilic desiccated body, a fact which is indirectly confirmed, for example, by the volume decrease which accompanies the drying of dispersed bodies such as concrete despite their considerable structural rigidity. Support of this conception of the role of the capillary forces is also found in the well-known method for obtaining xerogels (aerogels) from hydrogels through the replacement of a polar medium by a nonpolar one by passing through a series of intermediate media. These forces which are responsible for shrinkage, cracking and warping, for the production of strains and the formation of voids and internal fissures during the drying of jellies, and for other important phenomena as well, have not been directly studied up to the present time. Recently there has been pointed out the vital role which these forces play in forming the active surfaces of certain adsorbents [6], and catalysts [7].

By a direct, although summary, method we have detected and studied those forces, designated as the forces of capillary contraction (F_σ), which arise under dynamic conditions in drying films of high molecular and dispersed systems. The kinetics of their development during the drying process has been investigated.

It should be noted that although the great importance of the role of capillary forces acting in the surface at the air—liquid interface is acknowledged, it is still necessary to take into account the cohesive interaction between the macromolecules or particles of the solid phase. This force acts through the liquid molecular layers in very narrow openings, pores and microfissures where the properties of the liquid on the solid surface are altered and there is a corresponding increase in the force of capillary contraction. To a certain degree, the forces of coagulation attraction also appear here. As the liquid residues are removed, the influence of the surface of the solid phase gradually makes itself felt to a greater and greater extent. The capillary forces disappear at absolute desiccation and the remaining effect is that of the intermolecular (cohesional) forces in their pure form. Thus the investigated force of capillary contraction is a complex quantity requiring a most thorough study.

Measurements were carried out on various high polymer films and dispersed systems using an apparatus which permitted the determination of F_σ over the entire course of the drying process, shrinkage being prevented in the direction of action of the forces which were being evaluated. Specimens were prepared in the form of strips, using powdered cement with a small addition of pulverized asbestos fibers (1.3%) which acted as a micro-protective medium to prevent accidental fissuring and thus considerably increase the reproducibility of the results. During drying in the dispersed condition, the pure asbestos itself almost completely failed to show forces of capillary contraction.

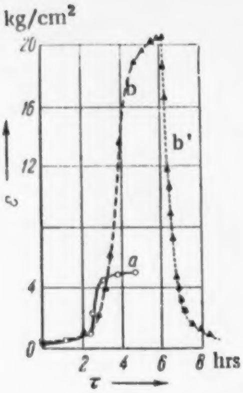

Fig. 1. a) Time of treatment, 22 hrs; b) 161 hrs; b') the rapid fall in F_σ resulting from the action of water vapors.

In Fig. 1, the ascending curves show the development of the forces of capillary contraction during the drying of two cement specimens which had been previously held for hardening in a moist medium for various periods. By comparing these two curves it is possible to see the effect of the hardening time of the cement on the forces of capillary contraction. It was also established that, up to setting, these forces were but weakly manifest in the drying cement.

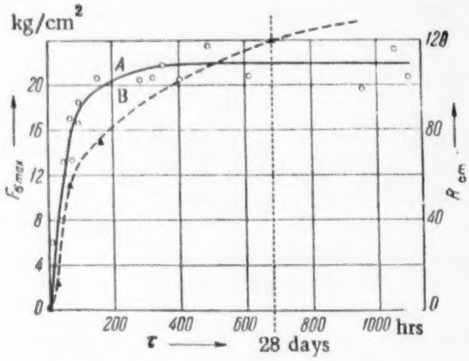

Fig. 2. The relation between the time of preliminary hardening and: A) the maximum value of the forces of capillary contraction; B) strength. 28 days is the standard time of hardening up to grade strength.

The dependence of F_σ on the time of preliminary hardening of cement specimens was investigated in detail. The experimental results obtained for specimens whose various times of hardening ranged over an interval of more than 1000 hrs are presented in Fig. 2 (A). For comparison there is given the curve B, which shows the increase in the strength of specimens which were prepared from a cement solution and had the form of cubes 3 cm on an edge. The analogous course of these two curves supports our argument [8] that the development and consolidation of the structure leads to an increase in F_σ. The true value of F_σ continually increases with the development of the microstructure but there is at the same time an increase in the resistance of the structure to the compressing action of the forces which are under study. It is clear that the value determined is essentially the difference of these two opposing forces. Initially the forces of capillary contraction predominate in this difference. After the maximum has been attained, there is an alteration in the relationship of these forces. On being considerably extended, i. e., with further increase in the structural strength, Curve A must begin to fall as a result of the disappearance of the meniscuses. From this it is easy to understand the inversion in the positions of the end segments of the curves in Fig. 2.

For each specimen, and at any stage in the drying up to attainment of the maximum of the force F_σ, the value of this force is rapidly reduced to zero by the action of water vapors under isothermal conditions. This diminution is indicated in Fig. 1 by the dotted falling branch b'. The water, adsorbing from the vapor and then undergoing capillary condensation, fills even the narrowest portion of the microfissures to bring about a decrease in the structural strength (in the general sense) and diminish the forces of capillary contraction, completely eliminating these latter in individual sections. The structural strains can then relax to zero. If the same specimen is again subjected to drying, F_σ rises to its previous maximum value. This takes place much more rapidly than it did the first time, a fact which indicates the presence of a moisture reserve in the deep-lying layers of the specimen .

There can be a repeated alteration between drying and the action of water vapors. This acts on the cement just as does a disintegrating, alternating internal mechanical effect, being accompanied by a gradual accumulation of irreversible structural changes, a decrease in the strength and an irreversible increase in volume [7]. This culminates in the formation and development of cracks. The role of the forces of capillary contraction in the processes of corrosion of concretes is here very clear.

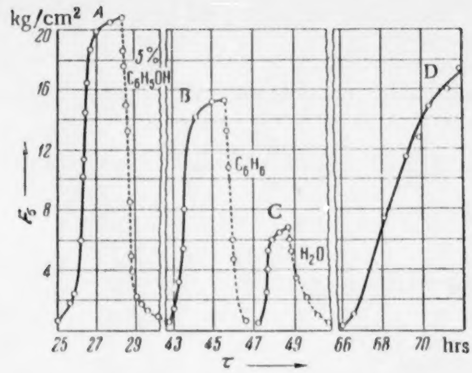

Fig. 3. The effect of the variation of the molecular nature of the liquid medium on F_σ. A) The ascending branch is for the second drying and the descending is for the decrease of F_σ under the action of the vapors of a 5% aqueous phenol solution; B) the maximum value of F_σ in the third drying is diminished by the action of sorbed layers of phenol, the descending branch showing the decrease in F_σ under the action of benzene vapors; C) the maximum is still further diminished under the influence of the adsorbed layers of phenol and benzene and under the action of pure water vapors the decrease in F_σ is very gradual because of the hysteresis of wetting; D) final drying.

These ideas concerning the surface mechanism of the action of the forces which are under study and the possibility of their control are confirmed by the experimental data which are presented in Fig. 3. Just as in Fig. 1, the rising segments of these curves reflect the increase of F_σ during the drying of a single specimen and the dotted, falling curves show its decrease under the action of the vapors of water and other liquids. Curve A indicates the course of this relationship in the second cycle (drying–wetting) in which the diminution of F_σ results from the action of mixed vapors of water and phenol (5% in the liquid phase). The influence of the phenol is manifest in a decreased surface tension in the surfaces of the contracting water meniscuses, or webs, between the neighboring structural elements and, possibly, in a certain hydrophobization of the surface of the solid phase and an additional adsorptional diminution of the structural strength. This effect is indicated in the subsequent drying (Curve B), in which the maximum proves to be considerably lowered.

A still greater lowering of the maximum value of F_σ is obtained by the subsequent action of benzene vapors on this same specimen (Fig. 3, C). This combined action of phenol and benzene proves, however, to be very transient so that after the specimen has been held, as usual, overnight in an atmosphere of water vapors, F_σ in the following drying once more rises and approaches the previous maximum value. The action of water vapors proceeds somewhat more slowly in the cycle C because of the considerable hysteresis in the wetting of the surface which is occupied by benzene and the phenol residues. There is also a retardation in the increase in F_σ during the following (final) drying, D. These results permit one to speak with assurance of the possibility of successfully combatting the destructive action of the forces of capillary contraction through the application of stable hydrophobizing sorbents.

It must be kept in view that in the course of the drying processes there can be in a single system a simultaneous and complex interaction between the forces due to capillary contraction and those arising from the strength-decreasing adsorbed hydrate layers. This is realized quite markedly in rapid drying, the considerable forces of capillary contraction and the high moisture gradients then causing great strains to develop in the surface layers of the structure, "predisintegration zones" (Rebinder) being produced. Here along the freshly formed surfaces in the nucleating region of microfissures there penetrate molecular layers of water and dissolved materials, these coming from the deeper lying, more moist layers to exert a disintegrating action. Thus the alteration of drying and wetting acts the more aggressively the sharper is the transition between the opposing processes which are replacing one another.

Generalizing the results which are presented here and those which have been obtained earlier, it can be said that under atmospheric conditions and with sharp changes in the moisture of the surface layers of cement and other organic and inorganic hydrophilic materials, there occurs a continuous and very complex interplay of the oppositely directed but continuously connected molecular-surface forces of capillary contraction on the one hand and of the strength-diminishing adsorbed hydrate layers on the other. The action of these forces is the cause, not only of the corrosion of concrete, but also of many other phenomena in nature and in technical work.

The authors express their deep appreciation to Academician P. A. Rebinder for his interest in this work and for his very valuable suggestions.

LITERATURE CITED

[1] P. A. Rebinder, Jubilee Collection Dedicated to the 30th Anniv. of the Great Oct. Socialist Rev.* (Acad. Sci. USSR Press, 1947),part 1, p. 533.

[2] P. A. Rebinder, Symposium, New Physicochemical Methods for Investigating Surface Phenomena [in Russian] (Acad. Sci. USSR Press, 1955), p. 5.

[3] P. A. Rebinder and G. I. Loginnov, Problems in the Construction of Electrostations (Materials Conference) [in Russian] (Acad. Sci. USSR Press, 1955).

[4] N. V. Mikhailov and P. A. Rebinder, Colloid J. 17, vol. 2 (1955).**

[5] P. A. Rebinder, Papers on the Chemistry of Cement [in Russian] (Moscow, 1956), p. 125.

[6] I. E. Neimark, Progr. Chem. 25, vol. 6, 748 (1956).

[7] I. V. Rostovtseva, Dissertation, Rostov-on-Don State Univ. 1954.

[8] M. S. Ostrikov and B. I. Razvodov, Communications, D. I. Mendeleev All-Union Chem. Soc. 1, 22 (1947); M. S. Ostrikov, S. I. Pakhomov, and N. P. Sinel'nikov, Bull. Acad. Sci. USSR, Phys.-Tech. Sci. Series No. 4, 119 (1956).

Received July 17, 1958

The Rostov-on-Don State University and
The Rostov Engineering-Construction Institute

---

* In Russian.

** Original Russian pagination. See C. B. translation.

THE COEFFICIENT OF DIFFUSION IN LIQUIDS

G. M. Panchenkov

(Presented by Academician A. V. Topchiev, July 8, 1957)

In our work on the theory of liquid viscosities [1] we have started from the supposition that there is a force of attraction acting between "conjugate" molecules which are separated from one another by a distance greater than the equilibrium distance, r_0, at which the potential energy is a minimum. Bonding will arise here between two molecules belonging to two liquid layers if these molecules have a total kinetic energy less than the energy of binding and certain supplementary conditions are fulfilled, and this system then behaves as a single "kinetic unit" over a finite period of time which is not in excess of the half period of vibration.

On the other hand, bonding cannot arise if the total kinetic energy of a pair of oppositely moving molecules is greater than the bond energy, and the molecules will then move independently of one another. Under the definite conditions which are indicated below, such molecules will have the possibility of passing from one liquid layer into a neighboring one, i. e., diffusion can take place. Thus the mean kinetic energy associated with the individual molecule which is capable of diffusion will be equal to

$$\varepsilon_D \geqslant {}^1/_2\,\varepsilon_0, \qquad (1)$$

ϵ_0 being the energy of a single liquid molecular bond.

As has been shown in our papers [1],

$$\varepsilon_0 = 2\lambda_{i0}/\gamma, \qquad (2)$$

λ_{i0} being the internal latent heat of evaporation of the liquid in vacuum and at absolute zero, and γ the coordination number of the liquid.

Since the distance between the molecules of a liquid is less than their linear dimensions, it follows that one other condition must be fulfilled in order that molecules pass from one layer into another: it is necessary that two molecules lying side by side in that layer into which the given molecule is diffusing should be separated by a distance which would permit the penetration of the latter, i. e., by a distance larger than the equilibrium distance.

The probability of such a favorable molecular distribution will be designated by W. From these considerations it follows that diffusion in liquids differs from diffusion in gases by the fact that all of the molecules in low pressure gases participate in the diffusion, whereas in the liquid diffusion involves only those molecules having energies in excess of ϵ_D and lying opposite to a free space. For gaseous "self diffusion," the kinetic theory leads to the following expression for the diffusion coefficient

$$D = {}^1/_8\,\pi\lambda\bar{c}, \qquad (3)$$

λ being the mean free path corresponding to the transfer of matter and $\bar{c}$, the mean molecular velocity.

According to what has been said above, it is necessary to write for liquids:

$$D = 2Wr_0\bar{c}, \qquad (4)$$

with r_0 representing the half equilibrium distance between molecular centers, the molecules being, for simplicity, considered as spherical. Since real molecules are not spherical they will be replaced in the following calculation by spheres of such effective radius as would lead to the behavior shown by the real molecules. The coefficient $\pi/8$ will be descarded since it is necessary to consider the molecular motion in two directions only (toward and away from the next layer). In liquids, the value of λ cannot exceed the mean distance between molecular centers. Transitions over greater distances have very low probabilities. The quantity r_0 can be easily determined from

$$r_0 = \sqrt[3]{3v_m / 4\pi N_0}, \tag{5}$$

v_m being the gram-molecular volume of the liquid and N_0, the Avogadro Number. The mean velocity is

$$\bar{c} = \int\limits_{c_D}^{\infty} \frac{c\,dN}{N}, \tag{6}$$

c_D being the velocity of those molecules having kinetic energies equal to ϵ_D. Setting the expression for dN/N from the Maxwell Distribution Law into Eq. (6), integrating and passing from velocities to energies, we obtain:

$$\bar{c} = \frac{2}{\sqrt{\pi}} \sqrt{\frac{2RT}{M}}\, e^{-\varepsilon_0/2RT} \left[\frac{\varepsilon_0}{2RT} + 1\right]. \tag{7}$$

In view of the fact that the separating of molecules from one another to free a place for a diffusing molecule is a process analogous to evaporation, the quantity W can be written as

$$W = e^{-2\lambda_{iT}/\gamma RT}, \tag{8}$$

λ_{iT} being the internal latent molecular heat of evaporation at the working temperature.*

Setting (5), (7) and (8) into (4) we obtain the final equation

$$D = 4\, \frac{\sqrt[3]{3}\, \sqrt{2R}}{\sqrt[3]{4\pi N_0}\, \sqrt{\pi}}\, \frac{v_m^{1/3} T^{1/2}}{M^{1/2}}\, e^{-2\lambda_{iT}/\gamma RT} e^{-\varepsilon_0/2RT} \left[\frac{\varepsilon_0}{2RT} + 1\right]. \tag{9}$$

Since Eq. (4) has been written for the process of "self diffusion," all of those quantities which characterize molecular properties (v_m, M, λ_{iT}, ϵ_0) must be considered as mean values for the substances composing the system.

Equation (9) gives the relation between the diffusion coefficient and the temperature, pressure and concentration, the quantities v_m and λ_{iT} being functions of the temperature, pressure and concentration and ϵ_0, a function of the concentration and pressure.

Under the condition that only neighboring molecules interact and that the relative concentration of neighbors is the same around any one molecule, it follows that for a solution consisting of two components [2]:

$$\varepsilon_0 = \varepsilon_{011} c_1^2 + 2\varepsilon_{012} c_1 c_2 + \varepsilon_{022} c_2^2, \tag{10}$$

ϵ_{0ij} being the bonding energy between molecules of the ith and jth types and c_1 and c_2, the mole fractions of the two solution components. Depending on the relationship between the quantities ϵ_{011}, ϵ_{022} and ϵ_{012}, the diffusion

---

* It is obvious that this expression is only valid when the attractive forces sharply diminish with increasing distance, i. e., when these forces can be neglected at an intermolecular distance equal to the molecular diameter. In the opposite case a quantity $\lambda < \lambda_{iT}$ enters into the exponent.

Calculated and Experimental Values of Diffusion Coefficients and Coordination Numbers of Liquids

T, °K	o-xylene—n-xylene					C_2H_5OH—C_2H_5OD					C_6H_6—C_6H_5D				
	d^t_4, $\frac{g}{cm^3}$	$\lambda_i T$, $\frac{cal}{mole}$	$D_{cal}\cdot 10^5$, cm²/sec	$D_{exp}\cdot 10^5$, cm²/sec	coordination no.	d^t_4, $\frac{g}{cm^3}$	$\lambda_i T$, $\frac{cal}{mole}$	$D_{cal}\cdot 10^5$, cm²/sec	$D_{exp}\cdot 10^5$, cm²/sec	coordination no.	d^t_4, $\frac{g}{cm^3}$	$\lambda_i T$, $\frac{cal}{mole}$	$D_{cal}\cdot 10^5$, cm²/sec	$D_{exp}\cdot 10^5$, cm²/sec	coordination no.
288.2	—	—	—	—	—	0.7936	7387	0.800	0.800	6.436	0.88408	7619	1.88	1.88	6.136
293.2	0.8704	9702	1.122	1.124	7.790	—	—	—	—	—	—	—	—	—	—
298.2	—	—	—	—	—	0.7851	7324	1.040	1.050	6.452	0.87340	7478	2.52	2.15	5.910
303.2	0.8627	9515	1.482	1.397	7.678	—	—	—	—	—	—	—	—	—	—
308.2	—	—	—	—	—	0.7764	7261	1.329	1.310	6.410	0.86268	7336	3.31	2.40	5.670
318.2	—	—	—	—	—	0.7677	7176	1.692	1.700	6.444	0.85190	7188	4.29	2.67	5.444
323.2	0.8462	9286	2.323	2.026	7.512	—	—	—	—	—	—	—	—	—	—
343.2	0.8297	8996	3.540	2.849	7.320	—	—	—	—	—	—	—	—	—	—

coefficient will vary linearly with the concentration or will pass through a maximum, a minimum or a point of inflection. The quantity ϵ can be easily evaluated from the temperature dependence of the liquid density and viscosity [1].

For a system of two liquids it is necessary to calculate the quantity λ_{iT} by a similar equation.

The extent to which the predictions of Eq. (9) agree with experiment can be seen from Table 1.

The diffusion coefficients of o-xylene in n-xylene were measured in our laboratory by T.S. Maksareva and V. V. Erchenkov, using a microdiffraction method. The values of the binding energy, ϵ_0, which were required for these calculations were found from the temperature dependence of the liquid density and viscosity [6] and proved to be as follows:

System	o-xylene—n-xylene	C_2H_5OH—C_2H_5OD	C_6H_6—C_6H_5D
ϵ_0, cal/mole	2117.7	3393.6	2343.1

In order to evaluate the diffusion coefficients it is necessary to know the coordination number, γ, for the system in question. This quantity has been evaluated from Eq. (9) using the diffusion coefficients at 15 and 20°.

Table 1 shows that in the systems o-xylene—n-xylene and benzene—monodeuterobenzene the calculated diffusion coefficients exceed the experimentally determined values more and more as the temperature rises. This is to be explained, on the one hand, by inaccuracies in the determination of the latent heat of evaporation at various temperatures and, on the other hand, by the fact that the coordination numbers of the liquids fall with rising temperatures. Small variations in the coordination numbers lead to a considerable change in the calculated diffusion coefficients. Values of the coordination numbers, as calculated from Eq. (9) and the experimentally determined diffusion coefficients, are presented in Table 1.

It is to be seen from this data that the coordination numbers for the systems o-xylene—n-xylene and C_6H_6—C_6H_5D diminish only slightly with temperature, but this leads to a discordance between the calculated diffusion coefficients and the experimental data when the coordination number found at any one temperature is employed in the calculations. In the case of the C_2H_5OH—C_2H_5OD system the coordination number is practically independent of the temperature and if any one of its values over a given temperature interval is employed in the calculations, the calculated diffusion coefficients prove to be in good agreement with the experimental data.

Similar calculations were carried out by us for a number of other systems and the agreement between theory and experiment proved to be good.

The quantity

$$-2\lambda_{iT}/\gamma T = \Delta S, \tag{11}$$

ΔS being the entropy change accompanying bond formation, calculated on a 1 mole basis. The temperature dependence of this quantity is covered by the expression

$$\frac{\partial \Delta S}{\partial T} = \frac{2}{\gamma} \frac{\Delta C_{\text{eq}}}{T}, \tag{12}$$

Δc_{eq} being the difference of the heat capacities of the equilibrium vapors and the liquid. If it is assumed that the quantity Δc_{eq} is independent of the temperature, then

$$\Delta S = \alpha \ln T + \beta. \tag{13}$$

α and β being constants.

Setting (11) into (9) and taking (13) into account, we obtain

$$D = 4 \frac{\sqrt[3]{3}\sqrt{2R}}{\sqrt[3]{4\pi N_0}\sqrt{\pi}} \frac{v_m^{1/3} T^{1/2}}{M^{1/2}} e^{\beta/R} \left[\frac{\varepsilon_0}{2RT} + 1\right] e^{(\alpha T \ln T - \varepsilon_0)/RT}. \tag{14}$$

According to calculations on many liquids

$$v_m^{1/3} T^{1/2} \left[\frac{\varepsilon_0}{2RT} + 1\right] \approx \text{const.} \tag{15}$$

Thus Eq. (15) can be written in the following form

$$D = A e^{(\alpha T \ln T - \varepsilon_0)/RT}, \tag{16}$$

where

$$A = \frac{4\sqrt[3]{3}\sqrt{2R}\, v_m^{1/3} T^{1/2}}{\sqrt[3]{4\pi N_0}\sqrt{\pi}} \left[\frac{\varepsilon_0}{2RT} + 1\right] e^{\beta/R}.$$

As calculation shows, Eq. (16) is in good agreement with experimental data.

If Eq. (16) is written in logarithmic form,

$$\ln D = \ln A + \frac{\alpha \ln T}{R} - \frac{\varepsilon_0}{RT}, \tag{17}$$

results, from which it is obvious that over a wide interval of temperatures ln D does not vary linearly with 1/T. Over narrow temperature intervals it can be considered that ln T = a − b/T, a and b being constant coefficients, and thus over such temperature intervals ln D does depend linearly on 1/T.

LITERATURE CITED

[1] G. M. Panchenkov, J. Phys. Chem. 24, 1390 (1950); Proc. Acad. Sci. USSR 50, 329 (1945); 51, 361, 453 (1946); J. Phys. Chem. 20, 811, 1011 (1946); 21, 187 (1947); The Theory of Liquid Viscosities [in Russian] 1947; Proc. Acad. Sci. USSR 63, 701 (1948).

[2] G. M. Panchenkov, Proc. Acad. Sci. USSR 51, 453 (1946); J. Phys. Chem. 20, 1011 (1946); The Theory of Liquid Viscosities [in Russian] 1947.

[3] K. Graupner and E. R. S. Winer, J. Chem. Soc. 1952, 1145.

[4] The Physicochemical Properties of the Individual Hydrocarbons [in Russian] vol. 5 (Moscow, 1954).

[5] Technical Encyclopedia, Handbook of Physical, Chemical and Technical Data [in Russian] 7 (Moscow, 1937).

[6] G. M. Panchenkov, J. Phys. Chem. 24, 1390 (1950).

Received June 25, 1957

The M. V. Lomonosov State University, Moscow

THE NATURE OF THE INTERACTION OF ANIONS AND WATER MOLECULES IN SOLUTION

Iu. P. Syrnikov

(Presented by Academician I. I. Cherniaev, June 17, 1957)

In considering hydration it is customary to make no fundamental distinction between the hydration of anions and cations, and the water molecule is looked upon as being a rigid dipole. Although such a simplified model is to a certain degree acceptable for the calculation of thermochemical quantities, it is inadequate for the study of the acoustical properties of solutions of strong electrolytes and for many problems. At the present time the acoustical properties of such solutions are being investigated in the Physics Faculty of the Leningrad State University [1-3]. It was the purpose of the present work to obtain the additional information which is required for the understanding of certain of these properties.

It is known that the water molecule consists of one electrically negative oxygen and two protons, that it possesses clearly expressed electropolar properties and that it can form hydrogen bonds. It is precisely through these bonds that the molecules are bound together in liquid water. At the present time [4], the hydrogen bond is considered to be closely related to the donor-acceptor bond. The formation of a hydrogen bond in the complex A—H . . . B—R results in a redistribution of the electron density, especially in the atom B; the H atom plays the role of an "acceptor," the B atom, the role of a "donor" and the electron of the B atom is then shared between it and the proton. This is the most fundamental characteristic of the hydrogen bond and one which sets it apart from other types of intermolecular action.

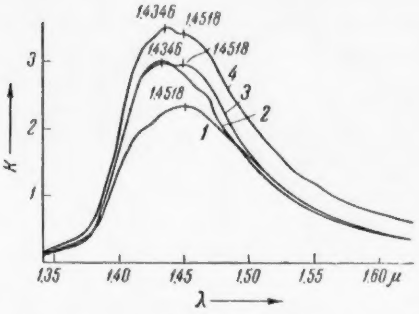

Fig. 1. The relation between the absorption coefficients of solutions and the wavelength. 1) Absorption in pure water; 2) absorption in a $NaNO_3$ solution (13.7 moles H_2O per 1 mole $NaNO_3$); 3) absorption in a $NaNO_3$ solution (31.6 moles H_2O per 1 mole $NaNO_3$); 4) absorption in a KNO_3 solution (31.6 moles H_2O per 1 mole KNO_3).

On dissolving in water, a strong electrolyte dissociates into an anion and a cation. The anion and cation interact with the water molecules and it is this interaction which is designated as hydration. It should be noted that various authors have read different meanings into the concept of hydration. By hydration we shall understand the interaction of an ion with the water molecules which are neighboring to it.

It is the electronegative part of the water molecule, or its oxygen, which approaches a cation in hydration, and thus the interaction between the cation and the water molecules is of a sharply different character from the binding of two water molecules with one another. The structure of the hydrate cloud of a cation must therefore differ from that of pure water.

The situation is different in the case of the hydration of an anion. The anion is a negative atom (or group of atoms) and it is the positive part, or the proton, of the water molecule which approaches it, several molecules of water simultaneously coming up to the anion to bind various protons to it. The excess electrons of the anion are shared between these several protons and the interaction between the anion and the water molecules participating in its hydrate layer is of the donor-acceptor type. For each "acceptor," or proton, there corresponds a fraction of an electron (at least such is the case with mono- and divalent anions). By their nature, such bonds are very close to, if not identical with, those existing between the molecules in pure water, i. e., they resemble hydrogen bonds.

The quantitative treatment of this type of interaction presents very great difficulties since it calls for the solution of the quantum mechanical many-body problem. It is of interest to experimentally confirm the suppositions advanced above. It is known that spectroscopy, and the spectroscopy of infrared absorption in particular, furnish the most direct method for detecting and studying hydrogen bonding. Although much work has been carried out on the infrared absorption specra of ionic solutions [5, 6], the O−H absorption band in solutions of strong electrolytes has not been specially investigated with a view to studying the interaction between water molecules and anions.

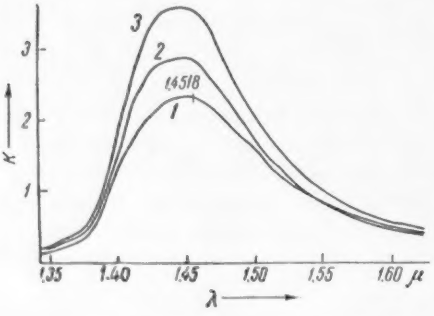

Fig. 2. The relation between the absorption coefficients of chloride solutions and the wavelength.
1) Absorption in pure water; 2) absorption in a NaCl solution (10.7 moles H_2O per 1 mole NaCl); 3) absorption in a KCl solution (16.5 moles H_2O per 1 mole KCl).

We have undertaken measurements of the infrared absorption of ionic solutions in the region of 1.35-1.60 μ (the first overtone of the O−H group).

It is known that the narrow band in the region of 1.36 μ which corresponds to the free O−H group in the water molecule gives way to a wide band displaced in the direction of longer wavelengths when this group enters into hydrogen bonding this displacement being approximately proportional to the energy of the hydrogen bonding. For any system it is thus possible to judge from the infrared absorption spectra the presence of free O-H groups and O-H groups which have entered into hydrogen bonding, and to approximately evaluate the energy of this bonding.

The measurements were carried out in the Academy of Wood Technology, using a manually operated spectrophotometer with a glass optical system. This spectrophotometer had a high resolving power (4 A per division of the recording cylinder), a grating with 600 lines per 1 mm being used as a spectral analyzer. Solutions of 8 salts with 4 different anions were studied. The results of these measurements are shown in Figs. 1-4. In calculating the absorption coefficients for these solutions, the optical density of each solution was divided by the concentration of the solvent water. From the data it is to be seen that even at saturation, the absorption bands in these ionic solutions, lie, to a first approximation, in the same region as the band in pure water, i. e., water molecules which are bound to the anions interact with the latter in approximately the same manner as do interacting water molecules. For certain anions the energy of this interaction is somewhat different from the energy of bonding between water molecules. Thus, for a saturated $NaNO_3$ solution the maximum of the absorption band lies at $\lambda = 1.4346\,\mu$ while the absorption maximum for water is at 1.4518 μ. For a KNO_3 solution in which the salt concentration is less, the absorption band had two maxima: one of these corresponds to the maximum in the saturated $NaNO_3$ solution and the other, to the maximum in pure water. A similar situation is observed in $NaNO_3$ solutions at a molar concentration equal to that of the KNO_3 solution.

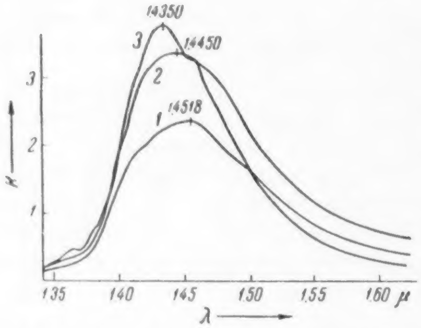

Fig. 3. The relation between the absorption coefficients of iodide solutions and the wavelength.
1) Absorption in pure water; 2) absorption in a CdI_2 solution (29.1 moles H_2O per 1 mole CdI_2); 3) absorption in a KI solution (9 moles H_2O per 1 mole KI).

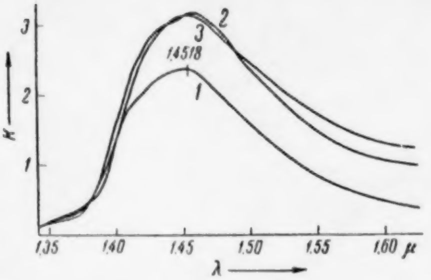

Fig. 4. The relation between the absorption coefficients of sulfate solutions and the wavelength. 1) Absorption in pure water; 2) absorption in a $MgSO_4$ solution (34.4 moles H_2O per 1 mole $MgSO_4$); 3) absorption in a $CdSO_4$ solution (25 moles H_2O per 1 mole $CdSO_4$).

It can thus be considered that the maximum at $\lambda = 1.4346\mu$ corresponds to the vibrational frequency of that O–H group which interacts with the NO_3^- anion. In the chlorides and sulfates the maximum of the absorption band falls at the same wavelength as in pure water. The absorption band in the KI solution has a maximum at $\lambda = 1.4350\mu$. The absorption band in CdI_2 is also displaced toward the region of shorter wavelengths although the salt concentration in this solution is considerably less than that of the KI solution, and the band corresponding to pure water predominates.

On the basis of these facts it can be said that there is agreement between the spectroscopic data and the hypothesis as to the interaction of anions with water molecules which has been advanced here. Since the water molecules interact with the anions and exist, from the direction of the latter, under conditions similar to those prevailing in pure water (i. e., they are bound to the anions by hydrogen bonds) it can be further supposed that the structure of the hydrate cloud of the anion would resemble that of water itself. From this point of view there are to be understood the results of A. Pasynskii [7] who, in determining hydration numbers acoustically, from the relative decrease in solution compressibility as compared with pure water, was led to values considerably lower than those obtained from thermochemical data. Such results can be explained by the fact that the water molecules are bound to anions by hydrogen bonds and the compressibility of the hydrate cloud of the anions is approximately the same as that of water itself, anionic hydration being accompanied by no diminution of the compressibility.

We express our deep thanks to I. G. Mikhailova, V. P. Karelova and V. V. Bazilevich for their valuable advice and suggestions.

LITERATURE CITED

[1] I. G. Mikhailov, J. Phys. Chem. 30, vol. 2, 466 (1956).

[2] I. G. Mikhailov and V. A. Shutilov, Bull. Leningrad Univ., Phys. and Chem. Series No. 16, vol. 3, 16 (1956).

[3] I. G. Mikhailov and Iu. P. Syrnikov, Symposium, The Application of Ultrasonics to the Investigation of Matter, vol. VI, Moscow Oblast Ped. Inst. 1958.*

[4] N. D. Sokolov, Progr. Phys. Sci. 57, 205 (1955).

[5] R. B. Barnes, R. C. Gore, U. Liddel, and V. Z. Williams, Infrared Spectroscopy (N. Y., 1944).

[6] L. Kellner, Reports on Progress in Physics 15 (1952).

[7] A. Pasynskii, J. Phys. Chem. 11, 606 (1938).

Received June 10, 1957

The A. A. Zhdanov State University, Leningrad, and
The Leningrad Academy of Wood Technology

---

* In Russian.

THE INFLUENCE OF SUBSTITUENTS ON THE PROPERTIES OF THE MOLECULES OF THE PARA-DISUBSTITUTED DERIVATIVES OF BENZENE

P. P. Shorygin and Z. S. Egorova

(Presented by Academician B. A. Kazanskii, September 11, 1957)

The frequencies of the more or less localized atomic vibrations in groups joined to the benzene ring are altered markedly by the introduction of a second substituent into the ring in the para-position. Thus under the influence of such substituents, the frequency of the valence vibration in the nitro group can be changed by 10-50 cm^{-1}. It is clear that these alterations are principally related to changes in the rigidity of the N—O bond.

The absorption spectra and certain other optical properties of the aromatic compounds are more sensitive to the effect of substituents than are the frequencies in the vibrational spectra. Despite difficulties in interpretation, the absorption spectra have in certain cases given valuable information concerning not only the excited state of the molecule but its basic state as well.

By drawing on various methods of investigation, it is possible to obtain a more well-rounded concept of the mutual effects of the atoms in complex molecules, the possibility being offered at the same time of verifying through one method conclusions drawn on the basis of another. This latter is particularly desirable in view of the fact that each of these methods has its own limitations and possible sources of errors and discrepancies.

In this work there have been studied the spectra and dipole moments of the para-derivatives of nitrobenzene, , with various substituents, X. The nitro group is one of the most electronegative radicals and in the derivatives of nitrobenzene the effect of electronegative substituents is expressed with particular clarity.

In Table 1 there are presented values of the following quantities:

1. The displacement ($\Delta\omega$) of the frequency of the symmetric valence vibration of the nitro group which results from the introduction of a substituent X, these values being obtained from measurements of the Raman spectra in benzene solutions (in both benzene and cyclohexane solutions, the frequency of the nitro group in unsubstituted nitrobenzene is equal to 1347.5 cm^{-1}).

2. The integral intensity coefficient I_{NO_2}, of this line in the Raman spectra, as measured in benzene solutions by a photographic method, using the mercury line 4358 A for excitation of the spectra ($^1/_{100}$ of the intensity of the 313 cm^{-1} line in CCl_4, reduced to 1 mole, was chosen as the unit; the accuracy was ± 10%).

3. The chracteristics of the intense absorption bands in the ultraviolet region; the wavelength λ, in A; the value of $\epsilon/1000$, ϵ being the molar (decimal) absorption coefficient at the band maximum; the oscillator strength, f, according to measurements in heptane solutions and the difference ($\Delta\lambda_1$) between the wavelengths of the intense absorption bands for the compounds 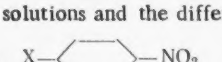 and $PhNO_2$, as obtained from measurements on benzene solutions. These spectra were measured with an SF-4 photoelectric spectrophotometer.

4. The difference ($\Delta\mu$) between the observed value of the dipole moment of 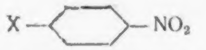 and the vector sum of the moments of 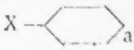 and 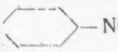 (in debyes, according to the data of

TABLE 1

Group X in X–⬡–NO_2	$\Delta\omega_{NO_2}$ cm^{-1}	I_{NO_2}	Ultraviolet spectra (in heptane)					$\Delta\lambda_1$ in benzene	$\Delta\mu$	α_{para}
			λ_1	$\frac{\varepsilon_1}{1000}$	f_1	λ_2	$\frac{\varepsilon_2}{1000}$			
–H	0	700	2520	9.6	0.27	—	—	0	0	0
$-SO_2R$	3	~800	2470	11.5	0.34	—	—	—	—	0.6
–F	0	900	2580	8.5	0.23	—	—	~80	0.1	0.05
$-CH_2Cl$	0	1100	2580	12	0.31	—	—	~80	0.1	0.2
$-CCl_3$	—	—	2550	14.5	—	—	—	—	—	0.4
–COOEt	~0	—	2540	13.5	0.36	—	—	~50	—	0.5
–CHO	~–2	1000	2580	16.5	0.41	—	—	~80	–0.1	0.4
–Cl	~–1	~1300	2670	11	0.29	—	—	130	0.15	0.2
–Br	~3	~1300	2700	12	0.30	—	—	170	0.15	0.2
–R	–2	1400	2650	10.2	0.28	—	—	130	0.1	–0.15
$-CR_3$	–2	1500	2650	10.5	0.29	—	—	130	0.1	–0.20
$-\underset{\cdot}{C}\cdot NR_2$	–2	1600	2620	~9	—	—	—	—	—	—
–I	0	2700	2880	12.5	0.32	2210	8	340	0.4	0.3
–C=C	—	—	2910	16	—	—	—	—	0.35	~0
–OH	–5	3200	2850	10.5	0.26	2190	9	390	0.7	–0.35
–OPh	–3cy	~3200	2930	15	0.37	2200	14	420	0.6	–0.3
–OR	–5	4000	2920	12	0.29	2200	9	460	0.45	–0.3
–SH	–7.5	5700	3050	12.7	0.32	2240	6	560	—	0.1
–Ph	–1.5	5500	2940	18	0.45	2220	12	440	0.3	~0
–NR·CHO	–6	5500	3040	12	0.35	2240	10	540	—	—
–SR	–3	16000	3260	15	0.30	2200	~7	780	0.6	–0.05
–C=C–Ph	–4.5cy	20000	3300	19	0.52	2370	13	720	0.5	—
–NHCOR	—	—	3000	15	—	~2200	12	—	—	~0
$-NH_2$	–12	20000	3190	15	0.37	2260	8	820	1.0	–0.65
–N : N·Ph	—	—	3250	24	0.64	2140	13	—	0.4	0.6
–NH·NH·Ph	–16	38000	3250	15	0.45	2300	14	890	—	—
$-NH\cdot NH_2$	–20	45000	3350	17	0.43	~2200	8	870	~2	–0.6
–NH·Ph	~–12cy	—	3530	21	0.42	2350	8	—	0.8	—
$-NR_2$	–28	170000	3540	20	0.41	2260	8	1210	1.4	–0.7
Ferrocene	~–10	—	3900 3120	4 16	0.06 0.37	2800	11	—	—	—

Notes. 1. The H atoms attached to carbons have been omitted in the formulas; R is the methyl group; for the unsubstituted nitrobenzene in benzene solution, λ_1 = 2620 A. The data for the 2200 A band are considerably less trustworthy than those for the neighboring bands. Weak absorption bands have not been taken into account. Values accompanied by the letters cy were obtained from measurements on cyclohexane solutions. In the compounds in which X = Cl, Br, NH·Ph, CHO and COOEt, the NO_2 frequency is split into 2 components; the table gives the total intensity and mean value of these frequencies.

2. T. I. Ambrush and M. A. Geiderikh synthesized the nitrodiphenyl, nitrohydrazobenzene, nitroazobenzene, nitroamine and certain other compounds and A. N. Nesmeianov and R. V. Golovna kindly supplied the p-nitrophenylferrocene, and the authors take this opportunity to express their thanks to them.

the literature on dipole moments in benzene), this quantity characterizing the additional displacement of the electrons (in the direction from X to NO_2) which results from the simultaneous presence of the two substituents X and NO_2.

5. The Hammett constant, σ_{para}, determined principally from the dissociation constants of X–⬡–COOH.

In characterizing the relationship between the properties of the compound X–⬡–NO_2 and the type of substituent X, we note that the electronegative and electropositive substituents affect the reactivity in opposite directions and the optical properties (I_{NO_2}, λ_1, f_1 and the polarizability) in the same direction.

The effect of an electropositive substituent on the X–⬡–NO_2 molecule is in every instance considerably greater than the effect of an electronegative substituent (the situation is reversed with the X–⬡–NR_2 molecule).

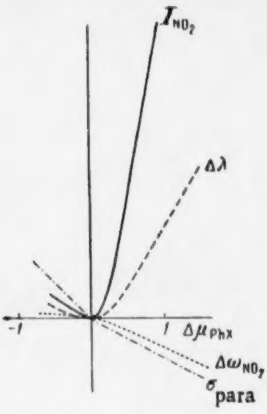

Fig. 1.

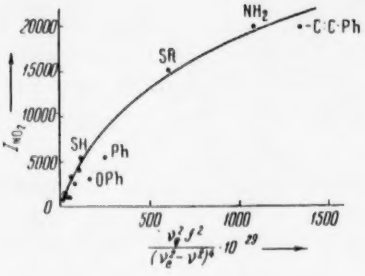

Fig. 2.

Figure 1 shows qualitatively the tendencies which are noted in the relationships between the quantities I_{NO_2}, λ_1, ω_{NO_2} in the X— — NO_2 molecules, the constants σ_{para} for the substituents X, and the anomalies in the dipole moments of the compounds PhX ($\Delta\mu_{PhX}$), as obtained from the data of [1].

The points corresponding to the values of I and λ for the substituents $C_6H_5\cdot$ and $CH_2:CH\cdot$ lie considerably above the indicated curves; such substituents have little influence on the dipole moments and chemical properties and strongly affect the optical characteristics.

Alkyl groups X act as weak electropositive groups in affecting the dipole moments of the nitro compounds. For molecules with branched and unbranched alkyl groups the difference between the investigated parameters (Table 1) does not exceed the possible experimental error. Differences in the values of the constant σ are more substantial, though it should not be forgotten that these quantities have a very approximate significance. It is not unusual that values of σ be given in the literature with third place accuracy, a fact which can easily lead to confusion and give the impression of great possibilities for the exact and independent characterization of substituents.

In any case, the passage from $-CH_3$ to $-CMe_3$ results in a quite insignificant alteration in the effects arising from the mutual influence of groups. The effect of methylation increases in the order $CH_3 < OH < SH < NH_2$.

The influence of Z on the spectra of the Z·NH— —NO_2 molecule is similar to the effect of this same substituent in the Z— —NO_2 molecule, but more weakly expressed. Through the bridges $\cdot CH_2\cdot$ and $\cdot CH_2\cdot CH_2\cdot$, the effect of the substituent Z is very small.

Sequences arranging the electropositive substituents according to their effect on the dipole moments, the frequency and intensity of the line of the nitro group, the absorption spectra and the exaltation of refraction (as well as those in terms of the values of the constant σ_{para}), are very similar. The divergencies which are noted in individual cases are frequently to be explained by differences in the experimental conditions (different solvents, etc.). It is, unfortunately, difficult to realize completely uniform conditions of measurement. Differences in the experimental conditions are not, however, the principal sources of these divergencies. It can be noted that the OH group influences dipole moments more strongly than does OR group whereas with the optical properties this effect is reversed. Essential differences can be noted between the effect of substituents on the chemical and the physical properties of a series of compounds (for example, ones in which X = SH, SR, C:C, C:C·Ph).

A more complete concordance is observed in the effects of substituents on the various optical properties of the X— —NO_2. molecule. On the other hand, considerable divergencies are noted with the monoderivatives of benzene PhX [1], this being related to the fact that in the compound $X\cdot C_6H_4\cdot NO_2$ (in distinction to PhX) there are close-lying intense absorption bands whose influence on the optical properties is predominant.

Judging from the data on the relation between I_{NO_2} and the frequency of the incident light and the dispersion of the refractive indices, it can be concluded that the intense absorption band of the para-derivatives of nitrobenzene which lies in the 2500-3500 A region is the one which principally determines the line intensity of the nitro group and the dispersion. According to calculations for n-nitroaniline, this band accounts to the extent of 90% for the observed dispersion at 4500-5500 A and the exaltation of refraction resulting from the introduction of the amino group (~ 8 cc).

The differences in the intensities of the NO_2 Raman line in the various compounds

is greater than it should be according to the relation $I \sim (\nu_1^2 - \nu^2)^{-2}$ and, as is to be seen from Fig. 2, less than would be expected from the expression

$$I \sim \nu_1^2 f_1^2 (\nu_1^2 - \nu^2)^{-4}. \tag{1}$$

These relations are obtained by differentiating the expression for the polarizability $\alpha = \text{const} \cdot \sum_e \frac{f_e}{\nu_e^2 - \nu^2}$ with respect to the nuclear coordinate:

$$\frac{\partial \alpha}{\partial Q} = \text{const} \sum_e \frac{1}{\nu_e^2 - \nu^2} \frac{\partial f_e}{\partial Q} - \frac{2\nu_e f_e}{(\nu_e^2 - \nu^2)^2} \frac{\partial \nu_e}{\partial Q}$$

(ν being the frequency of the incident light and $\underline{e}$, the index of the electron level).

Equation (1) more or less satisfactorily describes the relation between I_{NO_2} and ν (at constant ν_1, i. e., with one and the same compound), but, as is to be seen from Fig. 2, gives large divergencies when ν_1 varies at constant ν (i. e., in a series of nitro compounds with varying ν_1, excitation of the spectrum being by one and the same frequency ν). If account is taken of the differences in the anisotropy of the scattering tensors, these divergencies are still more pronounced.

These divergencies do not show the character of a completely random distribution of points, a gradual departure from linearity being noted. Within the framework of the semiclassical treatment of Raman spectra, this divergence can be ascribed to the diminution of the quantity $\partial \nu_e / \partial Q$ in a series of nitro compounds (in compounds showing closely neighboring absorption bands, damping can also result).

According to one approximation for the symmetrical vibration of the nitro group of n-nitroaniline, the derivative of the polarizability of the molecule with respect to the nuclear coordinate q_{N-O} amounts to about 100 A^2. If it is assumed that

$$\frac{\partial \alpha_X}{\partial q} = -14 \cdot 10^9 f_1 \nu_1 (\nu_1^2 - \nu^2)^{-2} \frac{\partial \nu_1}{\partial q} \ \text{Å}^2,$$

and account is taken of the fact that the absorption band is polarized in the X direction (setting for f_1 the value 3·0.37) the derivative $(\partial \nu_1 / \partial q)_0$ should be of the order of 20,000 cm^{-1}/A; such a value is completely possible for variations of the equilibrium distance of separation between the N and O atoms in electronic excitation of the order of magnitude 0.03-0.1 A.

LITERATURE CITED

[1] P. P. Shorygin and Z. S. Egorova, Proc. Acad. Sci. USSR 117, 5 (1957).*

Received June 27, 1957

The L. Ia. Karpov Physicochemical Institute and
The N. D. Zelinskii Institute of Organic Chemistry
of the Academy of Sciences of the USSR

---

* See C. B. translation.

ELECTRONOGRAPHIC INVESTIGATION OF THE STRUCTURE OF THE MOLECULE OF LITHIUM OXIDE

P. A. Akishin and N. G. Rambidi

(Presented by Academician N. N. Semenov, August 2, 1957)

There have hitherto been no experimental data in the literature on the structure of the molecule of lithium oxide; all that was known was an approximate calculated value of the Li—O distance, obtained by Brewer and Mastick [1] on the basis of an ionic model. The obtaining of experimental data on the configuration and geometrical parameters of the lithium oxide molecule in the gas phase is of interest in connection with the theory of the structure of the molecule, and is necessary for the calculation of thermodynamic functions and of the equilibrium constants of some gas reactions by the methods of statistical thermodynamics.

This paper deals with the experimental determination of the geometrical structure of the Li_2O molecule by means of the diffraction of fast electrons by a stream of vapor.

The measurements were made with an MGU electronograph for investigating the molecular structures of substances of low volatility, fitted with a sector device. A high temperature evaporator with an ampule heated by electron bombardment was used to produce the stream of vapor; lithium oxide was evaporated from a molybdenum ampule at 1300-1350°. The electronograms of the vapor were recorded on diapositive film (GOST 2817-50, light sensitivity 0.7 units) with an exposure of 15 sec to 1.5 min. Since under the experimental conditions the intensive radiation from the red-hot evaporator strongly illuminated the film, completely masking the diffraction pattern, we used special methods for screening the emulsion — a) aluminum foil, 5-7μ thick, was stretched taut on a metal frame and placed close to the emulsion, and b) a thin layer of black India ink was sprayed onto the emulsion and washed off before development. Preliminary observations of the electronograms of crystalline ZnO and $CdCl_2$ vapor, using normal and screened film, showed the applicability of this technique.*

The lithium oxide (purity 99.62%) was made by thermal decomposition of lithium nitrate in a silver crucible.**

Using an s^2-sector, seven sets of electronograms of lithium oxide vapor on 2-3 films were obtained, each with a different electron wavelength in the range 0.0443-0.0488 A (λ was determined from electronograms of standard crystalline ZnO, obtained before and after the electronograms of the vapor).

The electronograms of the vapor had 3-4 clear interference rings, and the diffraction pattern showed a distribution of intensity of scattered electrons little different from a damped harmonic function (Fig. 1).

It should be noted that, though the sector method provided good electronograms of lithium oxide vapor, the use of a microphotometer for their interpretation offers no particular advantages over the visual method for determinations of simple molecular structures (for linear tetratomic molecules see [3], for complex molecules [10]).

The electronograms of lithium oxide vapor were analyzed by the method of radial distribution [4] and by the method of successive approximations [5]. The radial distribution curve was calculated by the equation

---

* Details of the apparatus and the method of investigating inorganic compounds of low volatility are described in [2].

** Our thanks are due to I. A. Savich', V. G. Kniaginina, and N. I. Pecherova who prepared this material in the School of Inorganic Chemistry of the Chemical Faculty of the MGU.

$$D(r) = \int\limits_{0}^{s_{\max}} sI(s)\, e^{-\alpha s^2} \sin sr\, ds, \qquad (1)$$

where I(s) is the intensity of molecular scattering, determined visually;

$$s = \frac{4\pi}{\lambda} \sin \vartheta/2;$$

λ is the electron wavelength; ϑ is the angle of scattering; and α is a factor defined by the relation $\exp[-\alpha s_{\max}^2] = 0.1$. In the construction of the radial distribution curve, the experimental I(s) curve was extrapolated into the region of small s values ($0 \leq s \leq \leq 4$) as part of a theoretical scattering curve, based on a model of the Li_2O molecule with an angle of 110° between the bonds (the reasons for choosing this model are discussed below). The radial distribution curve had two peaks at values of r equal to 1.82 and 2.90 A (Fig. 2). The peak at 1.82 A was taken as corresponding to the interatomic distance Li–O. The peak at 2.90 A, from correlation of the areas under the distribution curve (ratio of areas found 9.4, theoretical 8.6), would naturally be assumed to represent the interatomic distance Li . . . Li; but its magnitude corresponded with the so-called diffraction effects, so that the above identification of the peak, although convincing enough, cannot be considered as complete. If it is accepted that the interatomic distance Li . . . Li in the lithium oxide molecule is 2.90 A, then the angle between the Li–O bonds should be close to 110°; this agrees with the information in the literature that the valency angle of oxygen is between 100 and 120° in most of its compounds which have been investigated [12]. It should also be noted that there is a theoretical basis [11] for supposing that the structure of the lithium oxide molecule should be similar to that of its nearest analog, the water molecule.

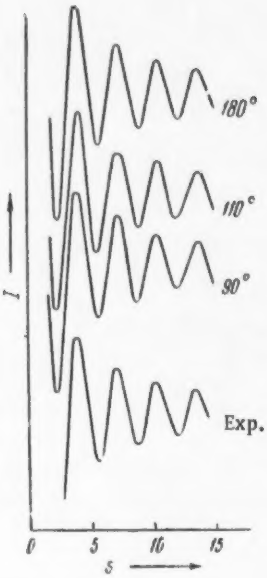

Fig. 1. Theoretical curves for the intensity of scattering of electrons, for different models of the Li_2O molecule , and the experimental distribution of intensity (visual appraisal of electronograms obtained by the sector method).

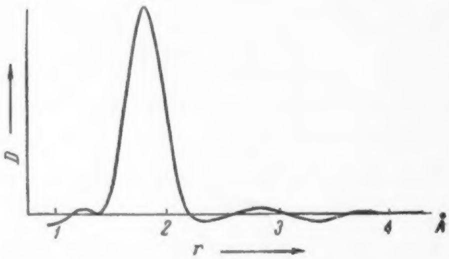

Fig. 2. Radial distribution curve of the Li_2O molecule, constructed in accordance with Eq. (1).

For the interpretation of the electronograms of lithium oxide vapor by the method of successive approximations [5], theoretical curves of I(s) were constructed for a series of molecular models with angles between the bonds varying in 10° steps between 180 and 90°. Figure 1 shows these theoretical curves for angles of 180, 110 and 90°, and it is evident that the I(s) curve is not very sensitive to changes in valency angle, a fact which is connected with the small part played by the Li . . . Li spacing in the total scattering by the Li_2O molecule. Indeed, the ratio of the scattering powers of the atomic nuclei corresponding to the interatomic distances Li–O and Li . . . Li, is

$$\frac{2z_{\mathrm{Li}}z_{\mathrm{O}}r\,(\mathrm{Li}-\mathrm{Li})}{z_{\mathrm{Li}}^2 r\,(\mathrm{Li}-\mathrm{O})} = 8.6,$$

so that the characters of both the theoretical and experimental I(s) curves are basically determined by scattering by the atomic nuclei forming Li–O linkages. Similar results have been observed in the electronographic investigation of vapor molecules of fluorides of elements in the 2nd group of the periodic system [3], in that the characters of their I(s) curves show little variation with a change in the valency angle F–Me–F, which was determined in this case by the radial distribution curve. Starting with the most probable of the triangular molecular models of lithium oxide, with an angle of 110° between the Li–O bonds, we have used the method of successive approximations (Table 1) to obtain the value 1.82 ± 0.02 A for r(Li–O).

TABLE 1

Molecule of Li_2O; $r_{theor.}$(Li–O) = 2.00 A

Max.	Min.	s_{theor}	s_{exp}	$\frac{s_{theor}}{s_{exp}}$	r_{exp} (Li–O)
1		3.95	4.40	0.898	1.80
	2	5.41	6.02	0.899	1.80
2		6.98	7.62	0.916	1.83
	3	8.70	9.47	0.919	1.84
3		10.15	11.21	0.905	1.81
	4	11.67	12.99	0.898	1.80
4		13.42	14.66	0.915	1.83
		Average mean		0.907	1.82
		Mean error		±0.008	± 0.01 A

Comparing this figure of 1.82 A for r(Li–O) of gaseous Li_2O molecules with the interatomic distance 2.00 A (calculated from the lattice constant a = 4.619 A [6]) in the crystal lattice, we obtain the characteristic difference of about 10%, which is recorded in the literature as the difference between the gas molecule and the crystalline lattice for a number of inorganic compounds.

It is interesting to compare the experimental value of the interatomic distance Li–O with approximate values calculated in different ways. Brewer and Mastick [1], on the basis of an ionic model, calculated that r(Li–O) = = 1.52 A. A value can be calculated from the empirical equation of Shomaker and Stevenson [7]

$$r(\mathrm{Li}-\mathrm{O}) = r_{\mathrm{Li}} + r_{\mathrm{O}} - \beta\,|x_{\mathrm{O}} - x_{\mathrm{Li}}|,$$

where r_{Li} and r_O are the covalent radii of the lithium and oxygen atoms, x_{Li} and x_O are the electrononegativities of the atoms, and β is an empirical constant. Using the values $r_{Li} = 1.34$ A, $r_O = 0.73$ A [8], $x_{Li} = 0.95$, $x_O = 3.50$ [9] and $\beta = 0.09$, we obtain a figure of 1.85 A for r(Li–O) (1.92 A if β is taken as 0.06 [8]). The closeness of the experimental value of r(Li–O) to that calculated from the Schomaker-Stevenson equation, and its greater difference from that calculated on an ionic model for Li_2O, are reasons for concluding that the bonds in the lithium oxide molecule are covalent in character. This agrees with some interesting results for crystalline lithium oxide recently published by Vainshtein and Dvoriankin [13], who compared the experimental curve of $f_{el}(s)$ for small angles of electron scattering with theoretical curves calculated for structures with covalent and ionic bonds, and concluded that the bonds in Li_2O were mainly covalent in character.

LITERATURE CITED

[1] L. Brewer and D. F. Mastick, J. Am. Chem. Soc. 73, 2045 (1951).

[2] P. A. Akishin, M. I. Vinogradov, et al., Instruments and Tech. Exp. 3, 2 (1958).

[3] P. A. Akishin and V. P. Spiridonov, Crystallography 2, 475 (1957).

[4] I. L. Karle and J. Karle, J. Chem. Phys. 17, 1052 (1949); 18, 957 (1950).

[5] L. Pauling and L. O. Brockway, J. Chem. Phys. 2, 867 (1934).

[6] G. B. Bokin, Introduction to Crystallography, p. 367 (1954).*

[7] V. Schomaker and D. P. Stevenson, J. Am. Chem. Soc. 63, 37 (1941).

[8] V. Gordi, V. Smit, and R. Trambarulo, Radiospectroscopy, p. 321 (1955).*

[9] W. Gordy and W. J. O. Thomas, J. Chem. Phys. 24, 439 (1956).

[10] J. M. Hastings and S. H. Bauer, J. Chem. Phys. 18, 13 (1950).

[11] J. A. Pople, Proc. Roy. Soc. A 202, 323 (1950).

---

* In Russian.

[12] P. Allen and L. Sutton, Acta Cryst. 3, 46 (1950);

[13] B. K. Vainshtein and V. F. Dvoriankin, Crystallography 1, 626 (1956).

Received July 30, 1957

M. V. Lomonosov Moscow State University

THE VAPOR PRESSURE OF CHROMIUM OVER CHROMIUM–IRON ALLOYS IN THE SOLID STATE

E. Z. Vintaikin

(Presented by Academician G. V. Kurdiumov, July 12, 1957)

The thermodynamic investigation of chromium-iron alloys is of interest, not only for its practical importance, but because it also provides new information for the development of the theory of solid solutions. The chromium-iron system shows complete miscibility in the solid state. At temperatures below 800°, with alloys of approximately equiatomic composition, a σ-phase is formed, which appears to be a chemical compound. When stainless chromium steels are annealed at 475°, embrittlement occurs, the cause of which is the subject of various and even contradictory suggestions [1-4]. In particular, in an investigation [3] of the cause of the brittleness of chromium steels, it was stated that there was segregation of the solid solution at 475°, and that this caused the embrittlement. The authors stated that the segregation was an intermediate process preceding the formation of the σ-phase. The second phase was successfully detected [2] in an alloy containing 27% Cr after prolonged (4 years) annealing at 482°. It was found to be a solid solution of chromium and iron, with a space-centered lattice and a chromium content of 80%.

The breakdown of solid solutions with a tendency to form chemical compounds is unusual, since usually there is a negative departure from ideality and a negative heat of mixing for the formation of a chemical compound or for any increase in order, while a necessary condition for breakdown with a fall in temperature is a positive heat of mixing. A knowledge of the thermodynamic properties of the chromium-iron system could, to some extent, help to form a correct picture of the behavior of the solid solution in this case. Also, a thermodynamic investigation of a system of such unusual behavior might assist in the creation of a more exact theory of real solid solutions.

Investigations of the thermodynamic properties of the chromium-iron system have been described in the literature. In the liquid state the system has been found [5] to show small negative departures from the law of ideal solutions. A value has been obtained [6] for the activity of the iron, and heats of sublimation have also been determined for iron-chromium alloys in the temperature range 1100-1300°. Consideration of this work, from the point of view of the general thermodynamic laws, suggested that the results obtained were incorrect. Indeed, according to the results of [6], the activity of iron in an alloy containing 10% chromium exceeds unity and has a value of 2 at 1100°. If this were true, the partial pressure of iron over the alloy should be greater than the vapor pressure of the pure metal at the same temperature. The existence of several maxima and minima in the curve showing the variation of thermodynamic activity with concentration is also inconsistent with the general theory of solutions. Finally, the statement, that the heat of sublimation of iron is 156 kcal/g-atom from a 50% Cr alloy is unlikely to be correct, since this would imply a great chemical affinity between iron and chromium, which in reality does not exist.

The object of this work was the measurement of the saturation vapor pressures of chromium over chromium-iron alloys in the temperature range 1100-1400°, in order to calculate the thermodynamic functions of these solutions. Knudsen's effusion method was used, with radiometric determination of the chromium condensed on targets. The principle of the method has been described in [10], and experimental details are given in [7]. Electrolytic iron and chromium, purified in hydrogen, were used to prepare the alloys; the chromium contained the radioactive isotope Cr^{51}. The metals were melted in an alundum crucible in a helium atmosphere. In all the measurements great care was taken to prevent a reduction in the chromium content of the surface of the alloy, by having the sample in the form of small filings. Special means were also used to reduce the time for degasifying. The measurements showed that impoverishment of the surface was so slight that it could be neglected. The values found for the vapor pressures of chromium over chromium-iron alloys could be represented by the following empirical equations

$$\log P\ (\text{in bars}) - \frac{18430}{T} + 11.653 \text{ for } 21.3 \text{ atom \% chromium}$$

$$\log P\ (\text{in bars}) - \frac{18500}{T} + 11.990 \text{ for } 41.4 \text{ atom \% chromium}$$

$$\log P\ (\text{in bars}) - \frac{18670}{T} + 12.122 \text{ for } 55.2 \text{ atom \% chromium}$$

$$\log P\ (\text{in bars}) - \frac{18730}{T} + 12.234 \text{ for } 75.5 \text{ atom \% chromium}$$

$$\log P\ (\text{in bars}) - \frac{18940}{T} + 12.388 \text{ for pure chromium}$$

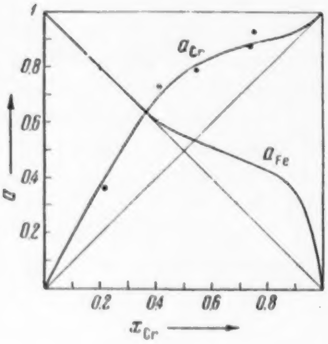

Fig. 1. Curves of thermodynamic activity in the system chromium-iron.

The results for the vapor pressure of pure chromium agree well with previous data [8, 9].

The thermodynamic activities of chromium and the heats of solution were calculated from the vapor pressure data. Figure 1 shows the variation of the activity of chromium with its molar concentration in chromium-iron alloys at a temperature of 1667°K. The same figure shows the variation of the activity of iron at 1667°K, calculated by means of the Gibbs-Duhem equation. The heats of sublimation and the partial heats of solution of chromium are shown in Table 1. The heats of solution of iron were calculated in the evaluation of the heats of solution of chromium by the Gibbs-Duhem equation.

The activities and heats of solution were used to calculate the integral molar thermodynamic functions — change in heat content ΔH and change in free energy ΔF:

$$\Delta H = x_{Cr}\Delta\overline{H}_{Cr} + x_{Fe}\Delta\overline{H}_{Fe},$$
$$\Delta F = RT\,(x_{Cr}\ln a_{Cr} + x_{Fe}\ln a_{Fe}).$$

The entropy ΔS was obtained from the well-known equation: $\Delta F = \Delta H - T\Delta S$. This function is shown in Fig. 2. It is evident from the figure that solid solutions of chromium and iron show a positive deviation from ideal behavior, and excess of thermodynamic potential over the ideal occurs in principle for the calculation of the positive heat of mixing, while the figure shows that the entropy of mixing is very close to the ideal. It should be noted that the heat of mixing curve is not symmetrical with respect to the equiatomic composition, and that the maximum lies on the chromium side. The figure shows that the alloys have a positive heat of mixing, so that chromium-iron solid solutions are subject to segregation. Extrapolation of the dependence of free energy on concentration makes it possible to

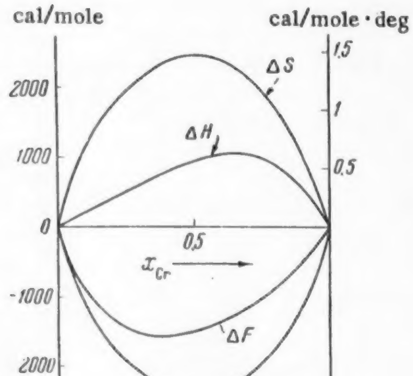

Fig. 2. Thermodynamic functions of the system chromium-iron.

TABLE 1

Mole-fraction of chromium, x_{Cr}	Heat of sublimation of chromium, kcal/g-atom	Heat of solution of chromium, $\Delta\bar{H}_{Cr}$, kcal/g-atom
0.214	84.4	+2.3
0.414	84.7	+2.0
0.552	85.5	+1.2
0.755	85.8	+0.9
1.000	86.7	0

estimate the critical temperature for breakdown, and this was found to be 600°C. It should be noted that the results in this paper indicate that the maximum of the decomposition curve is for a chromium-rich mixture.

Thus the results of this work confirm that the embrittlement at 475° is the result of a process of segregation [2-4].

It is possible, on the basis of data in the literature and the results of this investigation, that the α-solution at 475° can either change into the σ-phase or break down into two solid solutions. And, since the formation of the σ-phase proceeds extremely slowly, only the second alternative occurs in practice.

The author expresses his deepest gratitude to Academician G. V. Kurdiumov and Professor L. A. Shvartsman for their interest in this work and for a number of valuable suggestions.

LITERATURE CITED

[1] H. S. Link and P. W. Marshall, Trans. Am. Soc. Metals 44, 549 (1952).

[2] R. M. Fisher, E. J. Dulis, and K. G. Carrol, J. Metals 5, 690 (1953).

[3] A. J. Lena and M. F. Hawkes, J. Metals 6, 607 (1954).

[4] E. Baerlecken,and H. Fabritius, Stahl und Eisen 77, 1774 (1955).

[5] A. P. Liubimov and A. A. Granovskaia, The Use of Radioactive Isotopes in Metallurgy 34, 95 (1955).

[6] L. I. Ivanov and M. P. Matveeva, Proc. Acad. Sci. USSR 111, 1271 (1956).*

[7] Iu. V. Kornev and V. N. Golubkin, Physics of Metals and Metallography 1, 286 (1955).

[8] R. Speiser, H. L. Johnston, and P. Blackburn, J. Am. Chem. Soc. 72, 4142 (1950).

[9] E. A. Gulbransen and K. F. Andrew, J. Electrochem. Soc. 99, 402 (1952).

[10] E. Z. Vintaikii, Proc. Acad. Sci. USSR 117, 4 (1957).**

Received August 10, 1957

Institute of Metallography and Physics of Metals of the Central Research Institute of Ferrous Metallurgy

---

* Original Russian pagination. See C. B. translation.

** See C. B. translation.

THE EFFECT OF AN EXTERNAL ELECTRIC FIELD ON THE ADSORPTIVE POWER OF A SEMICONDUCTOR

F. F. Vol'kenshtein and V. B. Sandomirskii

(Presented by Academician N. N. Semenov, July 25, 1957)

According to the electronic theory of chemisorption, the application of an electric field, in changing the concentration of free current carriers in a semiconductor, should alter its adsorptive power [1]. One of the authors has previously pointed out the possibility of the existence of this effect [2].

If a plate of semiconductor is subjected to a homogeneous electric field acting at right angles to its surface, then the concentration of current carriers will be increased on one surface and decreased on the other. The adsorptive power of each surface will change correspondingly. The changes in adsorptive power do not compensate each other, so that the total adsorptive powers of the semiconductor will be different in the presence and in the absence of the electric field.

We shall call the increase or decrease of adsorptive power in the electric field electroadsorption and electrodesorption, respectively. The object of this work is to estimate the possibility of observing this effect experimentally, which depends on the magnitude of the change in pressure in the reactor when the field is applied and the corresponding value of the field.

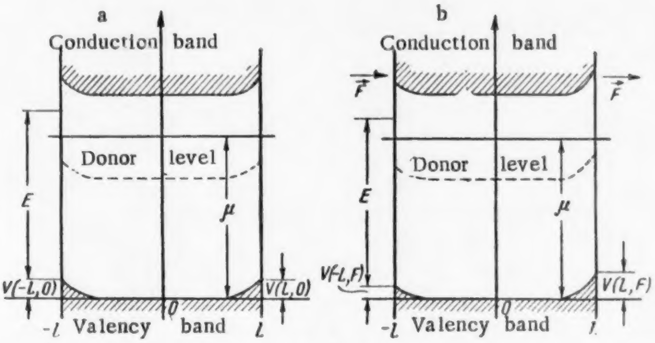

Fig. 1. Diagram of energy levels a) in the absence of an external electric field, and b) in the presence of the field.

Consider the adsorbent in the form of a plate of thickness 2L in the direction of the $\underline{x}$ axis and of much larger dimensions in the directions of the $\underline{y}$ and $\underline{z}$ axes. On the surfaces $x = \pm L$ (Fig. 1) molecules are adsorbed with a corresponding local surface energy level $\overline{E}$. To be more precise we shall consider the adsorption of acceptor molecules on a p-type semiconductor. The crystal is exposed to a homogeneous electric field of strength F, acting at right angles to the surface.

To simplify the calculation we shall make the following assumptions: a) the thickness of the crystal is much less than the length of the screening l; hence, the position (relative to the energy zones) of the Fermi level μ in the center of the crystal does not change when the field is applied; b) there is a Boltzmann distribution of electrons in all the energy levels in the crystal (both in the absence and in the presence of the electric field); c) surface zones are absent; d) there are only two types of bonds between the adsorbed molecules and the surface – "weak" and "strong" acceptor bonds [3].

A diagram of the energy levels in the absence and in the presence of the electric field is given in Fig. 1. The potential energy of an electron is designated by $V(x, F)$. We can say that $V(0, 0) = V(0, F) = 0$. Clearly $V(-L,0) = V(L,0)$.

It is supposed that the crystal is in a reactor of constant volume, v, filled with gas at pressure p_0. When the field F is applied, the gas pressure becomes p. The problem consists in determining the dependence of p/p_0 on F. From the condition for adsorptive equilibrium at not too great a pressure, we have [4]

$$N_1(0) = N_2(0) = \frac{\gamma p_0}{1-\eta(0)}, \quad N_1(F) = \frac{\gamma p}{1-\eta_1(F)}, \quad N_2(F) = \frac{\gamma p}{1-\eta_2(F)}, \tag{1}$$

where $N_1(F)$ and $N_2(F)$ are the numbers of molecules adsorbed on unit areas of the corresponding left and right-hand surfaces (Fig. 1); $\eta_1(F)$ and $\eta_2(F)$ are the fractions of the molecules which are strongly bound [5] to the corresponding surfaces [obviously $\eta_1(0) = \eta_2(0) = \eta(0)$]; γ is the adsorption coefficient of the Langmuir equation.

From the equation of state for an ideal gas and from (1), it follows that

$$\frac{p_0}{p} = \frac{1}{2}\left\{\frac{1-\eta(0)}{1-\eta_1(F)} + \frac{1-\eta(0)}{1-\eta_2(F)}\right\}. \tag{2}$$

From (2) it may be concluded that $\gamma kT \frac{S}{v} \gg 1$, where S is the area of each of the two adsorbing surfaces, k is the Boltzmann constant and T is the absolute temperature. (It may be noted that the opposite case, $\gamma kT \frac{S}{v} \ll 1$, corresponds to the disappearance of the effect when $\frac{p}{p_0} = 1$.)

If Poisson's equation is applied to the volume of the semiconductor and integrated once, then, corresponding to the two boundary conditions at $x = \pm L$, we obtain two equations containing the unknowns $\eta_1(F)$, $\eta_2(F)$ and p. These two equations, together with (2), form a complete system of equations for determining the effect under consideration. But, since it proves to be impossible to find an analytical form for the dependence of p/p_0 on F in the general case, some special cases will be considered.

Suppose that

$$\eta(0) \ll 1. \tag{3}$$

This signifies that, in the absence of the electric field, the majority of the adsorbed molecules are "weakly" linked to the surface. From (3) it follows that $\eta_2(F) < \eta(0) \ll 1$, so that (2) becomes

$$\frac{p_0}{p} = \frac{1}{2}\left[\frac{1}{1-\eta_1(F)} + 1\right]. \tag{4}$$

From (4) it is evident that $p_0/p \geq 1$, i. e., only electroadsorption can occur within the limits of this model We shall consider the case where

$$\frac{p_0}{p} \gg 1, \tag{5}$$

corresponding to a large value of the effect.

By using an obvious expression for $\eta_1(F)$ [5] and assuming (5), we obtain from (4)

$$\frac{p}{p_0} = 2e^{\frac{E-\mu+V(-L,\,F)}{kT}}. \tag{6}$$

It is easy to find an expression for $e^{-\frac{V(-L,\,F)}{kT}}$, using one of the equations obtained by applying the boundary conditions to the integrated form of the Poisson equation, and assuming that

$$\frac{|V(-L,F)|}{kT} \gg 1 . \tag{7}$$

Putting this expression in (6), we obtain a relation between the magnitude of the effect and F

$$\frac{p}{p_0} = 2\left(\frac{\varepsilon kT}{ql}\right)^2 e^{\frac{E-\mu}{kT}} \frac{1}{F^2}. \tag{8}$$

Here ϵ is the dielectric constant of the semiconductor, q is the absolute value of the charge of an electron.

It is not difficult to show that, according to (8), Assumptions (3), (5) and (7) can be interpreted as follows:

$$p_0 \gg \frac{\varepsilon kT}{4\pi q^2 \gamma l} e^{-\frac{E-\mu}{2kT}}; \tag{9}$$

$$F \gg \begin{cases} \frac{\varepsilon kT}{ql} e^{\frac{E-\mu}{2kT}} + 8\pi q \gamma p_0 & \text{when} \quad E \gg \mu; \\ \frac{\varepsilon kT}{ql} + 8\pi q \gamma p_0 & \text{when} \quad E \ll \mu. \end{cases} \tag{10}$$

Thus, under Conditions (9) and (10), the effect is large and its value is given by Eq. (8).

Some numerical values may be inserted. Suppose that $\epsilon = 10$, $T = 300°K$, $l = 10^{-4}$ cm, $\gamma = 10^{-2}$ mm Hg/A^2, $E-\mu = 0.1$ ev. Then from (9) and (10) we have $p_0 \gg 1.5 \cdot 10^{-6}$ mm Hg and $F \gg 10^2$ v/cm. This calculation shows that, under the conditions assumed, the effect of electroadsorption should clearly be detectable experimentally.

LITERATURE CITED

[1] F. F. Vol'kenshtein, Problems of Kinetics and Catalysis 8, 79 (1955).

[2] F. F. Vol'kenshtein, Problems of Kinetics and Catalysis 8, 201 (1955).

[3] F. F. Vol'kenshtein and S. Z. Roginskii, J. Phys. Chem. 29, 3 (1955).

[4] F. F. Vol'kenshtein and Sh. M. Kogan, Bull. Acad. Sci. USSR, Div. Chem. Sci. 916 (1957).*

[5] V. B. Sandomirskii, Bull. Acad. Sci. USSR, Phys. Ser. 21, 211 (1957).

Received July 18, 1957

Institute of Physical Chemistry of the Academy of Sciences of the USSR

---

* Original Russian pagination. See C. B. translation.

DEPENDENCE OF THE YIELD OF FORMALDEHYDE IN THE OXIDATION OF METHANE ON THE CONCENTRATION OF HOMOGENEOUS INITIATOR, THE AMOUNT OF INERT GAS AND THE CONDITION OF THE WALLS OF THE REACTION VESSEL

N. S. Enikolopian and G. V. Korolev

(Presented by Academician N. N. Semenov, July 30, 1957)

It was shown previously [1] that the yield of stable intermediate products (SIP) from complex chain reactions, in which both the formation and consumption of SIP occur only by a chain mechanism, is not a function of the formation-rate and termination constants or of degenerate branching of the chains. This is so for any chain lengths in the case of the spontaneous formation of "slow" active centers; but, when "fast" active centers are formed, it only happens at sufficiently long chain lengths.

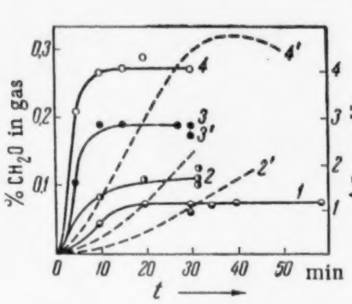

Fig. 1. Yield of CH_2O and increase of pressure in the uninitiated oxidation of CH_4. Mixture $CH_4 : 2O_2$, pressure 150 mm Hg, temperature 512°C. 1, 2, 3, 4) Curves of build-up of CH_2O; 1',2', 3', 4') manometric curves (1' coincides with the x axis); 1, 1') clean vessel; 2,2') H_2F_2 vessel; 3, 3') $K_2B_4O_7$ vessel; 4, 4') H_2F_2 vessel and an N_2 pressure of 300 mm Hg.

The yield of SIP, being a function only of the velocity constants of the elementary reactions of chain formation and of the concentrations of initial and intermediate products, does not depend on the diameter or nature of the walls of the reaction vessel, on dilution of the mixture with an inert gas or on the concentration of initiating radicals, and in this sense has a limiting value. The existence of limiting yields of SIP in complex reactions has been investigated in the case of the homogeneous oxidation of methane [1].

If, besides the chain mechanism for the consumption of SIP, there is a molecular mechanism with a velocity of the same order, then the yield of SIP will fall below the limiting value. In this case, a change in the reaction conditions, which affects the relative speeds of the chain and molecular processes of consumption of SIP, will alter the yield of SIP. This is confirmed by the experimental results given below for the yields of formaldehyde in the homogeneous oxidation of methane. The apparatus and experimental technique have been described previously [1].

The experiments on the uninitiated oxidation of CH_4 were carried out in three quartz reaction vessels, each of diameter 45 mm, whose surfaces had been treated in different ways: 1) the vessel had been given no special treatment ("clean" vessel); 2) the vessel had been washed with hydrofluoric acid (H_2F_2 vessel); 3) the vessel had been washed with a 1% solution of $K_2B_4O_7$ ($K_2B_4O_7$ vessel).

The experimental results (Fig. 1) showed that the yield of CH_2O depended on the state of the reactor surface. Thus, under these conditions for the oxidation of CH_4, the yield of CH_2O did not reach its limiting value, so that the rates of removal of CH_2O by molecular and chain processes were of the same order.

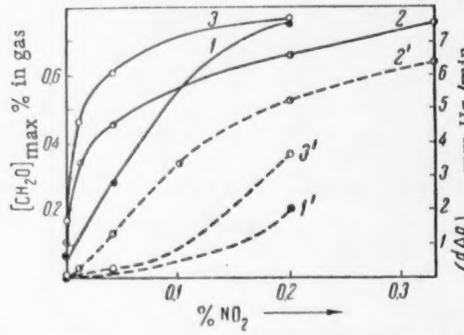

Fig. 2. Dependence of the maximum speed of oxidation of CH_4 and of the yield of CH_2O on the concentration of added NO_2. Mixture $CH_4 : 2O_2$, pressure 150 mm Hg, temperature 512°C. 1, 2, 3) Yields of CH_2O; 1', 2', 3') maximum rates in terms of Δp; 1, 1') clean vessel; 2, 2') H_2F_2 vessel; 3, 3') $K_2B_4O_7$ vessel.

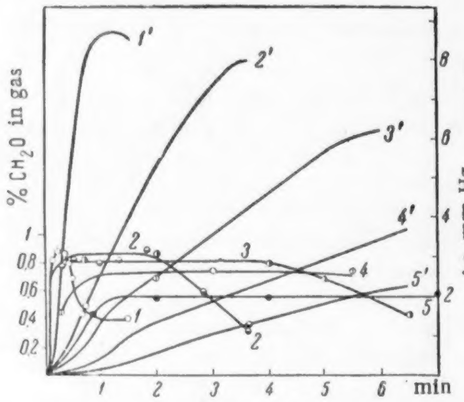

Fig. 3. Yield of CH_2O and increase in pressure for the oxidation of CH_4 in the presence of various additions of NO_2. Mixture $CH_4 : O_2$, pressure 100 mm Hg, temperature 512°C, $K_2B_4O_7$ vessel. 1, 2, 3, 4, 5) Curves of build-up of CH_2O; 1', 2', 3', 4', 5') manometric curves. Content of NO_2 in mixture: 1, 1') 0.65%; 2,2') 0.32%; 3,3') 0.16%; 4,4') 0.08%; 5,5') 0.04%.

There could be two reasons for this dependence of the yield of CH_2O on the nature of the reactor surface: 1) destruction of active centers on the surface took place in the kinetic or diffusion-kinetic region; 2) heterogeneous destruction of CH_2O occurred in the kinetic or diffusion-kinetic region.

In the first case, a decrease in the effective constant of destruction (ϵ) of the active centers on the surface, when changing from one vessel to another, would lead to an increase of the stationary concentrations of all the active centers in the reaction system, and this, in turn, would increase the proportion of chain to molecular removal of CH_2O, with the result that the yield of CH_2O would shift toward its limiting value, i. e., it would increase. Obviously, if ϵ increased on changing from one vessel to another, then the yield of CH_2O would decrease because of the increase in the proportion of molecular to chain removal of CH_2O.

In the second case, a decrease in the velocity constant (C) of the heterogeneous removal of CH_2O, when changing from one vessel to another, would be accompanied by an increase in the yield of CH_2O because of the reduction in the proportion of molecular removal of the aldehyde. And, vice versa, an increase in C would reduce the yield of CH_2O.

It is obvious that dilution of the reaction mixture with nitrogen, by hindering the diffusion of radicals and molecules to the walls, must increase the yield of CH_2O, if chain termination and decomposition or oxidation of CH_2O on the walls (or even one of these processes) occurs in the diffusion or diffusion-kinetic zone (dilution with nitrogen will reduce the values of ϵ and C).

It was found that addition of 300 mm Hg of N_2 to 150 mm Hg of the mixture $CH_4 : 2O_2$ considerably increased the yield of CH_2O and the rate of increase of pressure during the oxidation, which is a measure of the concentration of active centers, for all three vessels. The most pronounced effect of dilution with nitrogen was observed with the H_2F_2 vessel (Fig. 1, curves 4 and 4').

It is also obvious that addition to the reaction mixture of substances which form active centers spontaneously must increase the yield of CH_2O, because of the increase in the proportion of chain to molecular reaction. When the concentration of radicals becomes so large that molecular removal of CH_2O becomes negligibly small compared with removal by chain reaction, the yield of CH_2O will attain its limiting value. Such an increase in the concentration of active centers can only increase the rate of oxidation, but the yield of CH_2O will remain constant.

Figure 2 shows the results of experiments on the oxidation of methane in the presence of different amounts of NO_2. It can be seen that raising the NO_2 concentration from 0 to 0.2-0.3% produces a 4-8-fold increase in the yield of CH_2O; there was a simultaneous marked increased in the rate of oxidation. It can also be seen that, when

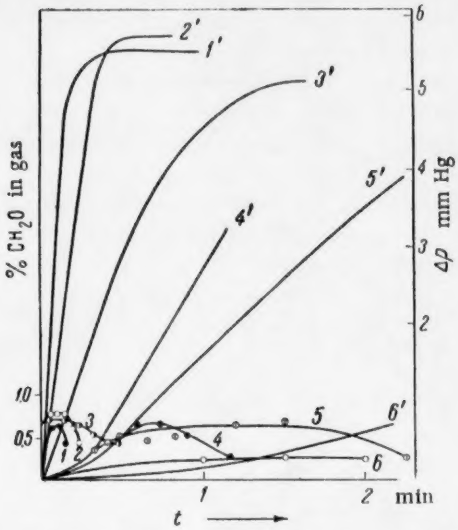

Fig. 4. Rate of oxidation of CH_4 and limiting yields of CH_2O for initiation with added NO_2 and Cl_2. Mixture $CH_4:O_2$, pressure 36 mm Hg, temperature 610°C, $K_2B_4O_7$ vessel, 1, 2, 3, 4, 5, 6) curves for build-up of CH_2O, 1', 2', 3', 4', 5', 6') manometric curves. Content of additive in mixture: 1, 1') 0.13% NO_2; 2,2') 0.065% NO_2; 3,3') 0.02% NO_2; 4,4') 0.5% Cl_2; 5, 5') 0.3% Cl_2; 6, 6') without additive.

the concentration of NO_2 in the mixture was increased, the yield of CH_2O approached the same limiting value (0.75-0.80% in the gas) for all three vessels.

Unfortunately, it was not possible to investigate the effect of concentrations of NO_2 greater than 0.2-0.3%, because the maximum of the curve relating CH_2O concentration and time became narrower with increasing amounts of NO_2, and above 0.2-0.3% of NO_2 the maximum became so acute that the experimental error was of the same order as any possible increase in the maximum. For this reason, a series of experiments was carried out in which NO_2 was added to mixtures containing less oxygen. It is clear from the curves in Fig. 3 that raising the NO_2 content from 0.160 to 0.650% considerably increased the rate of oxidation, but was practically without effect on the yield of CH_2O. For $[NO_2] < 0.162\%$ the yield of CH_2O became a function of the NO_2 concentration in the mixture.

Thus, with a high enough concentration of active centers in the reaction system, the yield of SIP reached its limiting value. It is clear that the value of this limiting yield will not depend on the means of obtaining the concentration of active centers, since it only matters that the chain mechanism should overwhelmingly preponderate over the molecular reaction for the removal of SIP. In particular, if there is a high enough concentration of chain carriers produced by the addition of initiators, the yield of SIP should not depend on the chemical nature of the initiators.

To prove this experimentally, two parallel series of experiments were carried out, using NO_2 and Cl_2 as initiators. The results are shown in Fig. 4, and it is clear that, while variation of the concentration of initiator had a strong effect on the rate of oxidation, it was practically without influence on the yield of CH_2O, so that oxidation was taking place in the limiting region. With NO_2 as initiator the maximum concentration of CH_2O in the gas obtained was 0.64-0.74% (curves 1, 2, 3), and with Cl_2 as initiator it was 0.64%, so that the limiting yield of CH_2O was practically the same in the two cases. For comparison, the yield of CH_2O (Fig. 4, curve 6) and the velocity (curve 6') are shown for the uninitiated reaction under the same conditions.

Thus, the above results show that, in the uninitiated oxidation of methane, there is a molecular mechanism for the removal of formaldehyde whose speed is comparable with that of the chain mechanism, so that the yield of CH_2O in the uninitiated oxidation is a function of the reaction conditions (the nature of the reactor walls, the pressure of inert gas, etc.) and is considerably below its limiting value. When the concentration of active centers in the reaction system is raised, the yield of CH_2O increases to a limiting value, which does not depend on the state of the reactor walls nor on the nature or concentration of the initiating free radicals.

LITERATURE CITED

[1] N. S. Enikolopian, G. V. Korolev and G. P. Savushkina, J. Phys. Chem. 31, 4 (1957).

Received July 30, 1957

Institute of Chemical Physics of the Academy of
Sciences of the USSR

THE EFFECT OF TRIBENZYLAMINE ON THE REACTION OF REDUCTION OF THE PERSULFATE ION

N. V. Nikolaeva-Fedorovich and L. A. Fokina

(Presented by Academician A. N. Frumkin, July 27, 1957)

It has recently been established that surface-active organic cations increase the rate of reduction of anions by means of their adsorption over the whole range of potential [1]. The accelerating effect of organic cations ceases at a sufficiently negative potential because the large organic cations are ousted from the metal/solution boundary by inorganic cations and water molecules. The increase in the rate of reduction of anions may explain the decrease in the negative value of the ψ_1-potential (the potential at the radial distance of the reacting particle from the surface of the electrode) or the change in the ψ_1-potential from a negative to a positive value [1, 2].

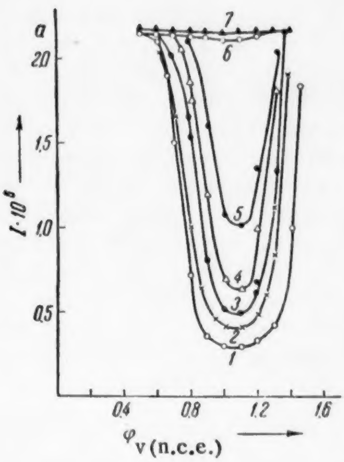

Fig. 1. Polarization curves for the reduction of 10^{-3} N $K_2S_2O_8$ + 10^{-3} N H_2SO_4 with addition of tribenzylamine: 1) without addition, 2) 1/100, 3) 1/50, 4) 1/40, 5) 1/30, 6) 1/10, 7) 1/5 saturated with tribenzylamine.

It is known from the literature that one of the most effective organic cations is tribenzylamine [3]. But A. A. Kriukova and M. A. Loshkarev [3], when investigating the effect of tribenzylamine on the reduction of the $S_2O_8^{2-}$ anion in the presence of 1N H_2SO_4, found that it caused a decrease instead of an increase in the rate of reduction. The authors consider that the effect of organic cations cannot be explained as the result of their causing a change in the ψ_1-potential, but is similar to the action of molecular additives which retard the reduction of $S_2O_8^{2-}$. However, both the range of potential in which the retardation of the rate of reduction occurs, and the increase in the rate of reduction long before the desorption potential, indicate that there may be a different reason for the retarding effect in this case.

We have investigated the influence of tribenzylamine on the reduction of the persulfate anion at a dropping mercury electrode.

In dilute solutions of supporting electrolyte, at potentials more negative than the electrocapillary maximum of mercury, the reduction of $S_2O_8^{2-}$ on the mercury electrode is a slow process, since the approach of the $S_2O_8^{2-}$ anions to the surface of an electrode is retarded by electrostatic repulsion [4]. In the polarization curve there was a fall in the current and a subsequent recovery at more negative potentials. Figure 1 shows that the addition of increasing concentrations of tribenzylamine to 10^{-3} N $K_2S_2O_8$ produced a decrease in the fall of current, i. e., an increase in the rate of reduction of $S_2O_8^{2-}$ (a solution 10^{-3} N in sulfuric acid was necessary, as the solubility of tribenzylamine is negligible in neutral and alkaline solutions). Increasing the concentration of tribenzylamine produced an increase in the current at the minimum of the curve. At $^1/_5$ of the saturation concentration of tribenzylamine the drop in current completely disappeared. Thus, as with the addition of other organic cations, the introduction to the solution and adsorption of tribenzylamine increased the rate of reduction of the persulfate anion.

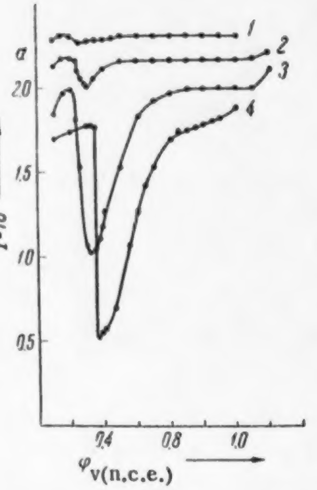

Fig. 2. Polarization curves for solutions of 10^{-3} N $K_2S_2O_8 + 10^{-3}$ N $(C_6H_5CH_2)_3N$ in the presence of H_2SO_4 at concentrations: 1) 10^{-2} N, 2) 10^{-1} N, 3) 1 N, 4) 6 N.

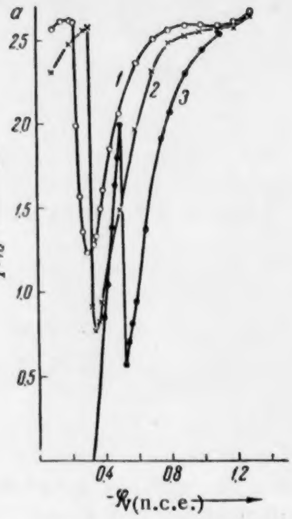

Fig. 3. Polarization curves for solutions of 10^{-3} N $K_2S_2O_8 + 10^{-3}$ N $(C_6H_5CH_2)_3N$ with addition of: 1) 1N H_2SO_4, 2) 1 N HCl, 3) 1 N HBr.

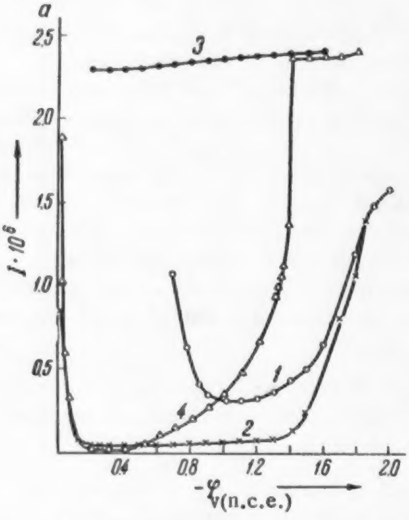

Fig. 4. Polarization curves for solutions: 1) 10^{-3} N $K_2S_2O_8$, 2) 10^{-3} N $K_2S_2O_8$ + saturated camphor, 3) 10^{-3} N $K_2S_2O_8$ + 1 N Na_2SO_4, 4) 10^{-3} N $K_2S_2O_8$ + + 1 N Na_2SO_4 + saturated camphor.

But, on increasing the concentration of H_2SO_4, tribenzylamine caused a decrease in the rate of reduction of $S_2O_8^{2-}$ at the same potentials as described in the work of A. A. Kirukova and M. A. Loshkarev. Figure 2 shows that the retardation of the reduction of $S_2O_8^{2-}$ occurred when both tribenzylamine and anions of supporting electrolyte were present together. The retardation was specially pronounced at potentials more positive than the point of zero charge on the mercury, and increased with increasing concentration of the anions of supporting electrolyte. When the concentration of H_2SO_4 was 0.1 N, the retardation of the reaction appeared at $\varphi = -0.5$ v with respect to the normal calomel electrode (n.c.e.), but, when the concentration of H_2SO_4 was increased to 6 N, a drop in current was clearly noticeable at $\varphi = -0.8$ v to n.c.e.

An increase in the adsorption of the anions of the supporting electrolyte also increased the retardation by tribenzylamine of the reduction of the persulfate anion. Figure 3 shows the polarization curves for the reduction of $S_2O_8^{2-}$ in the presence of 10^{-3} N tribenzylamine and 1 N H_2SO_4, HCl or HBr (the 10^{-3} N solution of tribenzylamine in all the acids was obtained by heating). The results demonstrate that the retarding effect increased for the series $SO_4^{2-} < Cl^- < Br^-$.

The retardation of the reduction of anions, when active anions and organic cations are adsorbed simultaneously, has been noted previously for the effect of tetrabutylammonium sulfate on the reduction of $K_2S_2O_8$ in the presence of 1 N KCl and 1 N KBr [5], and for the action of tetrabutylammonium sulfate and tetrabutylammonium iodide on the reduction of the copper-pyrophosphate complex [6].

These effects can be explained as follows. It follows from the electrocapillary measurements that surface-active anions are adsorbed in the presence of active cations, such as tetrapropylammonium, on a negatively charged surface [7, 2]. So that the organic cations, when added on their own, increase the rate of reduction of the anion, but, in the presence of surface-active anions, they form a surface layer with these anions, which retards the rate of reduction of the reducible anion.

In contrast to organic cations, which accelerate the reduction of anions, neutral organic molecules retard this reaction [8, 9]. We selected camphor and a mixture of β-naphthol, thymol and diphenylamine as examples of effective organic additives having a molecular character [10]. The introduction of a saturated solution of camphor to 10^{-3} N $K_2S_2O_8$ caused a powerful retardation of the rate of reduction of $S_2O_8^{2-}$ (Fig. 4). Desorption of camphor occurred at the potential $\varphi = -1.4$ v to n.c.e.; at this point the rate of reaction increased sharply, and the curve subsequently merged with that for the solution without camphor. Thus, camphor was found to have a retarding effect in the region of its adsorption and at low concentrations of supporting electrolyte (Fig. 4, curve 2). Increasing the concentration of supporting electrolyte to 1 N produced, in this case, a different effect (Fig. 4, curve 4) to that observed with tribenzylamine as additive. In the range of potential -0.2 to -0.4 v, there was some increase of the retardation, associated with the salting out effect of the electrolyte on camphor [10].* In the region of more negative potentials, camphor produced, not an increase, but a marked decrease in the retardation, associated with the adsorption of cations of supporting electrolyte. That the adsorption of cations of supporting electrolyte already occurred at $\varphi = -0.5$ v is obviously associated with the fact that camphor shifts to the point of zero charge on the side of more positive potentials. Similar phenomena were observed by T. V. Kalish and A. N. Frumkin [9]. With a saturated solution of a mixture of β-naphthol, thymol and diphenylamine as additive, the same phenomena were observed as with camphor. But the range of potential in which retardation was observed was considerably narrower than in the presence of camphor.

In conclusion we would like to thank Academician A. N. Frumkin for his constant guidance and exceptional interest in this work.

LITERATURE CITED

[1] A. N. Frumkin, Trans. 4th Conference on Electrochemistry (Moscow, 1956); S. Siekierski, Roczn. Chem. 30, 1083 (1956); N. V. Nikolaeva-Fedorovich and B. B. Damaskin, Trans. Conference on the Influence of Surface-Active Substances on the Electrodeposition of Metals, Vilna (1957), p. 33.

[2] A. N. Frumkin and N. V. Nikolaeva-Fedorovich, Reports MGU No. 4 (1957).

[3] A. A. Kriukova and M. A. Loshkarev, Trans. Conference on Electrochemistry, (Acad. Sci. USSR Press, 1953), p. 276.

[4] G. M. Florianovich and A. N. Frumkin, J. Phys. Chem. 29, 1829 (1955); A. N. Frumkin and G. M. Florianovich, Proc. Acad. Sci. USSR 80,907 (1954).

[5] A.P. Martirosian and T. A. Kriukova, J. Phys. Chem. 27, 851 (1953); A. Frumkin, Proc. 2nd World Congress on Surface Activity (London, 1957).

[6] E. A. Ukshe and A.I. Levin, Trans. Conference on the Influence of Surface-Active Substances on the Electrodeposition of Metals, (Vilna, 1957), p. 181.

[7] A. N. Frumkin, Electrocapillary Phenomena and Electrode Potential(Odessa, 1919).**

[8] H. Laitinen and E. Onstott, J. Am. Chem. Soc. 72, 4565 (1950).

[9] T. V. Kalish and A. N. Frumkin, J. Phys. Chem. 28, 801 (1954).

[10] M. A. Loshkarev and A. A. Kriukova, J. Phys. Chem. 23, 209 (1949).

[11] V. V. Losev, Proc. Acad. Sci. USSR 111, 626 (1956).***

Received June 22, 1957

---

* The salting out effect described by V. V. Losev [11] should be observed in solutions completely saturated with camphor, but this was, probably, not completely achieved in our experiments.

** In Russian.

*** Original Russian pagination. See C. B. translation.

SOME SPECIAL FEATURES OF THE RADIATION DESTRUCTION OF POLYMERS

A. B. Taubman and L. P. Ianova

(Presented by Academician V. A. Kargin, July 10, 1957)

The degradation (depolymerization) of polymers by the action of high energy radiation is accompanied by the formation of gases, which, being a high state of supersaturation, exert a considerable internal strain on the material and accelerate its disintegration.

It is difficult to establish directly a connection between the radiation stability of a polymer and the quantity of gas formed from it on irradiation [1], but this is not the result of a weak effect of gas formation on disintegration, and is due to the complex nature of the processes of radiolysis which lead to the formation of gaseous products of destruction. A number of the features of this process can be revealed by simultaneous exposure of the polymer to radiation and elevated temperature, and, in this paper, we have investigated gas formation and its effects on disintegration of the polymer, when polytetrafluoroethylene (PTFE), polymethyl methacrylate (PMMA) and polyethyl (PE) were exposed to a beam of fast electrons at different temperatures.

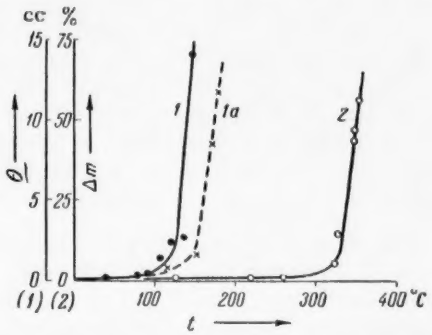

Fig. 1. Gas formation from polymers, on irradiation, as a function of temperature. 1 and 1a) Polymethyl methacrylate; 1 plasticized with 6% of dibutyl phthalate, 1a unplasticized. Dose $E_0 = 4.3 \cdot 10^{21}$ ev/cm^3, power of dose $E = 14.4 \cdot 10^{18}$ ev/cm$^3 \cdot$sec, $\tau = 5$ min. 2) polytetrafluoroethylene; $E_0 = 12.7 \cdot 10^{21}$ ev/cm^3, $E = 42 \cdot 10^{18}$ ev/cm$^3 \cdot$sec, $\tau = 5$ min.

The samples were heated electrically and irradiated in a special cell. The temperature was measured with a thermocouple having one junction embedded directly in the sample. The electron beam was produced by an accelerator with a tension of 600-900 kv, and its dosage power was $E \sim 2 \cdot 10^{17}$-$4 \cdot 10^{19}$ ev/cm^3. sec.

The thickness of the sample (2-3 mm) always exceeded the depth penetrated by the electrons. The quantity of gaseous products formed was determined by measuring the loss in weight (Δm) of the samples of PTFE and the volume of gas (Q) obtained when the samples of PMMA were dissolved in dichloroethylene.

It is clear from Fig. 1 that the process of gas formation, on exposure of the polymer to radiation at elevated temperature, is peculiar. For instance, with PTFE, the gas formation was negligible, amounting to a hundredth of a percent, over a wide range of temperatures, and, even at 250°, Δm did not exceed 0.5%. But in the region near the melting point, about the point at which PTFE becomes a viscous liquid (~ 330-350°), gas formation accelerated rapidly, so that the sample lost about half its weight in 5 min irradiation. After somewhat longer irradiation the sample was completely converted into gaseous products.

A similar dependence of the rate of destruction on temperature at a constant value of the radiation dosage was found with PMMA. Figure 1 shows that the quantity of gas formed was inconsiderable up to 100-110°, but increased very rapidly, as with PTFE, at the temperature at which the polymer begins to soften. The bubbles of gas, being unable to escape from the sample, converted the latter to a sponge whose volume was 5-10 times greater than the original. For unplasticized PMMA (the sample discussed above contained 6% of dibutyl phthalate) the change described occurred, as might be expected, at a higher temperature of 150-170° (dotted curve 1a of Fig. 1).

Finally, the same effect of a rapid increase in the destruction rate was observed at 110-120° for PE. In this case it is important to note that the increase in the intensity of radiolysis affected the mechanical properties of the sample considerably less than irradiation below the temperature of this transition.

The general character of this phenomenon, of a rapid increase in the destruction of a polymer by radiation within the narrow temperature range of melting (softening) of the material, clearly shows the reversibility of the radiolysis reaction, which leads to the formation of gaseous products. The gases dissolved in the polymer form a highly supersaturated solution, and, since their escape from the system by diffusion is slow [2], they strongly oppose any increase in the concentration of the solution or, which is equivalent, any increase in pressure. But, when the polymer becomes a viscous liquid, the rate of diffusion is greatly increased, the degree of supersaturation falls and the formation and growth of a new gas phase is facilitated.

The rapid escape of the products of destruction from the reaction zone shifts to the left the equilibrium of the reversible process — destruction $\rightleftarrows$ recombination of free radicals — so that there is a sudden increase in the rate of radiolysis. In consequence, a given dose of radiation can cause quite different degrees of destruction in the two temperature zones, below or above the region of rapid change in the curve relating gas formation with temperature. Since the greater mobility of the macromolecules in the region above the change in the curve allows complete relaxation of the strain created in the material, the large quantity of gas formed has less effect on the mechanical properties of the polymer than the small quantity of gas produced at temperatures below the change in the curve.

This draws attention to the part played in the destruction of the polymer by internal strains caused by gas formation, even when the gas cannot escape from the supersaturated solution to form a new phase. It also evidently explains why there is no relation between the stability of a polymer and the quantity of gas evolved on irradiation. The effect described, of a sudden increase of the intensity of destruction and gas formation, is not connected with the activation temperature of the radiolysis reaction, for, if it were, there would be a continuous increase with rise in temperature. Whereas the change in the speed of the process occurs abruptly, over a narrow range of temperature.

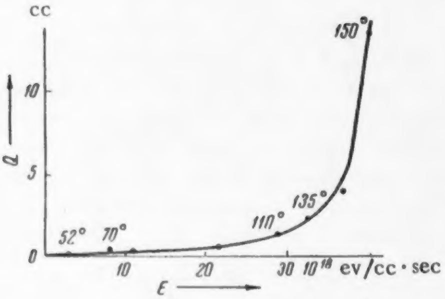

Fig. 2. Relation between gas formation in polymethylmethacrylate and the power of the dose at constant dosage. $E_0 = 1.8 \cdot 10^{21}$ ev/cm^3 = const, E was varied from 0.67 to $40 \cdot 10^{18}$ ev/cm^3 · sec.

The dependence of the process of gas formation by irradiation on the condition of the polymer was also shown by the breach of the rule of the equivalent effect of equal doses, independent of the power of the dose, which has been established in a number of cases of degradation by radiation. This is clear from Fig. 2, which shows, for PMMA, the variation of the quantity of gas liberated from the sample with the power of the dose (E). the reason for the abrupt bend in this curve is that the E values used were high enough for the radiation to raise the temperature of the sample, and, with the higher values of E, to convert it into the viscous liquid state. This occurs within a narrow zone in which the ionizing action of the radiation and the liberation of heat are a maximum, in accordance with the form of the curve for the distribution of the absorption of energy from decelerating electrons as a function of the thickness of the sample, which has a very pronounced maximum in this zone [3] (with PMMA, for example, with an electron speed corresponding to a tension of 900 kv, this zone lies at a depth of about 1.65 mm). So that in the range of E ~ 30-35 · 10^{18} ev/cm^3 · sec, for which the temperature of the sample reached t ≅ 110-130°, gas formation was greatly increased. It is interesting to note that if, from the temperatures of the sample given for each experimental point of the curve $Q = \varphi(E)$ (Fig. 2) a curve was constructed for $Q = f(t)$, the latter practically coincided with curve 1 of Fig. 1, which gives a similar relationship $Q = \psi(t)$. This showed that there is a definite relation between Q and t, although in a number of cases the results of irradiation would be different, according to whether the temperature taken was that reached by preliminary heating in an oven (conditions of Fig. 1) or was the result of the process of irradiation (conditions of Fig. 2).

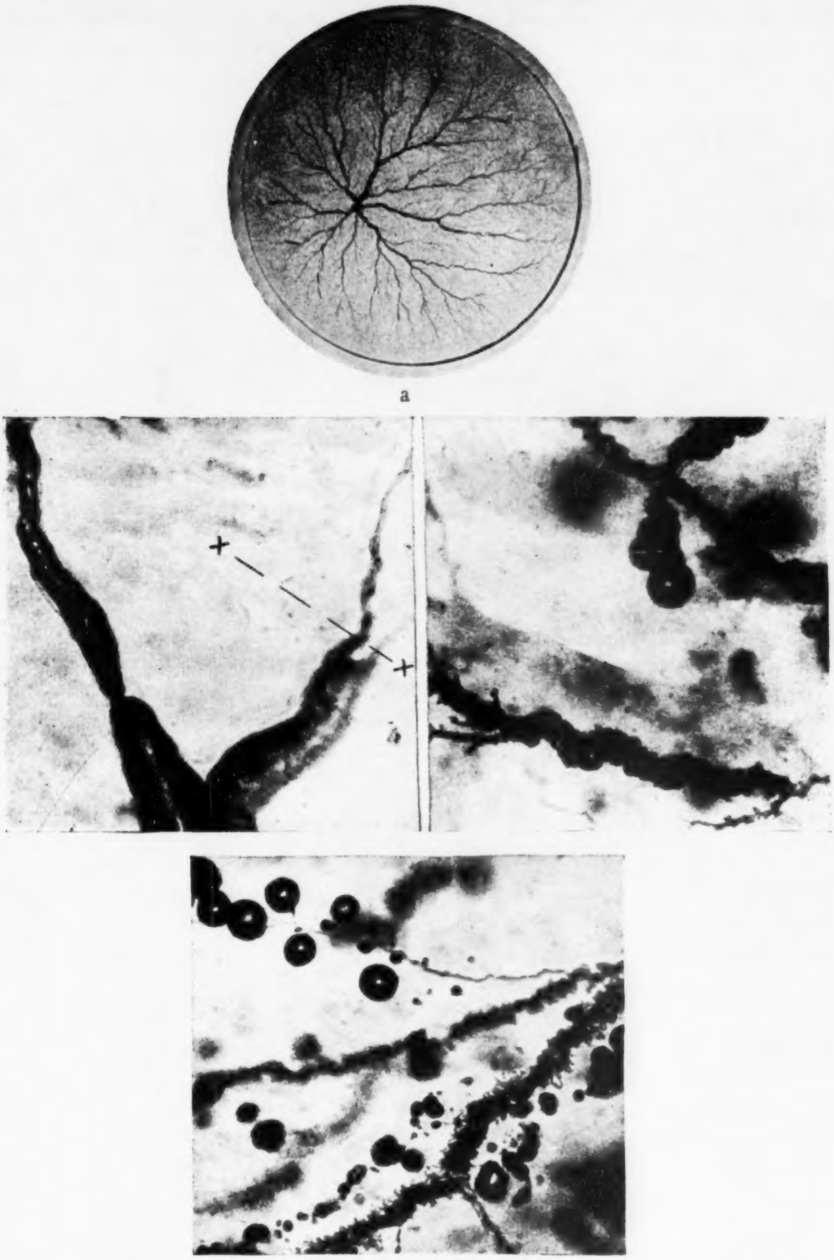

a

b

Fig. 3. a) Formation of cracks in polymethylmethacrylate, $E_0 = 0.17 \cdot 10^{21}$ ev/cm^3, $E = 8.5 \cdot 10^{18}$ ev/cm$^3 \cdot$sec, $\tau = 20$ sec; b) the development of cracks in polymethylmethacrylate and the formation from them of gas bubbles, $E_0 = 0.65 \cdot 10^{21}$ ev/cm^3, $E = 32.4 \cdot 10^{18}$ ev/cm$^3 \cdot$sec, $\tau = 20$ sec (150×).

The reversible character of the process of destruction also provides an explanation of the formation, on irradiation with electrons, of woodlike cracks, which have been studied in detail on glassy polymers [4]. We also obtained them on PE. Our results showed that, in contrast to the adsorption mechanism proposed in [4], the formation of these cracks (Fig. 3a) should be considered as the result of gas formation, and the cracks themselves as canals, through which the gas moves. Without giving details of these results, we show microphotographs (Fig. 3b), which illustrate the genetic connection between these cracks and gas bubbles. It is clear from these that a thin crack was formed where the sample of PMMA was only feebly irradiated by the electron beam (to the right of the line x-----x), while, where the beam exerted its full dosage, the cracks rapidly developed into cavities filled with gas. Depending on the conditions of gas formation in different parts of the sample, determined by the distribution of absorption or the energy of irradiation in relation to area and thickness, the cracks may: 1) widen considerably and turn into canals, forming an incompletely developed system, and slowly, because of the high viscosity of the medium, merge the bubbles with each other, or 2) not widen very much and develop into separate, isolated, fully formed bubbles (Fig. 3b).

Thus the cracks arise as a result of the strains in the material caused by the formation of gas and, once formed, they provide a means for reducing the degree of supersaturation of the solution and for liberating the excess of gas.

LITERATURE CITED

[1] V. S. Karpov, Session Acad. Sci. USSR on Peaceful Uses of Atomic Energy, Div. Chem. Sci. (1955), p. 3.

[2] R. Berrer, Diffusion in Solid Bodies (IL, 1948).*

[3] J. G. Trump and R. I. van de Graaff, J. Appl. Phys. 19, 7, 566 (1948).

[4] B. L. Tsetlin, N. G. Zaitseva, and V. A. Kargin, Proc. Acad. Sci. USSR 113, 2 (1957).**

Received July 6, 1957

Department of Disperse Systems of the Institute of
Physical Chemistry of the Academy of Sciences of
the USSR

---

* Russian translation.

** See C. B. translation.

THE EFFECT OF RATE OF DEFORMATION ON THE RATE OF THIXOTROPIC RECOVERY OF ALUMINUM NAPHTHENATE GEL AND AN OSCILLOGRAPHIC METHOD OF RECORDING STRAIN-DEFORMATION CURVES

T. G. Shalopalkina and A. A. Trapeznikov

(Presented by Academician S. I. Vol'fkovich, July 18, 1957)

It has been shown [1, 2] that the thixotropic properties of a gel-type system can be estimated from the growth of the tensile strength, P_r, and of its quasi-equilibrium value, $P_s{}^*$, for the system at rest after breaking up the structure.

The basis for the investigation of thixotropy is the application of a destructive influence to the system at a velocity gradient $\dot{\epsilon}_{\text{destr.}}$, which must somehow be determined. But in many investigations of thixotropy this condition has not been fulfilled or stated (for instance, when the structure is broken up in a standard way in some type of mixer). Subsequent measurement of the recovery of the structure must also be performed at a determined velocity gradient $\dot{\epsilon}_{\text{meas.}}$. The following two methods can be used for this: I) $\dot{\epsilon}_{\text{destr.}} = \dot{\epsilon}_{\text{meas.}}$, and II) $\dot{\epsilon}_{\text{destr.}} \gg \dot{\epsilon}_{\text{meas.}}$ By the use of both methods it is possible to make an adequate study of the phenomenon of thixotropy and to elucidate the specific features of the structure of the system under investigation.

In the region of small $\dot{\epsilon}$, the compensation method, providing a constant value of $\dot{\epsilon}$ over the whole range of deformation [4], is completely reliable for obtaining $P(\epsilon)$ curves, which characterize the important rheological properties of the system. To obtain $P(\epsilon)$ curves for large values of $\dot{\epsilon}$, we have developed a method of oscillographic recording.

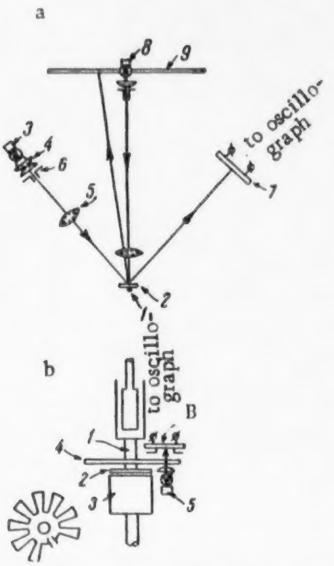

Fig. 1. Method of oscillographic recording of $P(\epsilon)$ curves. a) Recording of P, b) recording of ϵ and $\dot{\epsilon}$.

The arrangement for recording P, or the angle of rotation φ of the inner cylinder in the method of constant Ω (the rotation of the outer cylinder at a fixed speed), was as follows (Fig. 1a). On the axis of the inner cylinder, 1, there was fixed a mirror 2, and this was illuminated by a beam of light from the lamp, 3, through the condenser, 4, the focussing lens, 5, and the slit, 6, which gave a rectangular section to the beam. The light was reflected from the mirror to a selenium photocell, 7, whose area of illumination was limited by a special rectangular mask. The photocurrent, proportional to the illuminated area, was fed to the plates of the oscillograph. The construction of the apparatus allowed for the measurement of different ranges of φ. The dynamometer loading was such that $\varphi \leq 5°$, and in a number of cases φ was only 2-3°, which, with a limit of defomation $\theta_r = 100\text{-}200°$, practically ensured the condition $\dot{\epsilon} = \text{const}$. On the same axis of the cylinder there was another mirror, reflecting the image of a slit illuminated by a second lamp, 8, onto a scale, 9, for visual readings.

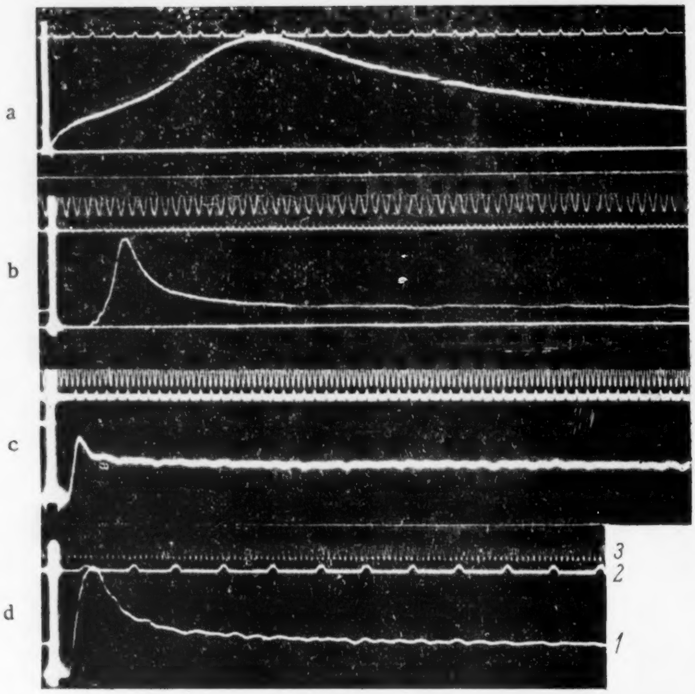

Fig. 2. Oscillograms of aluminum naphthenate gel and typographic ink No. 56. 1) Curves measuring the angle of rotation, φ, of the inner cylinder; 2) record of the angle of rotation, θ, of the outer cylinder; 3) record of time, τ. a) $\dot{\epsilon} = 1.45$, b) $\dot{\epsilon} = 490.2$, c) $\dot{\epsilon} = 152$, d) $\dot{\epsilon} = 34.3 \text{ sec}^{-1}$.

It was particularly valuable to be able to record simultaneously on a film both φ(i. e., P) and the angle of rotation, θ, of the outer cylinder, i. e., the deformation, ϵ, and the rate of deformation, $\dot{\epsilon}$. The recording of ϵ was done as follows. On the axis of the cylinder, 1 (Fig. 1b), there was fitted a disc, 4, rigidly connected to the top plate, 2, of a magnetic coupling, 3. The disc had radial slits every 20°, and underneath,a lamp, 5. Above the slits was a photocell, 6, the current from which was led to the plates of the oscillograph. The angle, θ, was recorded on the film in the form of a series of peaks. For example, $\epsilon = \epsilon_r$ was obtained by counting the number of peaks up to $P = P_r$ on the $P(\epsilon)$ curve. The simultaneous recording of τ in the form of a sinusoidal curve made it possible to calculate $\dot{\epsilon}$ (Fig. 2).

The application of this method to a 2% gel of aluminum naphthenate (plant experimental batch No. 24 [4]) in petroleum served to elucidate a number of new features of thixotropy in medium and high ranges of $\dot{\epsilon}$.

For example, Fig. 3a shows the curves of $P_r(\tau_{\text{rest}})$ and $P_s(\tau_{\text{rest}})$ for three values of $\dot{\epsilon}_{\text{meas.}}$, characterizing the recovery of the structure of the system after its destruction at $\dot{\epsilon}_{\text{destr.}} = \dot{\epsilon}_{\text{meas.}}$ (method I).

The experiments were carried out as follows* [1]. The fully recovered system was deformed at rate $\dot{\epsilon}$ to the condition where $P = P_s$. The system was then allowed to rest for a time τ_{rest}, and measurements were made at values of $\dot{\epsilon}_{\text{meas.}}$ up to $\dot{\epsilon}_{\text{destr.}}$. Figure 3a shows that, as $\dot{\epsilon}$ increased, the final maximum value of $\Delta P = P_r - P_s$, characterizing the thixotopric effect for each value of $\dot{\epsilon}$, greatly increased. But, with the growth of $\dot{\epsilon}$, the time for full recovery, τ_r (the time for P_r to reach the horizontal part of the curve) fell, so that the speed of thixotropic recovery increased. For example, when $\dot{\epsilon}$ was changed from 1.45 to 1450 sec^{-1}, τ_r decreased from 10 hrs to 1 min. Using logarithmic coordinates, the relation between τ_r and $\dot{\epsilon}$ appeared as a straight line (Fig. 3a).

---

* The radius of the outer cylinder was $R_2 = 1.500$ cm, that of the inner cylinder $R_1 = 1.402$ cm.

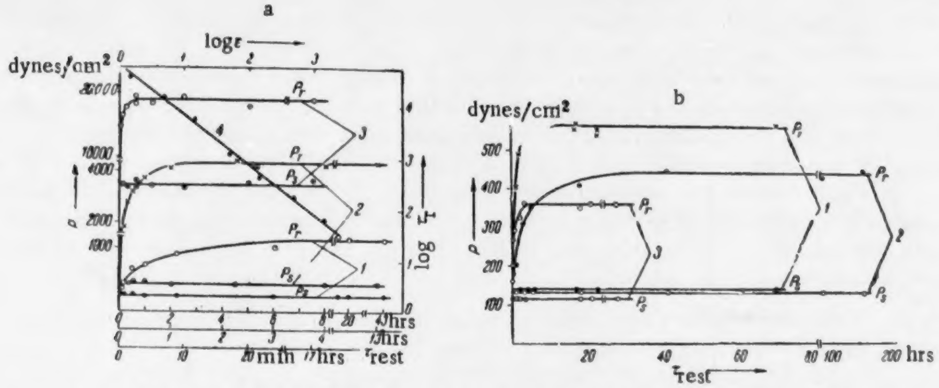

Fig. 3. Kinetics of thixotropic stiffening. a) At $\dot{\epsilon} = 1.45\ \text{sec}^{-1}$ (1), $\dot{\epsilon} = 14.51\ \text{sec}^{-1}$ (2), $\dot{\epsilon} = 490.2\ \text{sec}^{-1}$ (3) and $\log \tau_b = f(\log \dot{\epsilon})$ (4); b) $\epsilon = 1.45\ \text{sec}^{-1}$ (see explanation in text).

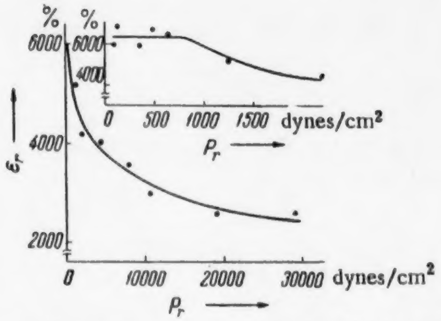

Fig. 4. Relation between ϵ_r and P_r (P_r changes in the same way with $\dot{\epsilon}$).

These results led to the following conclusions:

1) The strength of the structure, P_r, for different values of $\dot{\epsilon}_{destr.} = \dot{\epsilon}_{meas.}$ is determined by different elements of the structure, distinguished by their rates of recovery.

2) The elements of the structure on which P_r depends for small values of $\dot{\epsilon}$ do not determine P_r for large values of $\dot{\epsilon}$. But this is not due to irreversible destruction of the structure at high $\dot{\epsilon}$. This was shown by the coincidence of the values of τ_r (10 hrs) obtained for the same values of $\dot{\epsilon}_{destr.} = \dot{\epsilon}_{meas.} = 1.45\ \text{sec}^{-1}$ in two experiments (curve 1 of Fig. 3a and curve 1 of Fig. 3b), i. e., before and after measurement at all the $\dot{\epsilon}$ values given in Fig. 3a (curve 1 of Fig. 3b was obtained with a structure that had been allowed to recover for a long time after the preceding treatment of the system). It may be supposed that the more rapid recovery of the structure at high $\dot{\epsilon}$ is connected with the destruction of that part of the structure which recovers slowly, as P increases to P_r.

3) The structural conditions corresponding to τ_r for different values of $\dot{\epsilon}$ are not identical, in spite of the attainment of full recovery of the structure at P_r.

In addition to the reversible destruction of structure which has been considered, there can also be an irreversible destruction of the structure. This was shown by the fall in P_r and P_s, when measured at a low $\dot{\epsilon}$ of 1.45 sec^{-1}, before and after subjecting the system to a high value of $\dot{\epsilon}$ (curve 1 of Fig. 3a and curve 1 of Fig. 3b, and also curves 1 and 2* of Fig. 3b). In this respect there is an analogy with the condensation and dispersion of structures in solid plastic systems [3].

Irreversible destruction of structure can occur as the result of aging of the system, and this was shown by the fall in P_r and P_s in curve 3 of Fig. 3b, obtained by method I, after an aging time τ_{age} = 1 month, compared with curve 2 of Fig. 3b. The small value of τ_r was due to the use of method I.

It is interesting to note the variation of the deformation ϵ_r determined at the maximum P_r of the $P(\epsilon)$ curve for different values of $\dot{\epsilon}$ (Fig. 4). Already, for the small $\dot{\epsilon}$ values at which the $P(\epsilon)$ curve showed a maximum P_r, ϵ_r was found to have its highest value, 6200% (averaged value). It remained constant over a range of $\dot{\epsilon}$ (or P_r), but further on, beginning at a relatively low $\dot{\epsilon}$ of 1.45 sec^{-1}, dropped appreciably. With a change of $\dot{\epsilon}$ from 1.45 to 1450 sec^{-1}, ϵ_r dropped to half its original value. The difference in the deformation, ϵ_r, may include elastic, viscoelastic and irreversible plastic deformations. The growth of $\dot{\epsilon}$ can lead to a decrease of the plastic deformation in consequence of a weakening of relaxation. At a high enough $\dot{\epsilon}$ the viscoelastic deformation can also decrease, because the particles coiled into spheres do not have time to unwind under the influence of viscous forces, and tear apart prematurely. It may be presumed that the observed fall in ϵ_r is mainly the result of a decrease in the irreversible deformation at small values of $\dot{\epsilon}$, and is due to the second mechanism for the highest values of $\dot{\epsilon}$. Difficulty in uncoiling of the spheres probably occurs in every viscoelastic system, but the value of $\dot{\epsilon}$ corresponding to the lowering of ϵ_r by this will be higher the more mobile are the structural elements and the lower is the viscosity η_r.

---

* Curve 2 of Fig. 3b was obtained by method II described above under the conditions $\dot{\epsilon}_{destr.} = 1450\ \text{sec}^{-1} \gg \dot{\epsilon}_{meas.} = 1.45\ \text{sec}^{-1}$. The structure of the system was destroyed (at $\dot{\epsilon}_{destr.}$) before each τ_{rest}. A feature of this method of measuring thixotropy, in contrast to method I, is a 10 to 40 hr increase in τ.

It was also noted that the tearing apart deformation ϵ_r decreased with increase of P_r by thixotropic recovery of structure (for example, from 7300 to 5400% at $\epsilon = 1.45$ sec^{-1}).

LITERATURE CITED

[1] A. A. Trapeznikov and V. A. Fedotova, Proc. Acad. Sci. USSR 95, 595 (1954).

[2] A. A. Trapeznikov and T. G. Shalopalkina, Colloid. J. 19, 232 (1957).

[3] E. E. Segalova and P. A. Rebinder, Colloid J. 10, 223 (1948).

[4] A. A. Trapeznikov and T. G. Shalopalkina, Colloid J. 17, 471 (1955);* A. A. Trapeznikov, Colloid J. 18, 295 (1956).*

Received July 12, 1957

Institute of Physical Chemistry of the Academy of
Sciences of the USSR

---

*Original Russian pagination. See C. B. translation.

ELECTRON–DIFFRACTION STUDY OF THE STRUCTURE OF BERYLLIUM HALIDE MOLECULES

P. A. Akishin, V. P. Spiridonov and G. A. Sobolev

(Presented by Academician N. N. Semenov, August 2, 1957)

The present communication is devoted to a study of the molecular structure of the vapors of the beryllium halides – fluoride, chloride, bromide and iodide – for which the literature gives no data on the geometrical parameters. The specimens used in the work were prepared as follows: BeF_2 – by the thermal decomposition of ammonium fluoberyllate; $BeCl_2$ – by the action of chlorine on metallic beryllium with heating; $BeBr_2$ – by the action of dry bromine on powdered beryllium in absolute ether with subsequent precipitation of the salt with absolute benzene; BeI_2 – by the action of hydriodic acid on powdered beryllium with heating. The specimens were purified by recrystallization from solvents and vacuum distillation.*

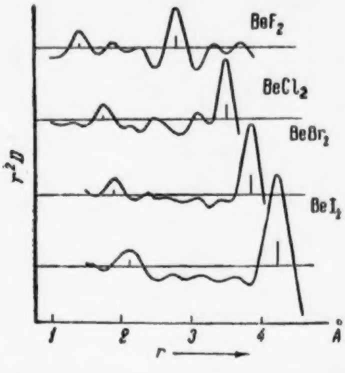

Fig. 1. Radial distribution curves for beryllium halide molecules.

The apparatus and method used to obtain the electron-diffraction patterns have been described earlier [1]. Because of the high hygroscopicity of the beryllium halides, they were loaded into the vaporizer ampoule in a dry box. Before the electron-diffraction patterns were recorded, all the materials were thoroughly degassed under high vacuum directly in the electron-diffraction apparatus. The electron-diffraction patterns were photographed on diapositive and ion-optical photographic film (NIKFI, type MK) with exposures of 2 to 30 sec.

8-10 series of electron-diffraction patterns (3 photographs per series) were obtained for all the beryllium halide vapors, at electron wavelengths from 0.0403 to 0.0627 A. The electron-diffraction patterns obtained had the following intensity distribution: the even maxima (2, 4, 6, 8, and 10th) were intense, while the odd maxima (3, 5, 7, and 9th) were less intense than the even maxima; the intensity of the even, and consequently, of the odd maxima falls regularly with increase in the scattering angle; at the same time the relative intensity of the odd maxima on going from beryllium fluoride to beryllium iodide increases; the minima preceding the even maxima are deep, while those preceding the odd maxima are shallow (see the experimental curves in Fig. 2).

The interpretation of the electron-diffraction patterns was made according to the Walter-Beach version of the radial distribution method [2] and also by the method of successive approximations [3]. The radial distribution curves $r^2D(r)$ for the molecules of all the beryllium halides studied (Fig. 1) have two clearly defined peaks which are naturally interpreted as the distances $r(Be-X)$ and $r(X-X)$, with the following values:

---

* We must express our thanks to A. V. Novoselovaia, K. N. Semenenko and A. S. Pashinkin for placing the above specimens at our disposal.

$BeF_2 : r(Be-F) = 1.43, \quad r(F-F) = 2.80A;$

$BeCl_2 : r(Be-Cl) = 1.77, \quad r(Cl-Cl) = 3.51A;$

$BeBr_2 : r(Be-Br) = 1.90, \quad r(Br-Br) = 3.84A;$

$BeI_2 : r(Be-I) = 2.12, \quad r(I-I) = 4.22A$

No other peaks which could be regarded as structural peaks were found on the radial distribution curves. Thus the data obtained by the radial distribution method indicate in every case that the electron-diffraction patterns of the beryllium halide vapors correspond to linear triatomic BeX_2 molecules.

Figure 2 shows the theoretical curves for the intensities of the scattered electrons, constructed for linear BeX_2 molecules, and these reflect clearly all the characteristic features of the electron-diffraction patterns obtained for the beryllium halide vapors. The results of the calculations using the method of successive approximations are given in Tables 1-4.

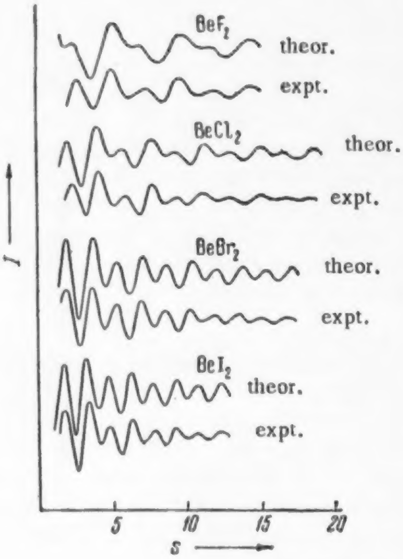

Fig. 2. Theoretical (valence angle 180°) and experimental intensity curves for beryllium halide molecules.

TABLE 1

BeF_2 Molecule; $r_{theor} = 1.40$ A

Max.	Min.	Intensity	s_{theor}	s_{exp}	$\frac{s_{theor}}{s_{exp}}$	r_{exp}, A
1		+10	2.44	2.81	(0.868)	(1.22)
	2	−14	3.68	3.94	(0.934)	(1.31)
2		+20	5.17	5.03	1.028	1.44
	3	−4	6.55	6.23	(1.051)	(1.47)
3		+2	6.92	7.27	(0.952)	(1.33)
	4	−8	8.22	8.45	0.973	1.36
4		+12	9.69	9.55	1.015	1.42
	5	−2	11.03	10.72	1.029	1.44
5		+1	11.42	11.79	0.969	1.36
	6	−5	12.71	12.91	0.985	1.38
6		+6	14.18	13.99	1.014	1.42
Mean value					1.002	1.40
Mean deviation					±0.022	±0.03

In our previous works [4-9] it was pointed out that a characteristic feature of the electron-diffraction patterns for the vapors of the halides of zinc, cadmium, magnesium, calcium, strontium and barium is the asymmetry of the contour of the diffraction rings, which is shown slightly in the case of the fluorides and increases on going to the chlorides, bromides and iodides (in some cases resulting in steps in the intensity from the outside of the ring), so that the accuracy of the determination of the valence angle according to the I(s) curves increases from the fluorides to the iodides (we would point out that in the majority of cases the question of the valence angle in the fluorides can only be decided by making use of the radial distribution data). Since in all the beryllium halides the charge of the halogen atoms exceeds the charge of the metal atom, the electron-diffraction patterns of the vapors show alternate maxima of high (even maxima) and low (odd maxima) intensities, which change their contour when the valence angle changes; at the same time the greatest sensitivity to variation in the valence angle X−Be−X is shown by the I(s) curve for BeF_2 and the least sensitivity by the curve for BeI_2. Since there is a reference in the literature [10] to the presence in beryllium halide vapors of dimeric molecules Be_2X_4, we have tested a number of models of the type Be_2X_4, taking beryllium chloride as an example:

1) model of the type (X = Cl)

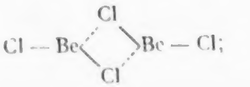

$$\mathrm{Cl-Be}\overset{\mathrm{Cl}}{\underset{\mathrm{Cl}}{\langle\,\rangle}}\mathrm{Be-Cl};$$

TABLE 2

$BeCl_2$ Molecule; r_{theor} = 1.76 A

Max.	Min.	Intensity	s_{theor}	s_{exp}	$\frac{s_{theor}}{s_{exp}}$	r_{exp}, A
1		+10	2.10	2.48	(0.847)	(1.49)
	2	−15	3.00	3.32	0.904	(1.59)
2		+20	4.08	4.13	0.988	1.74
	3	−6	5.02	5.18	0.969	1.71
3		+2	5.67	5.98	(0.948)	(1 67)
	4	−12	6.60	6.92	(0.954)	(1.68)
4		+10	7.65	7.69	0.995	1.75
	5	−3	8.61	8.57	1.005	1.77
5		+1	9.24	9.46	0.977	1.72
	6	−5	10.17	10.16	1.001	1.76
6		+4	11.23	11.04	1.017	1.79
	7	−2	12.17	12.09	1.007	1.77
7		+1	12.83	13.02	0.985	1.73
	8	−4	13.73	13.89	0.988	1.74
8		+3	14.80	14.80	1.000	1.76
	9	−1	15.73	15.68	1.003	1.77
9		+1	16.42	16.56	0.992	1.75
	10	−2	17.32	17.39	0.996	1.75
10		+1.5	18.37	18.24	1.007	1.77
Mean value					0.995	1.75
Mean deviation					±0.010	±0.02

TABLE 4

BeI_2 Molecule; r_{theor} = 2.10 A

Max.	Min.	Intensity	s_{theor}	s_{exp}	$\frac{s_{theor}}{s_{exp}}$	r_{exp}, A
1		+15	1.83	1.81	1.011	2.12
	2	−20	2.57	2.67	(0.963)	(2.02)
2		+20	3.37	3.40	0.991	2.08
	3	−6	4.13	4.18	0.988	2.07
3		+6	4.83	4.90	0.986	2.07
	4	−10	5.57	5.66	0.984	2.07
4		+10	6.37	6.36	1.002	2.10
	5	−3	7.13	7.12	1.001	2.10
5		+3	7.83	7.83	1.000	2.10
	6	−5	8.57	8.55	1.002	2.10
6		+5	9.37	9.25	1.013	2.13
	7	−1	10.13	10.05	1.008	2.12
7		+1	10.83	10.79	1.004	2.11
	8	−2	11.57	11.50	1.006	2.11
8		+2	12.37	12.22	1.012	2.13
Mean value					1.000	2.10
Mean deviation					±0.008	±0.02

TABLE 5

Geometrical Parameters of Linear Beryllium Halide Molecules

Compounds	Distance of Be — X, Å
BeF_2	1.40±0.03
$BeCl_2$	1.75±0.02
$BeBr_2$	1.91±0.02
BeI_2	2.10±0.02 *

TABLE 3

$BeBr_2$ Molecule; r_{theor} = 1.90 A

Max.	Min.	Intensity	s_{theor}	s_{exp}	$\frac{s_{theor}}{s_{exp}}$	r_{exp}, A
1		+15	2.00	2.02	0.990	1.88
	2	−20	2.83	2.97	0.953	(1.81)
2		+20	3.77	3.77	1.000	1.90
	3	−7	4.59	4.61	0.996	1.89
3		+8	5.33	5.39	0.989	1.88
	4	−12	6.15	6.22	0.989	1.88
4		+10	7.06	7.00	1.009	1.92
	5	−5	7.90	7.88	1.003	1.91
5		+4	8.63	8.66	0.997	1.89
	6	−8	9.45	9.50	0.995	1.89
6		+5	10.36	10.25	1.011	1.92
	7	−3	11.21	11.10	1.011	1.92
7		+2	11.93	11.87	1.006	1.91
	8	−4	12.77	12.64	1.010	1.92
8		+3	13.66	13.46	1.015	1.93
	9	−2	14.50	14.23	1.019	1.94
9		+1	15.23	15.03	1.013	1.92
	10	−3	16.05	15.84	1.013	1.92
10		+1 5	16.98	16.72	1.016	1.93
Mean value					1.005	1.91
Mean deviation					±0.009	±0.02

2) model of the type (X = Cl)

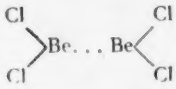

;

3) an octahedral model, in which four chlorine atoms are situated at the corners of a square, while two beryllium atoms lie on either side of the plane of the square at equal distances from it. It was found that the theoretical I(s) curves corresponding to the models 1-3 have no resemblance to the experimentally found intensity distribution in the beryllium chloride diffraction pattern.

On the other hand, diatomic molecules of the type BeX, if present in the vapor of the substances being studied, would give an intensity distribution (simple attenuated sine curve) differing sharply from the pattern obtained experimentally. From this it may be concluded that under the conditions of the electron-diffraction study carried out, the beryllium halide vapors either contain no dimeric (Be_2X_4) or diatomic (BeX) molecules, or else contain such small concentrations of these that they are outside the limits of the sensitivity of the electron-diffraction method. This is confirmed by approximate calculations made by Brewer [11], according to which, for example, 50% dissociation is not achieved for BeF_2 up to 3000°K, or up to 2000°K for $BeCl_2$.

Thus both of the methods used to interpret the electron-diffraction patterns of the vapors (the radial distribution method and the method of successive approximations) give concordant results for the configuration (linear structure) and geometrical parameters of the

---

* Table 1 in [14] shows a misprint in the value of the Be−I distance.

molecules of beryllium halide vapors (see Table 5) obtained for the first time in the present work.

It is interesting to note that the interatomic distances in the BeF and BeCl molecules (1.36 and 1.70, respectively), determined spectroscopically [12], are close to the interatomic distances in the BeF_2 and $BeCl_2$ molecules (see Table 5), differing from the latter by 0.04-0.05 A. There are no spectroscopic data for the BeBr and BeI molecules, but if it is assumed that the interatomic distances in these molecules are also less than the corresponding distances in $BeBr_2$ and BeI_2 by approximately 0.05 A, we obtain the values 1.86 and 2.05 A, respectively, which differ considerably from the values (Be—Br) = 2.05 A and (Be—I) = 2.33 A obtained in work by Margrave [13] based on an electrostatic model; this estimate must be taken as very approximate.

LITERATURE CITED

[1] P. A. Akishin, M. I. Vinogradov et al., Instruments and Tech. Exp. 3, 2 (1958).

[2] J. Walter and J. Beach, J. Chem. Phys. 8, 8, 601 (1940).

[3] L. Pauling and L. Brockway, J. Chem. Phys. 2, 12, 867 (1937).

[4] P. A. Akishin, L. V. Vilkov, and V. P. Spiridonov, Proc. Acad. Sci. 101, 1, 77 (1955).

[5] P. A. Akishin, V. P. Spiridonov, V. A. Naumov, and N. G. Rambidi, J. Phys. Chem. 30, 1, 155 (1956).

[6] P. A. Akishin, V. P. Spiridonov, G. A. Sobolev, and V. A. Naumov, J. Phys. Chem. 31, 2, 461 (1957).

[7] P. A. Akishin, V. P. Spiridonov, and G. A. Sobolev, J. Phys. Chem. 31, 3, 648 (1957).

[8] P. A. Akishin, V. P. Spiridonov, G. A. Sobolev, and V. A. Naumov, J. Phys. Chem. 31, 8, 1871 (1957).

[9] P. A. Akishin, V. P. Spiridonov, G. A. Sobolev, and V. A. Naumov; J. Phys. Chem. 32, 1, 58 (1958).

[10] O. Rahlfs and W. Fischer, Z. anorg. und allgem. Chem. 211, 349 (1933).

[11] L. Brewer, in the book: The Chemistry and Metallurgy of Miscellaneous Materials (N. Y.-Toronto-London, 1950), p. 193.

[12] G. Herzberg, Spectra of Diatomic Molecules (N. Y., 1950).

[13] J.Margrave, J. Phys. Chem. 58, 3, 258 (1954).

[14] P. A. Akishin and V. P. Spiridonov, Crystallography 2, 4, 475 (1957).

Received July 30, 1957

M. V. Lomonosov State University, Moscow

YIELDS OF FORMADELHYDE AND ACETALDEHYDE IN THE HIGH-TEMPERATURE OXIDATION OF ETHANE

N. S. Enikolopian and G. V. Korolev

(Presented by Academician N. N. Semenov, July 30, 1957)

The theories leading to the establishment of the limiting yields of stable intermediate products (SIP) in complex chain reactions [1] have been verified, taking the oxidation of methane as an example [1, 2]. The next most complex representative of the homologous series of paraffinic hydrocarbons – ethane – was chosen for the further examination of these theories.

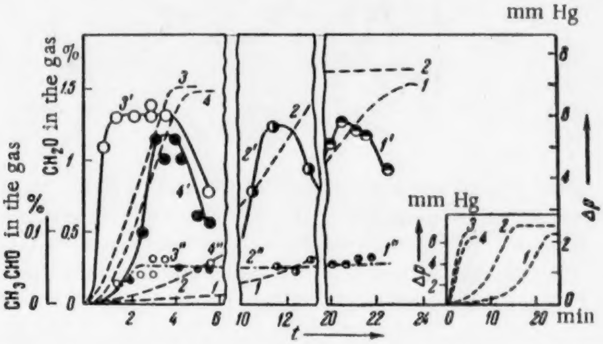

Fig. 1. The influence of additions of NO$_2$ and N$_2$ on the yields of aldehydes and on the manometric kinetics; T = 512°, pressure of the $C_2H_6 : 2O_2$ mixture 25 mm Hg; H_2F_2 vessel; dashed line) manometric kinetics; continuous curves) kinetics of increase in amount of CH_2O; dot-and-dashed line) kinetics of increase in amount of CH_3CHO; 1, 1', 1") no additives; 2, 2', 2") with 0.085% NO$_2$ added; 3, 3', 3") with 0.33% NO$_2$ added; 4, 4', 4") 10-fold dilution of the mixture with nitrogen.

A study has been made of the way in which the yields of the two SIP (formaldehyde and acetaldehyde) vary with variation in the conditions of high-temperature oxidation of C_2H_6. The apparatus and method of working have been described earlier [1]. The presence of a mixture of two aldehydes in the solution for polarographic analysis introduced no complications since the waves given by the two aldehydes are clearly differentiated in 0.05 N LiOH solution.

The experiments were carried out in two quartz reaction vessels with diameter 45 mm and volume 250 ml, the walls having been treated: 1) by washing with H_2F_2 (H_2F_2 vessel) and 2) by washing with 1% $K_2B_4O_7$ solution ($K_2B_4O_7$ vessel).

The results of experiments at low pressures (25 mm Hg) for mixtures relatively rich in oxygen ($C_2H_6 : 2O_2$) are given in Fig. 1, from which it can be seen that the addition of initiator radicals (NO$_2$) and dilution of the reaction mixture with an inert gas (N$_2$) considerably increase the concentration of active centers in the reaction system, as can be deduced from the sharp rise in the rate of increase in pressure. The yields of CH_2O and CH_3CHO remain practically unchanged, i. e., they do not differ from the limiting yields [1, 2].

The same experiments were repeated at a higher pressure, 53 mm Hg (see Fig. 2). The yield of CH_2O, as before, did not change with variation in the concentration of active centers over a wide range, and was approximately double the yield of CH_2O at a pressure of 25 mm Hg. We encountered an unexpected phenomenon with regard to the yield of CH_3CHO: at the very end of the conversion, when the chain processes in the system had slowed down appreciably, the rate of increase in the amount of CH_3CHO increased sharply ("jump") (as can be seen particularly clearly in curve 1 of Fig. 2), and a maximum value for the CH_3CHO concentration was reached at the moment when the rate of conversion, according to Δp, was already equal to zero.

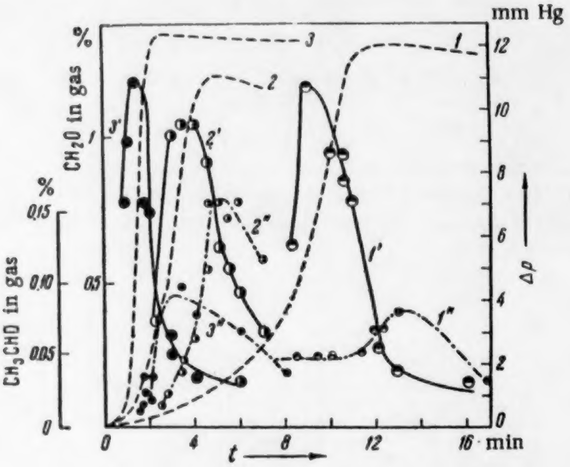

Fig. 2. The influence of additions of NO_2 and N_2 on the yield of aldehydes and on the manometric kinetics; T = 512°; pressure of $C_2H_6 : 2O_2$ mixture 53 mm Hg; H_2F_2 vessel; 1, 1', 1") without additive; 2, 2', 2") with 0.085% NO_2 added; 3, 3', 3") 7-fold dilution of the mixture with nitrogen. The other symbols are the same as in Fig. 1.

It is evident that at the moment when the rate in the reaction system, according to Δp, becomes equal to zero, the chain processes therein practically cease, since the high-temperature homogeneous oxidation of hydrocarbons in the gaseous phase necessarily involves the formation of CO, and this should be accompanied by an increase in the pressure. Consequently, the maximum CH_3CHO concentration, reached after the "jump," cannot be regarded as the maximum yield of SIP in the complex chain reaction and the theory of limiting yields cannot be applied to it. From this it follows that the formation of CH_3CHO after the reaction has stopped, according to Δp, is caused by some sort of molecular reaction of the original or intermediate materials.

Let us examine the question of the limiting yields of SIP in a complex chain reaction in which, together with the formation and disappearance of the SIP by chain processes, there also takes place not only the molecular decomposition of the SIP [2] but also molecular formation of the SIP. The case may then be represented in the form of a diagram

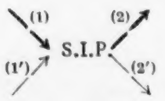

where the heavy arrows represent the chain processes and the light arrows represent the molecular processes. It is then necessary to distinguish the following three cases:

1) The stationary concentration of SIP which would be obtained if processes (1) and (2) alone were operating (purely chain yield) is higher than the stationary concentration which would be obtained if processes (1') and (2') alone were operating (purely molecular yield). In this case any change in the reaction conditions which leads to an increase in the concentration of active centers in the reaction system (initiation, dilution of the mixture with an inert gas, etc.) will increase the yield of SIP, since an increase in the concentration of active centers increases the part played by processes (1) and (2) in comparison with processes (1') and (2'), and the yield of SIP consequently approaches the purely chain yield.

2) The purely chain yield is less than the purely molecular yield. In this case an increase in the concentration of active centers in the reaction system leads to a reduction in the yield of SIP.

3) The purely chain yield is practically the same as the purely molecular yield. In this case, variation in the reaction conditions which influence the ratio of the rates of the chain and molecular processes of SIP formation and disappearance will not influence the yield of SIP.

It is practically impossible to distinguish case 1) from the case:

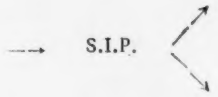

which is observed in the noninitiated or insufficiently initiated oxidation of methane [2], or to distinguish the case 3) from the case: ⇢ SIP ⇢ , which is observed in the oxidation of CH_4 when initiation has been sufficient [1].

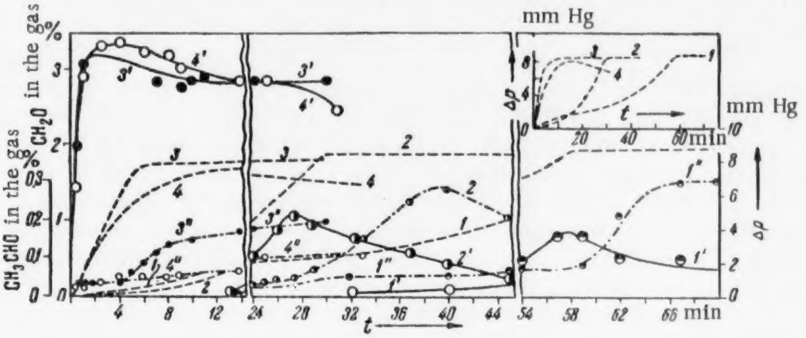

Fig. 3. The influence of the nature of the reaction vessel surface and of additions of NO_2 and N_2 on the yield of aldehydes and on the manometric kinetics; T = 452°; pressure of $2C_2H_6:O_2$ mixture 53 mm Hg; 1, 1', 1") without additive, in the H_2F_2 vessel; 2, 2', 2") 5-fold dilution of the mixture with nitrogen, in the H_2F_2 vessel; 3, 3', 3") with 1% NO_2 added, in the H_2F_2 vessel; 4, 4', 4") with 1% NO_2 added, in the $K_2B_4O_7$ vessel. The other symbols are the same as in Fig. 1.

The particular features observed in the kinetic behavior of CH_3CHO (the "jump" and the maximum concentration reached at $d(\Delta p)/dt \simeq 0$ may be explained if it is assumed that the case 2) above applies. It is then evident that as long as the concentration of active centers in the system is sufficiently high, the concentration of CH_3CHO in the system strives to maintain itself close to the purely chain level. With the reduction in the concentration of active centers at the end of the conversion, the part played by processes (1') and (2') increases in comparison with processes (1) and (2) and the yield of CH_3CHO increases towards the value of the purely molecular yield. An increase in the concentration of active centers in the system should, from this point of view, always lead to a reduction in the "pre-jump" concentration of CH_3CHO. If the concentration of active centers is sufficiently high for the molecular processes to be neglected in comparison with the chain processes, then the "pre-jump" yield of CH_3CHO will be the limiting yield. The experimental results given in Fig. 3 show that dilution of the mixture with nitrogen and addition of an initiator (1% NO_2) do indeed reduce the "pre-jump" yield of CH_3CHO, while the yield of CH_3CHO in the initiated reaction does not change on going from the H_2F_2 vessel to the $K_2B_4O_7$ vessel, although the rate of oxidation according to Δp, which is a measure of the concentration of active centers, is appreciably reduced. This enables us to regard the figure of 0.03% CH_3CHO in the gas as the limiting yield for the given temperature, pressure and mixture composition.

The maximum yield of CH_3CHO ("post-jump"), as can be seen from Fig. 3, undergoes no systematic change with change in the concentration of active centers in the reaction system (as should be expected on the basis of the interpretation put forward).

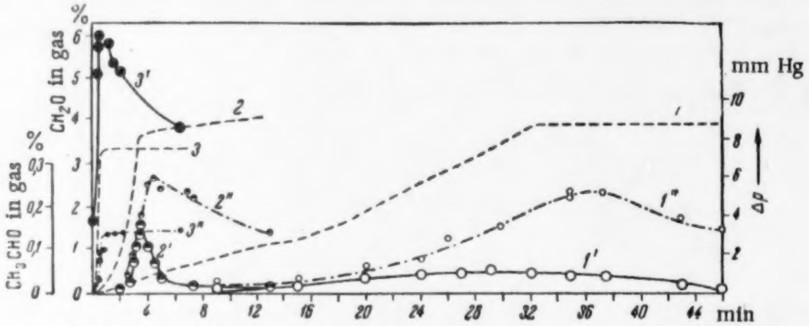

Fig. 4. The influence of the reaction vessel surface and additions of NO_2 on the yield of aldehydes and on the manometric kinetics; T = 512°; pressure of $2C_2H_6:O_2$ mixture 53 mm Hg; 1, 1', 1") without additive, in the $K_2B_4O_7$ vessel; 2, 2', 2") without additive, in the H_2F_2 vessel; 3, 3', 3") with 1% NO_2 added, in the $K_2B_4O_7$ vessel. The other symbols are the same as in Fig. 1.

It can be seen from Figs. 3 and 4 that the yield of CH_2O in the case of the mixture $2C_2H_6:O_2$ becomes a function of the reaction conditions: those conditions which lead to an increase in the concentration of active centers in the system increase the yield of CH_2O. Treatment of the reaction vessel with $K_2B_4O_7$ solution, as in the case of CH_4 oxidation [2], reduces the reaction rate, according to Δp, in comparison with the H_2F_2 vessel. In the noninitiated oxidation of C_2H_6, the change from the H_2F_2 vessel to the $K_2B_4O_7$ vessel is accompanied by a considerable reduction in the reaction rate and a simultaneous sharp fall in the yield of CH_2O (see curves 1' and 2' in Fig. 4). In the initiated oxidation of C_2H_6, the yield of CH_2O remains practically unchanged on going from the H_2F_2 vessel to the $K_2B_4O_7$ vessel (curves 3' and 4' in Fig. 3), which enables us to consider the yield of CH_2O in this case to be the limiting yield. Thus in the noninitiated oxidation of the mixture $2C_2H_6:O_2$, in contrast to the mixture $C_2H_6:2O_2$, the rate of the molecular decomposition of CH_2O becomes commensurate with the rate of its chain-process decomposition, and the yield of CH_2O becomes less than the limiting yield. With strong initiation, the rate of the molecular process is immeasurably smaller than the rate of the chain process and the yield is practically the same as the limiting yield.

LITERATURE CITED

[1] N. S. Enikolopian, G. V. Korolev, and G. P. Savushkina, J. Phys. Chem. 31, 4, 865 (1957).

[2] N. S. Enikolopian and G. V. Korolev, Proc. Acad. Sci. 118, 5 (1958).*

Received July 27, 1957

Institute of Chemical Physics, USSR Academy of Sciences

---

* See C. B. translation. P. 95, this issue.

THE REACTION OF METHYL RADICALS, PREPARED BY POLIANI'S METHOD, WITH DEUTERIUM

O. A. Ivanov, N. V. Fok, and V. V. Voevodskii

(Presented by Academician N. N. Semenov, July 26, 1957)

A number of works have recently appeared in the literature devoted to the study of the processes of thermal and photochemical decomposition of organic compounds forming the CH_3 radical in the primary decomposition stage, in the presence of molecular deuterium [1-5].

These studies are carried out for the most part in order to determine the rate constant for the elementary substitution reaction of the methyl radical:

$$CH_3 + D_2 = CH_3D + D.$$

In the works referred to, no methane containing more than one deuterium atom was detected. We would only point out that Nesby, Gordon and Smith [5], who carried out the photolysis of a mixture of acetone and deuterium in the presence of small amounts of mercury, found, together with CH_3D, a very small amount of CH_2D_2.

On the other hand, Mardaleishvili, Pariiskii, Poltorak and Voevodskii [6] have detected large quantities of extensively deuterated methane in a study of the reaction between deuterium and methyl radicals obtained by the interaction of H atoms, produced by an electrical discharge, with olefins. The authors suggest that these data can be taken as confirmation of the hypothesis which they previously put forward [7] regarding the existence of an exchange reaction between the hydrogen atoms in free radicals and molecular deuterium. These experiments were arranged in such a way as to exclude the participation of D atoms in the reaction, since the molecular deuterium in a number of experiments was added at a point in the stream where the reaction of H atoms with the unsaturated compounds could be considered to be complete.

The appearance of the polysubstituted methanes could not be related to the low pressures at which the experiments with the electrical discharge were carried out, since it was shown that in the photolysis of acetone and methyl iodide, a change in the pressure from several tens to several tenths of a millimeter of mercury did not result in the formation of extensively substituted methanes.*

An explanation of the above contradiction may be found in the different methods by which the methyl radicals are obtained. We therefore undertook a study of the reaction of D_2 with methyl radicals obtained by some other method.

We prepared methyl radicals by Poliani's method according to the reaction:

$$CH_3I + Na = CH_3 + NaI.$$

The reaction was carried out in the presence of molecular deuterium, which was used as carrier gas for the Na vapor. A diagram of the apparatus is shown in Fig. 1. The reaction vessel in which the streams of CH_3I and deuterium saturated with sodium vapor were mixed consisted of a quartz cylinder, connected via a nozzle with a small boat containing sodium, and via another nozzle with a flask containing CH_3I. The temperature of the boat containing the sodium was maintained at 450° during the experiments.

---

* These results were obtained by A. S. Chernysheva.

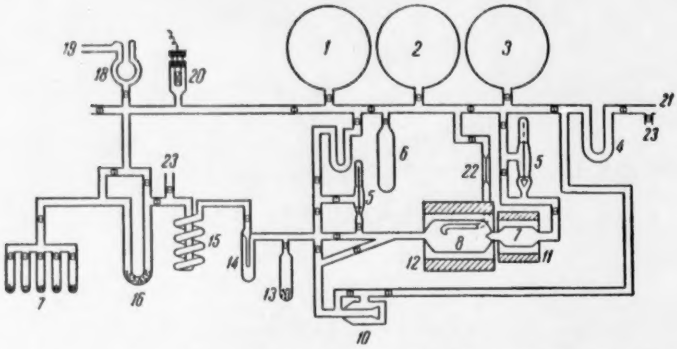

Fig. 1. Diagram of the apparatus. 1, 2, 3) Flasks with CH_3I, D_2 and H_2, respectively, 4) trap to collect mercury vapor from the manometer, 5) valves, 6) container with liquid CH_3I, 7) small boat containing Na, 8) reaction vessel, 9) nozzle, 10) diaphragm manometer, 11, 12) furnaces, 13) container with activated charcoal, 14) trap, 15) coil, 16) trap with activated charcoal, 17) battery for removing samples for analysis, 18) trap, 19) connection to pump, 20) thermocouple manometer, 21) connection to mercury manometer, 22) capillary, 23) connection to atmosphere.

In the cases where it was desired to exclude the three-dimensional reaction, the boat containing the sodium was not heated. The CH_3I pressure in the reaction vessel was equal to 0.5 mm Hg, D_2 pressure 10 mm, rate of flow of stream 8.5 cc/min. The reaction products, together with the saturated CH_3I, passed through a coil cooled with liquid nitrogen, where the methyl iodide, ethane and other condensable reaction products were frozen out. The methane and part of the deuterium were retained in a trap containing activated charcoal, which was placed beyond the coil and was also cooled by liquid nitrogen. At the end of the experiment the deuterium was pumped from this trap and the methane subjected to analysis. The mass-spectrometric analysis provided the information regarding the concentration of the different deuterated methanes. In the majority of experiments, the absolute quantity of methane was not determined.

In a number of experiments the inner surface of the reaction vessel was covered with sodium, deposited on the surface in the form of drops or in the form of a mirror. The drops were obtained either by rapidly heating pieces of sodium placed in the vessel so that they broke up into a spray, or by heating the sodium rapidly in the boat while a stream of deuterium was passed through. The mirror was obtained by gradually heating sodium placed in the vessel to 300°.

The deuterium used in the work was prepared electrolytically from D_2O and purified by diffusion through a palladium capillary. The CH_3I was distilled on a fractionating column (b. p. 41.5-42°, $n^{19} = 1.532$). The sodium used was chemically pure and was given no further purification.

The composition of the methanes obtained in the clean quartz vessel in the temperature range 20-480° was determined (Fig. 2). In these conditions the chief products are CH_4 and CH_3D. The quantity of polysubstituted methanes is small and only in a small temperature range close to 200° does it reach 18-20%. The ratio CH_3D/CH_4 increases in the temperature range 20-100° from 0.6 to 2, and remains unchanged on further increase in the temperature.

It was found that the deuterium content in the methanes formed altered considerably when metallic sodium from the stream was deposited on the surface of the vessel. Further experiments showed that the relationship between the percentage concentration of the various deuterated methanes and the temperature depended on the method by which the sodium was deposited on the surface.

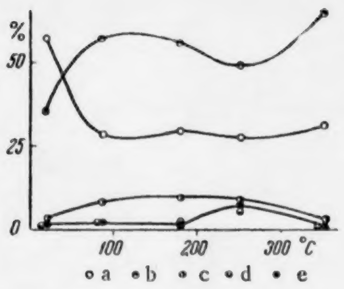

Fig. 2. The relationship between the temperature and the percentage composition of methanes obtained in the clean reaction vessel. a) CH$_4$, b) CH$_3$D, c) CH$_2$D$_2$, d) CH$_3$D,[*] e) CD$_4$.

When the surface of the vessel was covered with a sodium mirror (Fig. 3, I) the percentage concentration of extensively deuterated methanes (CD$_4$, CD$_3$H and CH$_2$D$_2$) at room temperature was 5-8 times greater than in a clean quartz vessel. When the temperature was increased the percentage of extensively deuterated methanes fell. It seems to us, however, that the fall is not connected with a reduction in the rate of formation of CD$_4$ and the other heavy methanes. It was shown by direct experimental measurement of the total concentration of methanes that when the temperature was increased to 70° the yield of methanes in the presence of the mirror increased by a factor of approximately 10. The fall in the percentage concentration of CD$_4$, CH$_2$D$_2$ and CD$_3$H may therefore be explained by the fact that a heterogeneous reaction is taking place on the surface of the sodium, leading chiefly to the formation of CH$_4$ and CH$_3$D.

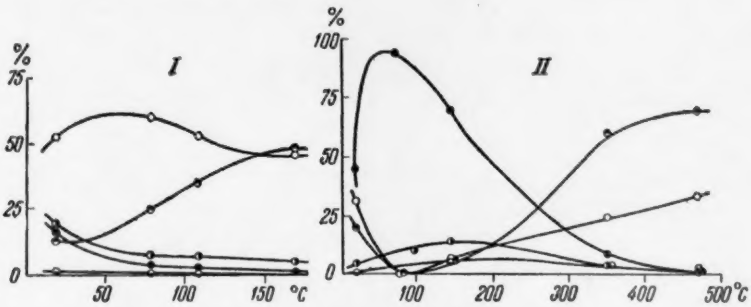

Fig. 3. The relationship between the temperature and the percentage concentration of methanes obtained in a vessel covered with a Na mirror (I) and with drops of Na (II). The symbols are the same as those used in Fig. 2.

It is important to note that light methane CH$_4$ undergoes no exchange with D$_2$ either in the presence of the mirror or in the presence of drops of sodium.

From these data, and also from the fact that the concentration of CD$_3$H is always lower than that of CD$_4$ and CD$_2$H$_2$, it follows that the extensively substituted methanes in our experiments could not have been formed as a result of the successive replacement of H atoms by D in saturated methanes. Thus no matter the mechanism by which CH$_2$D$_2$, CH$_3$D, and CD$_4$ are formed, this exchange should take place with the participation of methyl radicals.

The distribution of deuterated methanes in our experiments differs from the distribution in the experiments of Mardaleishvili, Pariiskii, Voevodskii and Poltorak [6], which evidently points to a different mechanism for their formation.

The part played by the Na surface in the exchange between CH$_3$ radicals and deuterium in our case cannot be doubted, but at the present time there are insufficient data available for the construction of a detailed mechanism which would explain the nature of the deuteration of methane or the maximum observed at a temperature of 70-80°.

---

[*] As in original. Probably CD$_3$H.—Publisher.

LITERATURE CITED

[1] T. G. Majury and E. W. R. Steacie, Canad. J. Chem. 30, 800 (1952).

[2] E. Whittle and E. W. R. Steacie, J. Chem. Phys. 21, 993 (1953).

[3] R. E. Rebbert and E. W. R. Steacie, Canad. J. Chem. 32, 113 (1954).

[4] R. D. Souffie, R. R. Williams, and W. H. Hamill, J. Am. Chem. Soc. 78, 917 (1956).

[5] M. Nesby, A. S. Gordon, and S. R. Smith, J. Am. Chem. Soc. 78, 1287 (1956).

[6] R. E. Mardaleishvili, G. B. Pariiskii, V. A. Poltorak, and V. V. Voevodskii, Bull. Acad. Sci. USSR, Div. Chem. Sci. 1956,* 516.

[7] V. V. Voevodskii, G. K. Lavrovskaia, and R. E. Mardaleishvili, Proc. Acad. Sci. 81, 215 (1951).

[8] H. V. Hartel and M. Polanyi, Z. phys. Chem. 11, 97 (1930).

Received July 19, 1957

Department of Chemical Kinetics, M. V. Lomonosov
State University, Moscow, and Institute of Chemical
Physics, USSR Academy of Sciences

ERRATUM

In the article of E.E. Segalova, V.N. Izmailova and P.A. Rebinder, "Investigation of the Kinetics of Supersaturation with Reference to the Formation of Crystallization Structures in the Hardening Process of Gypsum" which appeared in Proc. Acad. Sci. USSR 114, No. 3 (1957), the caption to Figure 3 should read :

The kinetics of structure formation in a suspension containing 30% of the hemihydrate of gypsum and various amounts of sand and dihydrate of gypsum, V/T = 0.5:

Curves	1	2	3	4	5	6	6	7
Sand, %	70	68	65	60	50	20	20	0
Dihydrate of gypsum,%	0	2	5	10	20	50	50	70

---

* Original Russian pagination. See C. B. translation.

PROCEEDINGS OF THE ACADEMY OF SCIENCES OF THE USSR

Section: PHYSICAL CHEMISTRY

VOLUME 118, ISSUES 1-6 JANUARY-FEBRUARY, 1958

CONTENTS

	PAGE	ISSUE	RUSS. PAGE
Electron-Diffraction Investigation of the Structure of the Chloroprene Molecule, P. A. Akishin, L. V. Vilkov, and V. M. Tatevskii	1	1	117
The Influence of Association of Organic Acids on Their Adsorption from Nonpolar Solvents, N. N. Griazev	5	1	121
On the Interaction of Ozone with Methyl Hydroperoxide, N. A. Kleimenov and A. B. Nalbandian	9	1	125
Investigation of the Mechanism of Electrolytic Formation and Decomposition of Percarbonate, Perborate and Perphosphate by the Isotope Method, I. F. Franchuk and A. I. Brodskii	13	1	128
The Free Energy, Heat and Entropy of the Adsorptional Displacement of Alcohols by Water from the Surface of an Oxide Catalyst, A. A. Balandin, O. K. Bogdanova, and A. P. Shcheglova	17	2	312
The Isotopic Exchange Between Gaseous Hydrogen and Solid Polymers Under the Action of Nuclear Radiations, Ia. M. Varshavskii, G. Ia. Vasil'ev, V. L. Karpov, Iu. S. Lazurkin, and I. Ia. Petrov	21	2	315
Adsorption from Three-Component Solutions, N. N. Griazev	23	2	317
The Influence of the Addition of Acids on the Kinetics of Acylation of an Aromatic Amine in an Inert Solvent, L. M. Litvinenko and D. M. Aleksandrova	27	2	321
The Electron Microscopic Investigation of Objects in a Gaseous Medium, I. G. Stoianova	31	2	325
Catalysis on Semiconductors in the Region of Intrinsic Conductivity, O. V. Krylov and S. Z. Roginskii	35	3	523
A Study of the Phase Composition and Adsorptive Properties of Iron–Carbon Catalyst, S. M. Samoilov, A. A. Slinkin, and A. M. Rubinshtein	39	3	526
The Kinetics of the Ionization of Molecular Chlorine, A. N. Frumkin and G. A. Tedoradze	43	3	530
The Chemically Nonuniform Structure of Sodium Borosilicate Glasses, N. S. Andreev and E. A. Porai-Koshits	47	4	735
The Effect of Oxygen on the Paramagnetic Resonance Absorption in $\alpha\alpha$-Diphenyl-β-picrylhydrazyl, N. S. Garif'ianov and B. M. Kozyrev	51	4	738
The Determination of Reaction Order from Acidity, A. I. Gel'bshtein and M. I. Temkin	53	4	740
The Action of Triethanolamine on Photographic Emulsions, A. P. Zhdanov, A. L. Kartuzhanskii, I. V. Ryshkova, and L. P. Shur	57	4	744

(continued)

CONTENTS (continued)

	PAGE	ISSUE	RUSS. PAGE
The Problem of the Reaction Path for Contact Oxidation on Semiconducting Catalysts (The Example of the Oxidation of Benzene), I. I. Ioffe and F. F. Vol'kenshtein	61	4	747
Capillary Contraction During the Drying of Jell Films and Dispersed Porous Bodies, M. S. Ostrikov, G. D. Dibrov, and E. P. Danilova	65	4	751
The Coefficient of Diffusion in Liquids, G. M. Panchenkov	69	4	755
The Nature of the Interaction of Anions and Water Molecules in Solution, Iu. P. Syrnikov	75	4	760
The Influence of Substituents on the Properties of the Molecules of the Para-Disubstituted Derivatives of Benzene, P. P. Shorygin and Z. S. Egorova	79	4	763
Electronographic Investigation of the Structure of the Molecule of Lithium Oxide, P. A. Akishin and N. G. Rambidi	83	5	973
The Vapor Pressure of Chromium Over Chromium–Iron Alloys in the Solid State, E. Z. Vintaikin	87	5	977
The Effect of an External Electric Field on the Adsorptive Power of a Semiconductor, F. F. Vol'kenshtein and V. B. Sandomirskii	91	5	980
Dependence of the Yield of Formaldehyde in the Oxidation of Methane on the Concentration of Homogeneous Initiator, the Amount of Inert Gas and the Condition of the Walls of the Reaction Vessel, N. S. Enikolopian and G. V. Korolev	95	5	983
The Effect of Tribenzylamine on the Reaction of Reduction of the Persulfate Ion, N. V. Nikolaeva-Fedorovich and L. A. Fokina	99	5	987
Some Special Features of the Radiation Destruction of Polymers, A. B. Taubman and L. P. Ianova	103	5	991
The Effect of Rate of Deformation on the Rate of Thixotropic Recovery of Aluminum Naphthenate Gel and an Oscillographic Method of Recording Strain-Deformation Curves, T. G. Shalopalkina and A. A. Trapeznikov	107	5	994
Electron-Diffraction Study of the Structure of Beryllium Halide Molecules, P. A. Akishin, V. P. Spiridonov, and G. A. Sobolev	111	6	1134
Yields of Formaldehyde and Acetaldehyde in the High-Temperature Oxidation of Ethane, N. S. Enikolopian and G. V. Korolev	115	6	1138
The Reaction of Methyl Radicals, Prepared by Poliani's Method, with Deuterium, O. A. Ivanov, N. V. Fok, and V. V. Voevodskii	119	6	1142